

Chlorophyll Fluorescence Spectrometer

Group 1

David Maria, Computer Engineering

Luke Preston, Electrical Engineering

Robert Bernson, Photonic Science & Engineering

Samuel Knight, Photonic Science & Engineering

Table of Contents

| | |
|---|----|
| 1. Executive Summary | 1 |
| 2. Project Description..... | 2 |
| 2.1 Motivation | 2 |
| 2.2 Project Goals and Objectives | 2 |
| 2.3 Requirement Specifications..... | 3 |
| 2.4 Engineering Trade-Off Matrix | 3 |
| 2.5 Block Diagram | 6 |
| 3. Constraints & Standards | 7 |
| 3.1 Standards | 7 |
| 3.1.1 RoHS Compliance | 7 |
| 3.1.2 Eye Safety..... | 8 |
| 3.1.3 FDA Performance Standards for Light-Emitting Products | 8 |
| 3.1.3 IEEE 802.15.1 - Bluetooth | 9 |
| 3.1.4 ISO/IEC 9899 – The C Language..... | 9 |
| 3.1.4.1 ANSI C (C89 / C90) | 10 |
| 3.1.4.2 C99..... | 10 |
| 3.1.4.3 C11..... | 10 |
| 3.1.4.4 C18..... | 11 |
| 3.1.5 Surface Quality for Optics..... | 11 |
| 3.1.5.1 US Standard MIL-PRF-13830B (Scratch-Dig) | 11 |
| 3.2 Constraints..... | 13 |
| 3.2.1 Economic | 13 |
| 3.2.2 Environmental | 13 |
| 3.2.3 Social | 14 |
| 3.2.4 Political..... | 14 |
| 3.2.5 Health and Safety..... | 14 |
| 3.2.6 Manufacturability | 15 |
| 3.2.7 Sustainability | 16 |
| 3.2.8 Time Constraints..... | 16 |
| 4. Project Research..... | 18 |
| 4.1 Similar Products | 18 |
| 4.2 Light Source | 18 |
| 4.2.1 LED | 20 |
| 4.2.2 Laser Diode..... | 22 |
| 4.2.3 Cuvettes | 26 |
| 4.2.4 Chlorophyll Sample Preparation | 27 |
| 4.3 Optics | 28 |
| 4.3.1 Filters | 28 |

| | |
|--|----|
| 4.3.2 The Slit | 30 |
| 4.3.2 Collecting & Focusing Optics | 30 |
| 4.3.3 Monochromator | 31 |
| 4.3.3.1 Prism | 31 |
| 4.3.3.2 Diffraction Grating..... | 34 |
| 4.3.3.3 Monochromator Conclusions..... | 37 |
| 4.4 Sensor System | 39 |
| 4.4.1 Linear Sensor Arrays | 39 |
| 4.4.1.1 AMS TSL1401CL..... | 40 |
| 4.4.1.2 AMS TSL3301CL..... | 40 |
| 4.4.1.3 Melexis MLX75306 3rd Generation..... | 40 |
| 4.4.2 Square CCD Sensors | 41 |
| 4.4.2.1 Renesas ISL29147 | 41 |
| 4.4.2.2 Texas Instruments OPT3002..... | 41 |
| 4.4.2.3 ON Semiconductor AR0130CS Series | 43 |
| 4.4.3 Sensor Comparisons | 44 |
| 4.4.4 Conclusion | 47 |
| 4.5 Electronics..... | 48 |
| 4.5.1 Printed Circuit Board..... | 48 |
| 4.5.2 PCB Design Software..... | 49 |
| 4.5.3 CPU | 50 |
| 4.5.2 ARM7 | 50 |
| 4.5.4 ARM Cortex-M | 51 |
| 4.5.5 Power Delivery | 52 |
| 4.5.6 Battery | 56 |
| 4.5.7 Battery Charging Circuit | 57 |
| 4.6 User Interface | 58 |
| 4.6.1 Smartphone Application (Wireless) | 59 |
| 4.6.2 Desktop Application (Wired) | 59 |
| 4.6.3 On-Board Touch Screen | 59 |
| 4.6.4 On-Board Display with Mechanical Buttons..... | 59 |
| 4.6.5 User Interface Comparison and Final Selection..... | 60 |
| 4.7 Wireless Communication | 60 |
| 4.7.1 Bluetooth Classic..... | 61 |
| 4.7.2 Bluetooth Low Energy..... | 62 |
| 4.7.3 Wi-Fi..... | 63 |
| 4.7.3 ZigBee Wireless Technology | 64 |
| 4.7.4 Wireless Communication Comparison and Final Selection..... | 64 |
| 4.8 Wired Communication | 65 |
| 4.8.1 UART | 66 |
| 4.8.2 I2C | 66 |

| | |
|---|-----|
| 4.8.3 SPI | 68 |
| 4.8.4 Wired Communication Comparison and Final Selections | 70 |
| 4.9 Bluetooth Module..... | 70 |
| 4.9.1 HC-05 | 70 |
| 4.9.2 RN42..... | 72 |
| 4.9.3 RN4020..... | 73 |
| 4.9.4 ESP32 | 74 |
| 4.9.5 Bluetooth Module Comparison and Final Selection..... | 74 |
| 5. Project Design..... | 76 |
| 5.1 Hardware Design..... | 76 |
| 5.1.1 Optical Cavity Design | 76 |
| 5.1.2 Optical Cavity Loss Calculations | 83 |
| 5.1.3 Electronics Design..... | 85 |
| 5.1.4 Laser Cavity Design | 92 |
| 5.1.5 Housing Design | 92 |
| 5.2 Software Design | 95 |
| 5.2.1 Embedded Software Design | 96 |
| 5.2.1.1 Block Diagram..... | 96 |
| 5.2.1.2 Image Sensor Interaction | 96 |
| 5.2.1.3 Bluetooth Sensor Interaction..... | 98 |
| 5.2.2 Mobile Application Software Design..... | 98 |
| 5.2.2.1 Block Diagram..... | 99 |
| 5.2.2.2 Bluetooth Communication Design..... | 100 |
| 5.2.2.3 Local Database Design | 100 |
| 5.2.2.4 Graphical User Interface Design..... | 102 |
| 5.3 Bill of Materials | 103 |
| 5.4 Design Summary..... | 103 |
| 6. Part Acquisition and Testing..... | 104 |
| 6.1 Introduction | 104 |
| 6.2 Status Summary..... | 104 |
| 6.3 Part Acquisition..... | 105 |
| 6.4 Hardware Testing | 105 |
| 6.4.1 RN4020 – Bluetooth Module Testing | 105 |
| 6.4.2 AR0130CS – CMOS Monochromatic Sensor Testing..... | 107 |
| 6.4.3 STM32F407VET6 – Development Board Testing..... | 109 |
| 6.4.4 Newport 33066FL01-270R Diffraction Grating Testing..... | 112 |
| 6.4.5 Laser Testing | 113 |
| 6.5 Software Testing | 114 |
| 6.5.1 Development Board Emulation | 114 |
| 6.5.2 Physical Measurements | 114 |
| 6.5.3 Mobile Application Automated Testing..... | 115 |

| | |
|---|------|
| 7. Administrative..... | 116 |
| 7.1 Milestones | 116 |
| 7.2 Budget and Avenues of Financing | 117 |
| 7.3 Division of Labor | 118 |
| 8. Project Summary/Conclusion | 119 |
| Appendix A – References | i |
| Appendix B – Permissions..... | iii |
| Appendix C – Extra Tables and Figures | viii |

List of Equations

| | |
|---|----|
| Equation 1. Comparison of bandgap energy (E_g) to energy of a photon ($h\nu$)..... | 20 |
| Equation 2. Relation between wavelength and frequency of a light wave | 20 |
| Equation 3. Deviation angle for a prism | 32 |
| Equation 4. Abbey number | 33 |
| Equation 5. Diffraction angle for a grating with light at normal incidence..... | 35 |
| Equation 6. Diffraction angle for a grating with light inbound from non-normal angle θ_i | 35 |
| Equation 7. Blazed grating equation..... | 36 |
| Equation 8. Calculating Power from Current and Voltage..... | 55 |
| Equation 9. Calculating Power from Energy and Time..... | 56 |
| Equation 10. Effective focal length of focusing mirror using slit size and angular dispersion | 80 |

List of Tables

| | |
|---|------|
| Table 1. Project deadlines | 17 |
| Table 2. Laser diode comparison | 24 |
| Table 3. Prism price comparison | 34 |
| Table 4. Groove spacing vs incidence angle..... | 37 |
| Table 5. Diffraction grating comparisons | 38 |
| Table 6. Sensor Electro-Optic Specifications | 47 |
| Table 7. Processor table of comparison | 52 |
| Table 8. Estimate of power consumption | 55 |
| Table 9. User Interface Method Comparison..... | 60 |
| Table 10. Traditional Bluetooth Specifications | 61 |
| Table 11. Bluetooth Low Energy Specifications | 62 |
| Table 12. Wi-Fi Specifications | 63 |
| Table 13. ZigBee Specifications | 64 |
| Table 14. Wireless Communication Comparison | 65 |
| Table 15. Wired Communication Technology Uses..... | 70 |
| Table 16. HC-05 Technical Specifications | 71 |
| Table 17. RN42 Technical Specifications | 72 |
| Table 18. RN4020 Technical Specifications | 73 |
| Table 19. ESP32 Technical Specifications | 74 |
| Table 20. Bluetooth Module Comparison..... | 75 |
| Table 21. Mirror prices and other metrics | 81 |
| Table 22. Table of expected interface losses | 83 |
| Table 23. Bluetooth Module IO Connectors..... | 90 |
| Table 24. CMOS Sensor IO Connections | 91 |
| Table 25. Mobile Application Design Choice Summary..... | 99 |
| Table 26. Bill of materials | 103 |
| Table 27. Part Acquisition Timeline..... | 105 |
| Table 28. RN4020 Testing Results | 107 |
| Table 29. Monochromatic Sensor Testing Results | 109 |
| Table 30. Development Board Testing Results | 112 |
| Table 31. Diffraction grating spec test..... | 112 |
| Table 32. Tested Specifications for Laser Module | 113 |
| Table 33. Milestones for Senior Design 1 | 116 |
| Table 34. Milestones for Senior Design 2 | 117 |
| Table 35. Budget details for CFS..... | 117 |
| Table 36. Division of labor for the CFS | 118 |
| Table 37. (Appendix) Efficiency and loss at relevant interfaces | viii |

List of Figures

| | |
|---|----|
| Figure 1. Engineering trade-off matrix | 4 |
| Figure 2. Block diagram and designation of responsibilities..... | 6 |
| Figure 3. Scratch-dig table of requirements..... | 12 |
| Figure 4. NFPA 704 diamond for acetone | 15 |
| Figure 5. Absorption spectrum of Chlorophyll <i>a</i> | 19 |
| Figure 6. Emission Spectrum of Chlorophyll <i>a</i> | 19 |
| Figure 7. Electron transitions in direct and indirect bandgap semiconductors. | 21 |
| Figure 8. Energy diagrams of absorption, spontaneous emission, and stimulated emission. | 22 |
| Figure 9. Fabry-Perot resonator cavity for a laser diode. | 23 |
| Figure 10. Schematic including dimensions for MZH8340550D-AL01A laser module. | 24 |
| Figure 11. Measured emission spectra of Chlorophyll <i>a</i> in Acetone based on various excitation wavelengths from 405nm to 440nm. | 25 |
| Figure 12. From left to right: Chlorophyll <i>a</i> sample diluted with 150mL (high concentration), Chlorophyll <i>a</i> sample after diluted until OD<0.1, pure acetone..... | 27 |
| Figure 13. A longpass optical filter and its wavelength-dependent transmission curve..... | 28 |
| Figure 14. A shortpass optical filter and its wavelength-dependent transmission curve..... | 29 |
| Figure 15. A bandpass optical filter and its wavelength-dependent transmission curve. | 30 |
| Figure 16. Example of deviating prisms..... | 31 |
| Figure 17. N-BK7 refractive index vs wavelength | 33 |
| Figure 18. Young's double slit | 35 |
| Figure 19. Dispersion comparison of a prism versus a diffraction grating..... | 39 |
| Figure 20. OPT3002 picture by TI (insert) | 42 |
| Figure 21. OPT3002 incidence angle vs normalized response curve | 42 |
| Figure 22. AR0130CS (ARDR) imaging sensor on a PCB | 44 |
| Figure 23. Internal Functioning of a 7805 linear regulator..... | 54 |
| Figure 24. Simplified schematic for the bq2970..... | 58 |
| Figure 25. UART Device Configuration | 66 |
| Figure 26. Serial over USB Communication | 67 |
| Figure 27. I2C Device Configuration | 67 |
| Figure 28. Multiple-Slave-Select SPI Configuration..... | 69 |
| Figure 29. Daisy Chain SPI Configuration | 69 |
| Figure 30. Dimensionless optical system design. | 76 |
| Figure 31. 90% sensor fill using the chlorophyll fluorescence spot. | 78 |
| Figure 32. Diffraction grating incidence angle vs angular dispersion at 600-700nm waveband . | 79 |
| Figure 33. Illustration of the geometric system between the diffraction grating and the focusing mirror (simplified) | 79 |
| Figure 34. Final optical system design with major angles and dimensions..... | 82 |
| Figure 35. Diffraction grating efficiency curve (source quality)..... | 84 |
| Figure 36. ARDR Monochrome Sensor quantum efficiency curve vs wavelength..... | 84 |
| Figure 37. Battery Charging Management Circuit | 86 |
| Figure 38. CMOS sensor 1.8 Volt supply | 87 |
| Figure 39. CMOS sensor 2.8 Volt supply..... | 87 |
| Figure 40. Laser Diode 3.0 Volt Supply | 87 |

| | |
|---|-----|
| Figure 41. ARM M-Processor and Bluetooth module power supply | 87 |
| Figure 42. Circuit schematic for the CFS | 89 |
| Figure 43. Dimensions of Laser Cavity | 92 |
| Figure 44. Complete housing design with dimensions, angles, and labels..... | 93 |
| Figure 45. Use Case Diagram | 95 |
| Figure 46. Embedded Software Block Diagram | 97 |
| Figure 47. Timing Diagram for Reading Pixel Data..... | 98 |
| Figure 48. Mobile Application Block Diagram | 99 |
| Figure 49. Entity Relationship Diagram for Application Database..... | 101 |
| Figure 50. GUI Design Sketch..... | 102 |
| Figure 51. RN4020 Bluetooth Module | 105 |
| Figure 52. RN4020 Individual Module Testing..... | 106 |
| Figure 53. RN4020 Integration Testing..... | 107 |
| Figure 54. AR0130CS Monochromatic Sensor | 108 |
| Figure 55. Monochromatic Sensor Configuration Testing | 109 |
| Figure 56. STM32 Development Board..... | 110 |
| Figure 57. Flashing Development Board..... | 111 |
| Figure 58. Testing Development Board..... | 111 |
| Figure 59. Richardson Diffraction Grating (unopened)..... | 112 |
| Figure 60. Setup for Measuring Laser Beam Spot Size..... | 113 |

1. Executive Summary

Plants are vital to human culture. They form the backbone of cultural ceremonies, social situations, medicines, decorations, food sources, oxygen production, and agriculture. It is important that plants stay healthy for all these applications. However, sometimes a plant might not be healthy even if its leaves aren't wilting. Ways of testing for plant health include soil examination, chemical analysis, and even trial-and-error horticulture practices. However, by using chlorophyll fluorescence spectroscopy, a general idea of plant health can be gained in only a few minutes.

A chlorophyll fluorescence spectrometer (CFS) tests for the presence of chlorophyll in flora by pumping a sample with ultraviolet light. This spectrometer is designed with portability and cost in mind. The device shines bandpass-filtered UV light from an LED through a collimating lens into a sample-holding area. The spectrum of the sample is focused through a focusing lens onto a diffraction grating. The grating splits the light into its component wavelengths and the light is sent to a linear CCD array. The signal is then processed from analog to digital and the spectrum of the sample is shown on a mobile phone screen.

Chlorophyll fluorescence gives information about the Photosystem II (PSII) protein complex, which is the first protein group chain involved in photosynthesis. Chlorophyll fluorescence intensity reveals information about how well PSII is using light energy absorbed by chlorophyll to power photosynthesis, and since PSII's efficiency is a general indicator of photosynthetic performance, chlorophyll fluorescence is the fastest method of testing the state of PSII. This spectrometer thus relies on the function of the PSII protein complex in plants to give meaningful data about the plant's health. If a certain plant's chlorophyll sample fluoresces lower than a known healthy plant, there could be evidence of stress, disease, infestation, or malnutrition. This device acts as a first indicator, preventing the need for lengthy chemical tests. Since light covers a large area, the device can also be used to judge the general health of plants in its vicinity, assuming all factors constant, which is a boon for greenhouses with strict environment and climate conditions.

This report documents the design process of the CFS. It starts with the description of the project and the motivations for choosing the topic. It will then describe requirement specifications such as cost, power supply, and device dimensions. There will be a research section describing each part chosen for the design and why that part was chosen. It will also briefly describe the trade-offs associated with the chosen parts compared to other considered parts. The report will then discuss the design constraints and engineering standards pertinent to the design. There will be a section following this describing the hardware and software design of the project with accompanying physics research. The report will then detail the administrative side of the project, such as budget, financing, and the project schedule template. The report will conclude with necessary references and an appendix for further references or for any material not significant enough to include in the body of the text.

2. Project Description

A CFS is an important tool for home horticulture enthusiasts, farmers, and pharmaceutical companies. It can accurately give a quick measure of a plant's overall health by observing how strongly a sample's chlorophyll fluoresces. The section herein describes the goals, motivations, requirements, and trade-offs associated with the CFS.

2.1 Motivation

Plants are an integral part of human culture. They help cure sicknesses, decorate space, are critical in art and architecture design, exchange carbon dioxide for oxygen, and many other functions. Like animals or family members, taking care of plants is a human imperative. It is important to understand when plants are stressed, sick, infested, or in need of different amounts of sunlight. The CFS is a tool that will provide a first-response overview of plant health, like a thermometer for a feverish toddler. Of course, once it has been established that a plant is unhealthy, then more specific measures can be taken to ensure the plant recovers adequately. The initial screening is the important part. Without it, it may be impossible to tell a plant is unhealthy until it is too late to save the plant.

2.2 Project Goals and Objectives

The goal of this project is to build a portable, cost-effective prototype of a fluorescence spectrometer that focuses mainly on measuring chlorophyll fluorescence. The prototype will meet the following goals.

Cost – The device will cost less to build and use than models currently on the market while performing the same tasks. The idea for this goal is to allow access for anyone who wants to monitor their plants' health and not limit it to only those with large or corporate budgets.

Size – The device will be portable and not overtly large, bulky, or cumbersome. The idea for this goal is to make the device easy to transport and store. Size is an important consideration for this device since many similar products are small enough to fit in the palm of a user's hand.

Ease of Use – The device will be simple, modest, and not over-designed. The device's interoperability with wireless communications will prevent the need for bulky cables and external storage. The idea for this goal is to make the device usable by anyone who has a smartphone. This goal goes in-hand with the Size and Cost goals.

Robust Quality – The device will be able to sustain normal wear-and-tear, will be watertight, and will be housed in material that can protect the delicate optics and electronics inside. The idea of this goal is to ensure that the sensitive optics and electronics do not get ruined or shifted out of place when the device is moved or dropped.

Utility Analysis – The device will be able to give a general classification of the sample’s health after fluorescence analysis. The idea of this goal is to make it easier for the user to understand the data. Some examples are “Good health”, “Average health”, “Fair health”, etc.

2.3 Requirement Specifications

This section details the requirement specifications for the CFS.

- The device will cost less than 500 USD to build to completion. This value includes all optics, electronics, computer hardware, software, and housing materials used for the final product. This value does not include test materials, simulation or design software used on license agreements, or previous prototypes.
- The device’s total volume will be less than or equal to 0.15 cubic meters.
- The device’s total power delivery to all power-requiring components will be less than or equal to 115 Watts.
- The device will have a battery that can last up to 6 hours independently, depending on the quantity of samples analyzed in that period.
- The device will house a wireless standard Bluetooth 4.0 Bluetooth Low Energy (BLE) mechanism which will provide fundamental communication for the user.
- The device’s radio power consumption will be between 10 and 500 microWatts.
- The total analysis time required to produce spectrum data for one sample will take less than 2 seconds.
- Each chlorophyll sample should have an optical density <0.1 so the fluorescing light is not reabsorbed by the sample

From the above requirement specifications, we have chosen the following three as the demonstrable requirements specifications to be used for the demonstration of our product.

- The device will house a wireless standard Bluetooth 4.0 Bluetooth Low Energy (BLE) mechanism which will provide fundamental communication for the user.
- The total analysis time required to produce spectrum data for one sample will take less than 2 seconds.
- Each chlorophyll sample should have an optical density <0.1 so the fluorescing light is not reabsorbed by the sample

2.4 Engineering Trade-Off Matrix

The engineering trade-off matrix for the CFS was designed to show the relationship between its engineering and marketing requirements. Fig. 1 is the matrix used for the CFS and is followed by a key describing the symbols used. An explanation with examples from the matrix follows Figure 1’s key.

The engineering requirements list the needs of the system from the point of view of a developer or engineer. Dimensions describes the volumetric size of the CFS in cubic meters and should be decreased to make the device portable. Power delivery shows how much power will be delivered to the circuits within and should be decreased so the device is economical and doesn't heat up. Power consumption describes how much power the internal battery will consume while powering the circuits and components within the device. This metric should be decreased so that the device lasts long amounts of time before needing a recharge. Cost describes how much money it will take to build and test the device and should be decreased for financial reasons. Wireless communication describes how wireless the device is, so this metric should be increased as much as possible. Total analysis time is the time spent analyzing information passed from the device to the processor and passing that on to the user, so it should be decreased.

| | | | Engineering Requirements | | | | | |
|--------------------------------------|----------------|---|--------------------------|----------------|-------------------------|---------|---|---------------------|
| | | | Dimensions | Power Delivery | Power Consumption | Cost | Wireless Communication | Total Analysis Time |
| | | | - | - | - | - | + | - |
| Marketing Requirements | Cost | - | ↑ | ↑ | ↑ | | ↓ | ↓ |
| | Size | - | ↑ | | | | | |
| | Ease of Use | + | ↑ | | | ↑ | ↑ | ↑ |
| | Robust Quality | + | ↓ | | | ↓ | ↑ | |
| Targets for Engineering Requirements | | | ≤ 0.15 cubic meters | ≤ 115 Watts | 6 hours of battery life | ≤ \$500 | Bluetooth 4.0 Bluetooth Low Energy (BLE) | < 2 seconds |

Figure 1. Engineering trade-off matrix

Key

↑↑ = Strong positive correlation. Advancing both metrics can be done without sacrifices and will produce corresponding net positives.

↑ = Positive correlation. Advancing both metrics can be done without sacrificing anything from either.

↓ = Negative correlation. Advancing one metric causes a sacrifice in the other correlated metric.

↓↓ = Strong negative correlation. Advancing one metric causes great sacrifices in the other correlated metric.

- = Negative polarity. This metric aims to be decreased in the project.

+ = Positive polarity. This metric aims to be increased in the project.

Green = Engineering Requirements chosen for demonstration.

The marketing requirements detail the qualitative metrics that the CFS aims to reach during the design process. Cost, as previously discussed, describes how much the device will cost. It is important that this metric is decreased as low as it can go. Users of the CFS will appreciate a cheaply priced, quality product. Size is the same as the engineering requirement's Dimensions, but for marketing requirements, it describes the general size of the device. Users of the CFS will want a device that isn't cumbersome or bulky—something they can carry around or install in place without disturbing their daily routines. Ease of Use describes how accessible the CFS is for the lay user. Since the CFS has built-in wireless capabilities, it is easy to sync up a data stream with the user's smartphone rather than having them deal with installing a program on their computer and offloading data using hard wires or cables. Robust Quality says that the product should be resistant to damage, stable, and not easily broken. Since the CFS houses sensitive optics and communication technologies, robustness is a very important metric.

Consider the Dimensions engineering requirement and the Size marketing requirement shown in Figure 1. Size and Dimensions both have a negative direction. Their correlation is ↑. As the Size of the device is decreased in its negative direction, the Dimensions of the device will also decrease in its own negative direction. They are positively correlated with ↑ since either metric can be advanced in their direction without sacrificing anything in the corresponding metric.

Now consider the Wireless Communications engineering requirement and the Cost marketing requirement in Figure 1. Cost has a negative direction and Wireless Communications has a positive direction. Their correlation is ↓. If Cost is decreased, or advanced negatively, Wireless Communications will be harder to implement and will also decrease negatively, which is the opposite of Wireless's positive direction. On the other hand, if more Wireless Communications are added, advancing the direction positively, the Cost of the device will increase, advancing Cost positively (or in the negative of its negative direction). For this reason, the correlation between these two metrics is ↓.

2.5 Block Diagram

Figure 2 shows the division of responsibilities and overall schematic of the chlorophyll fluorescence spectrometer. The device starts with an input optical source that excites a sample of isolated chlorophyll diluted to the spec given in the requirement specifications. The fluorescent light is passed into the optics area of the device where the optics will separate the spectrum and pass it to the sensor array. The light will be converted from an analog signal to a digital signal and sent to a central processing unit. The unit will feed the information into a software interface which will display the spectrum and may allow for user input. The device may require a modulator for the light source; however, given the slow photo-quenching effect inherent in chlorophyll, this is unlikely. The CFS is completed with an option to offload data using external storage. Even though the device will communicate wirelessly, the team wanted the CFS to give the user an option to port the information over to a personal computer or other device for analysis.

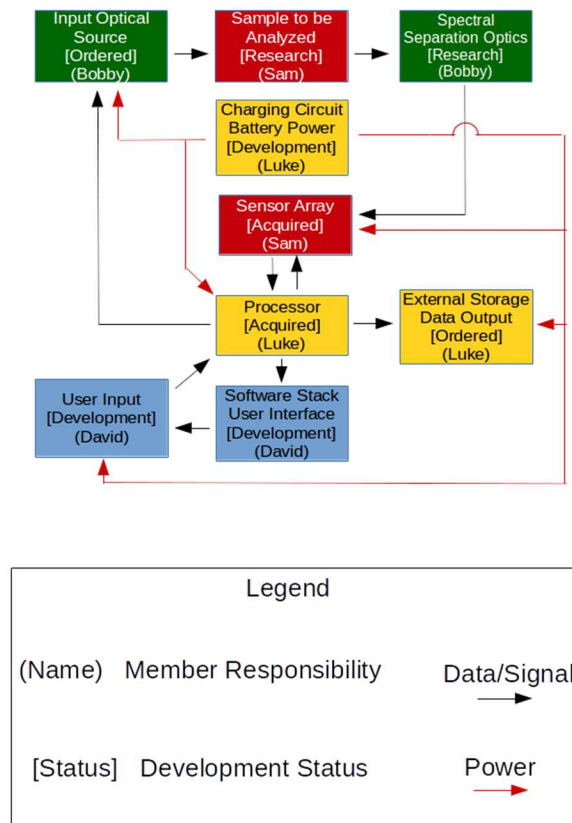


Figure 2. Block diagram and designation of responsibilities

3. Constraints & Standards

The section that follows details the constraints and standards applicable to the CFS. The standards section describes guidelines by which the CFS will be engineered. The constraints section describes rules which the CFS must follow. Together, these two engineering requirements will promote a sturdy product that is built to last, is marketable, and is not dangerous to introduce to the market.

3.1 Standards

A standard is an established way of doing things that ensures interoperability. Without engineering standards, the use of technology in the engineering industry, including the CFS, would be severely limited. The wide variance in how products are built and operated would cause tremendous mismatches in the markets. Products that should work naturally together, such as bolts and ceiling fans, home plumbing fixtures, and the modules in a modern computer would not work together if standards were not around.

Standards ensure the health and safety of the people who work with and use the product every day. Standards also ensure that the product itself is safe and does not cause undue harm to those who seek to operate it. According to senior engineers and standard accreditation organizations, following and identifying standards is an expected part of good engineering practice. As such, a working list of considered standards for the CFS has been listed below. Each standard is highlighted, is overviewed, and is briefly discussed with respect to its relevance to the project. Following the standards section is a discussion on theorized and known engineering constraints for the CFS.

3.1.1 RoHS Compliance

The Restriction of Hazardous Substances Directive (RoHS) is a European Union directive which was ratified in 2003. The RoHS restricts the amounts of certain materials which are allowed to be included in electronic devices. The RoHS is related to the Waste Electrical and Electronic Equipment Directive, which categorizes electronics and sets recycling goals. There are ten chemicals listed in the RoHS standard, which are lead, mercury, cadmium, hexavalent chromium, polybrominated biphenyls, polybrominated diphenyl ether, bis(2-ethylhexyl) phthalate, butyl benzyl phthalate, dibutyl phthalate, and diisobutyl phthalate. Prior to July 2019, only the first six materials were restricted. The changes were made with the release of RoHS 3. Exemptions in the RoHS allow lead for use in high temperature solders as well as solder for use in servers, storage and network equipment.

We will use RoHS compliant solders for this device—specifically, when soldering the image sensor. In order to achieve RoHS compliance, we will use lead free solder and screen each component and material that we use to ensure that none of the listed hazardous materials make their way into our project.

3.1.2 Eye Safety

Whenever a light source is involved, it is important to wear proper protective equipment to reduce injuries to the eye. Our CFS will incorporate a laser diode so it is important to recognize the standards of operation when operating a laser. The American National Standards Institute (ANSI) has written the ANSI Z136 set of standards to outline the safe use of lasers. ANSI has put categorized lasers into four main hazard classifications:

- Class I: Incapable of producing damaging radiation levels during operation
- Class II: Emits light in the visible portion of the spectrum
- Class III (a and b): Medium-power laser, may be hazard under specific viewing conditions, does not pose a fire or diffuse-reflection hazard
- Class IV: High-power laser, the direct beam can be hazardous to the skin and eye, may also pose a fire or diffuse-reflection hazard

The laser diode used in this CFS fall in the category of a Class 3b laser. This means while the laser is turned on and used for testing, proper eyewear must be worn such as UV blocking lenses. Besides eye injury, the laser does not pose much risk of injury. In the final product the laser will be set in housing where the laser will be unable to make direct contact with the eyes of the person operating the device.

3.1.3 FDA Performance Standards for Light-Emitting Products

The laser module we ordered came from a company outside of the United States. While this product was being shipped to the United States, it was required to fill out two forms, one which identifies the importer to the Department of Homeland Security and another to ensure the radiation standards of the imported equipment are up-to-date.

To fill out the form of “Declaration for Imported Electronic Products Subject to Radiation Control Standards,” it was necessary to locate the correct part of the Electronic Code of Federal Regulations, specifically Part 1040.10 on Radiation-Emitting Electronic Products. Part 1040 provides a general overview of both medical and non-medical radiation-emitting electronic products and the requirements the FDA must both verify and enforce when these products are imported into the United States.

The FDA “defines a radiation-emitting electronic product as any electrically-powered product that can emit any form of radiation on the electromagnetic spectrum.” The laser module for our device certainly fits this definition. In order to ensure that our laser module meets FDA standards, the applicability section of Part 1040.10 on laser products was referenced. Our group is manufacturing an electronic product (the CFS) and using the laser module as a component in the final product. Therefore, our laser module meets the required standards due to Part 1040.10 clause (1) which states that lasers manufactured or assembled after August 1, 1976 meet standards if they are “sold to a manufacturer of an electronic product for use as a component in such electronic product.” [eCFR]

3.1.3 IEEE 802.15.1 - Bluetooth

IEEE 802.15 is a set of standards from The Institute of Electrical and Electronics Engineers (IEEE) which defines standards related to Wireless Personal Area Networks (WPAN). While there are 10 major working areas under the IEEE 802.15 group, only the 802.15.1 substandard is relevant to this project. This standard is relevant to this project because we plan on using Bluetooth Low Energy, which is a wireless communication technology that falls under the 802.15.1 standard, to send analysis results from our device to a user-controlled device that will server as the main user interface.

The IEEE project 802.15.1 has defined a WPAN standard specifically based on the Bluetooth Foundation Specifications. The latest version of this standard, the IEEE Std 802.15.1™-2002, was published in June of 2002, and mainly focuses on defining the physical layer and media access control specifications for Bluetooth communication.

3.1.4 ISO/IEC 9899 – The C Language

ISO/IEC 9899 is an international standard which defines the C Programming Language. This standard was jointly defined by International Electrotechnical Commission and the International Organization for Standardization. The standard for the C language defines the syntax and constraints of the language and the semantic rules for the language.

For this reason, it is important for users of the language to be familiar with the different version of the C standard, and their differences, so that they can know what syntax and features are supported by the C standard version that they are implementing. This standard is relevant to our project because a large portion of the software that will be written for this project will embedded software which will be written using the C programming language. Because we will be writing C code, it is best practice to choose a single version of the C standard to target and adhere to the restrictions of that standard to avoid portability issues.

Although this standard defines the syntax and constraints of the language, there is no official standardized style guide for the C language. Having a set of defined style standards is important when developing an application to ensure that the code that is being written is all consistent style-wise. Style consistency increases the readability of the code and can make sure that best-practices be followed when formatting code to avoid for common mistakes. Because the C language has no official style guide, will define out own style guide for the development of this project. The code formatting standard that our team has defined for ourselves will include restrictions such as requiring meaningful names for all constants and variables, restricting the use of camelCase, defining indentations to be 4 spaces wide, requiring open braces be on the same line as the conditional or function, and other style restrictions.

The following sections of this report contains details about the major versions of the C standard, and the main differences between them. For this project we will be adhering to the C99 standard, for portability reasons.

3.1.4.1 ANSI C (C89 / C90)

ANSI C is a term commonly used to refer to the original group of C standards, also known as C89 and C90. Although these are the original C standards, they are not commonly used due to being outdated and lacking compatibility and usability features that were introduced in later versions of the C standard. The ANSI C standards have been officially withdrawn by their authors.

3.1.4.2 C99

The C99 standard was adopted in March 2000 by ANSI, and is known to be the most portable version of the C standard. The portability of this standard means that code compiled using the C99 standard is more likely to be supported on a wider array of devices than code compiled using later version of the C standard, which may have features that are too advanced or for which support was never implemented for some devices. This is especially important when dealing with Embedded programming, since many devices have been around for a long time and are not frequently updated. This version of the C standard improved the language by adding new data types and core language features, as well as improved compatibility with C++. A more detailed list of the additions made in this standard can be found in the list below.

- Better support for IEEE floating point standard
- Added the following built-in data types:
 - Long
 - `_Bool`
 - `_Complex`
 - `_Imaginary`
- Added new core language features:
 - static array indices
 - designated initializers
 - compound literals
 - variable-length arrays
 - flexible array members
 - variadic macros
 - the “restrict” keyword
- Improved compatibility with several C++ features

3.1.4.3 C11

The C11 standard was published in 2012 and is currently the previous version of the C standard. The C11 standard attempted to modernize some of the aspects of the language by doing things like improving Unicode support for the language, adding the “Generic” keyword, add a multi-threading API, and adding support for Atomic types. All of these additions work to modernize the language and make it fit in to the modern programming language landscape. Although these features modernize the language, 2012 is fairly recent as long as hardware manufacturing goes so the C11 standard is not as portable as the C99 standard, as not all hardware, especially embedded, has caught up with this standard.

3.1.4.4 C18

The C18 standard was published in 2018 and is mainly a “bug fix” release. No new features were added in this release over the previous C11 standard, as the only purpose of this release was to fix bugs that were introduced in the previous standards and make the programming language more stable.

3.1.5 Surface Quality for Optics

Optics are incredibly sensitive instruments since the subject they deal with—light—is very sensitive to any effects imposed on it. A major effect for consideration, especially when lenses and mirrors are considered, is the surface quality assured by the supplier of an optical component. In this section, the surface quality standard will be examined and discussed with respect to its relevance to the project.

3.1.5.1 US Standard MIL-PRF-13830B (Scratch-Dig)

The United States Military Standard Performance Specification MIL-PRF-13830B classifies optical surface quality using a “scratch-dig” system found in just about every optical manufacturer’s catalog. Optics must both comply with the standard listed above if either is desired by the manufacturer for use in military systems. Considering this is where an immense amount of money is made in the optics field, following this standard is good economic practice.

Following this standard is also good safety practice since a scratch or dig in an optic, particularly in laser applications, can cause immense laser-induced damage especially in ultrafast applications. Since the CFS uses a laser as its pump source, all optics should comply with the scratch-dig standards set forth in the MIL-PRF-13830B document to prevent any laser light from interacting with or damaging components within the optical cavity.

“Scratches” are marks on the surface of the optic. They are quantified with one of five numbers: 10, 20, 40, 60, and 80, with 10 being the lightest class of scratch and 80 being the darkest class of scratch. There is no metric given for the scratches, and according to further research, the scratches are arbitrary numbers that a human inspector assigns to a scratch under certain illumination conditions not described in the MIL-PRF-13830B document. The sum of all the lengths of all scratches in a single scratch brightness class cannot exceed one-quarter of the diameter of the optic as described in 3.5.2.1.

“Digs”, as defined in section 3.5.3.1 of the document, are the physically allowed diameters of the defect in units of 1/100 mm. If a dig is irregularly shaped, the average of the length and width is used as the dig magnitude. These dig numbers are then converted from 1/100 mm to a numeric signified with a pound sign. For example, if a dig is 0.8mm in diameter, it has Dig # 80. According to 3.5.3.2, the total number of digs cannot exceed one per 20mm of diameter or the total additive dimensions cannot exceed 1/20 of the total optical diameter.

The reason these metrics are so important is the level of scrutiny at which it forces manufacturers to quality control their optics. The higher the numbers are in the scratch and dig classifications, the less likely the chance the optic has at being used in a government system, which will cost the company a lot of money.

The ideal optic has no scratches and no digs, but due to how optics are manufactured, even optics designed for immense precision will not have 0-0 classifications. In fact, the closest to a 0-0 classification is 10-5 standard used for laser cavity mirrors, particularly in the ultraviolet but less so in the infrared. The ideal 0-0 optic would also have ideal lossy surfaces that only lose power based off their reflectance of light. While these optics simply do not exist, the discussion of their effects and their close neighbor (the 10-5 standard) is pertinent to show how important scratch-dig is to the selection of optical components.

The most common standard for commercially available optics is 40-20, circled in Figure 3. This is a scratch class of 40 and Dig # 20. As can be seen in Figure 3, there is no magnifying power or focal length requirement for the optics in this category, leading to an immense amount of freedom for the optical designers to manipulate.

TABLE I Surface Quality Requirements

| Focal planes and near focal planes | | | Central zone 1/2 diameter of surface | | Outer Zone | |
|------------------------------------|------------------|-------------------|--------------------------------------|-----|------------|-----|
| Beam diameter (mm) | Magnifying power | Focal length (mm) | Scratch | Dig | Scratch | Dig |
| Over 5..... | | | 80 | 50 | 80 | 50 |
| 4-5..... | | | 60 | 40 | 60 | 40 |
| 3.2-4..... | | | 60 | 30 | 60 | 40 |
| 2.5-3.2 | | | 40 | 20 | 60 | 40 |
| 2.1-2.5..... | | | 40 | 15 | 60 | 30 |
| 1.6-2.1..... | | | 30 | 10 | 40 | 20 |
| 1.0-1.6..... | | | 20 | 5 | 40 | 15 |
| 0.6-1.0..... | | | 15 | 3 | 30 | 10 |
| 0.4-0.6..... | | | 10 | 2 | 20 | 5 |
| 0.2-0.4..... | | | 10 | 1 | 15 | 3 |
| 0.2..... | 20-10 | 12.5-25 | 10 | 1 | 15 | 3 |
| 0.4..... | 10-5 | 25-50 | 10 | 2 | 20 | 5 |
| 0.6 | 5-3.3 | 50-75 | 15 | 3 | 30 | 10 |
| 1.0..... | 3.3-2 | 75-125 | 20 | 5 | 40 | 15 |
| 1.6..... | 2-1 | 125-250 | 30 | 10 | 40 | 20 |

Figure 3. Scratch-dig table of requirements

Republished under AMSC N/A FSC 6650 Distribution Statement A (Approved for public release; distribution is unlimited).

Precision and ultrafast lasers usually require 20-10 minimum due to how sensitive a laser is to light propagation and reflection. The CFS, not requiring too much precision, will be using primarily 40-20 optics since these are the most commercially available systems. 40-20 optics are low cost, meet United States military specifications, and are readily available for purchase which translates to low lead times on shipping and arrival, translating further to more testing time.

3.2 Constraints

Constraints are design decisions imposed by the environment or designer that impacts or limits the design. They act as pseudo-guidelines for the CFS. Constraint requirements often violate the abstractness property of engineering requirement specifications, but in this section, they are treated as guidelines for ethical, safe, and intelligent engineering work.

3.2.1 Economic

Economic constraints are going to be an important limitation for our senior design project. We have not been sponsored by a private company or by the University so we will be financing the design ourselves. For this reason, great care and deliberation must be taken to reduce the cost as much as possible. We have decided to split the cost equally across four students. In order to keep the cost down, we are going to avoid overdesigning and choose the components which meet the need and are good enough, not necessarily the highest quality components money can buy.

It is possible to spend as much as you want to on a CPU into the thousands of dollars, however in our case that would not result in a higher quality device for measuring chlorophyll content. Running over budget and unable to complete the project is a danger that we will avoid. The marketability of our device improves as well as we keep the cost lower. Should we choose to manufacture our device for sale, a lower cost makes the product more attractive to customers and improves the volume of sales. The budget for our device will be limited to \$500 which includes all components, electronics, hardware, software, optics and materials that we will be using.

3.2.2 Environmental

Environmental constraints are factors in which the testing and development of a device is limited by its surrounding environment. For chlorophyll to fluoresce and for the emitted light to be collected properly, certain environmental conditions must be met. There must be little to no natural or randomly polarized light interfering with the fluorescent light. This can cause destructive interference will occur and will impede an adequate amount of the desired light from reaching the detector. It should be noted that the samples we are testing are constrained by environmental factors. We are only testing samples that can be easily found in our immediate location. However, our device will be used to test and monitor plant health so it should be able to be used for any sample in an environment where chlorophyll extraction is possible.

Another environmental constraint to consider is how our procurement of samples will affect the health of a plant. A leaf or leaves are going to have to be removed from the tree or bush to be sampled in the CFS. This affects the plant's health in a way that must be examined. Generally speaking, removal of plant leaves is not unhealthy for a plant. It does not affect plant growth, internal health, or susceptibility to diseases and infections. In fact, removing leaves from a plant is considered a healthy part of maintenance, similar to getting

a haircut. Proper removal of plant material helps a plant continue to grow without becoming deformed, bent, or unruly. [HGIC] As such, removal of plant material for the purposes of integration into a sample for the chlorophyll fluorescence spectrometer has no environmental constraints because its own sampling activity benefits the environment.

3.2.3 Social

Social constraints are patterns of societal and cultural behavior which can impede the development of a device. The CFS does not have any major social constraints limiting it; however, there are government regulations applicable to the operation of the optical source used in the CFS. These standards are discussed in more detail in 3.1.2 Eye Safety, the subsection of 3.1 Standards.

3.2.4 Political

Political constraints include limitations on the project placed by the government policies and political weather in the area the project is being designed. After researching the political cloud surrounding chlorophyll fluorescence spectrometers, it was determined that no political constraints are applicable to the CFS. There are, however, political constraints that prevent the importation of laser sources and parts from certain overseas countries.

3.2.5 Health and Safety

A first thought for health and safety should be how the chlorophyll is extracted. Primarily, for preparing samples, acetone will be used to extract chlorophyll from plant samples such as pine needles, leaves, and flowers. Acetone is a flammable, volatile liquid compound with a strong odor. It is dangerous to drink and has non-zero NFPA 704 codes outlined in Figure 4. Acetone 1 in the Health code, meaning “Exposure would cause irritation with only minor residual injury.”

Acetone ranks 3 in the Flammability code, which describes “Liquids and solids (including finely divided suspended solids) that can be ignited under almost all ambient temperature conditions.” Acetone ranks 0 in the Instability-Reactivity code, meaning that it is “Normally stable, even under fire exposure conditions, and is not reactive with water.” It is important, therefore, when preparing solutions for testing that the acetone is kept away from open flames, used in a well-ventilated area, and is not allowed to contact the skin, eyes, or mouth.

Acetone can be toxic when inhaled and therefore should only be used to create chlorophyll solutions in a well-ventilated area. It is also dangerous to ingest or drink, but only in large quantities since the body is naturally adept at breaking down large amounts of acetone. [HL.A] As such, the acetone used for the project will be labeled at all times and no drinks will be allowed in sample preparation areas. This will prevent cross-contamination of safe liquids with the unsafe acetone.



Figure 4. NFPA 704 diamond for acetone

Republished under public domain use.

There is also concern with the battery and power supply of the device. A battery which operates at too high voltage will heat up quite a lot and could either overheat the device, causing a burn on someone handling it, or the battery could simply explode. The power supply has a similar problem; if too much voltage is supplied to any one part of the device, that device may burn out, fail, and/or cause a fire. As such, it is important that the power supply be designed very carefully using the power constraints given in the data sheets of the chosen components.

The light source for the CFS is centered in the low visible, upper ultra-violet range. The eye cannot see ultraviolet light and thus cannot contract the pupil to protect the rods, cones, and retina from damage. It is therefore important that the light source is encased in the CFS such that stray light does not leak out and damage the eye. This is covered in greater detail in 3.1.2 Eye Safety, the subsection of 3.1 Standards.

3.2.6 Manufacturability

Manufacturability constraints are design constraints that limit our design based on the ease with which the design can be constructed or mass-produced. “Design for manufacturability”, or DFM, is a common engineering practice which requires the engineers designing a product design the products to maximize the ease with which those products can be manufactured. This engineering practice is necessary for commercial products to increase profit margins and reduce the possibility of quality issues arising due to a difficult to manufacture product.

For the CFS, the main manufacturability constraint which we will comply with is following Design for Manufacturability best practices for our PCB design. Designing a PCB with manufacturability in mind reduces the cost of our PCBs and will allow us to manufacture more copies of the PCB in a shorter amount of time. Having a short manufacture time for our PCB is important because it provides us with a quick turnaround time if we find an issue with our PCB during the testing phase and need to make changes to the PCB design and order a new one. The cheaper cost associated with a manufacturable PCB will allow us to order more copies of the PCB for use in prototyping and testing. An example of PCB design manufacturability best practice is to choose components that can be placed and soldered by machines in the factory, which cheaper, faster, and more precise than using components that must be soldered by hand.

While we will be following Design for Manufacturability constraints for our PCB design, we will not be constraining our general product assembly to manufacturability constraints. We have chosen not to complicate our design by requiring a chassis design that can be manufactured at scale due to the fact that all of the assembly for our project will be done by hand. In the event that the CFS transitions into a commercial product, a re-design would be necessary to allow for automated assembly and increased manufacturability.

3.2.7 Sustainability

Sustainability constraints are design constraints that limit our design based on the reliability and durability of the product over a long period of time. The lifespan of a device is an important aspect to potential customers, and it is important for us to constrain our design in such a way that we can ensure the longevity and durability of our product.

The main sustainability constraint for the CFS is that our design must be water-resistant. This is because our CFS may be used in many different environments and will likely be used around plants. Areas with plants are generally either outdoors or near sprinkler systems, both of which put the sensitive electronics on-board the device at risk of being water damaged.

Another constraint for this device is that the device must be secured in such a manner that small drops or impacts will not compromise the integrity of the chassis. This is important because the optical elements within the measurement device are extremely sensitive and could quickly become damaged beyond repair if the chassis of the device were to be opened.

3.2.8 Time Constraints

Time constraints will be one of the biggest challenges for our design team. We have two semesters to research, design, build, test, iterate, and present our device. During this time, we each have other obligations in our schedules and will be compelled to dedicate time to developing this project every week. Procrastination is an easy way for us to waste our time and end up with nothing to present at the end of Senior Design 2 and receive a failing grade. Another danger is feature creep.

The possibilities for our design are potentially endless and for that reason it is important that we limit the scope of our project early on. This way we will not have an ever-expanding list of features to add which becomes more than we can realistically produce in the 8 months that we are allowed to work on this project. Time constraints related to milestones and deadlines for this project are dictated by the senior design curriculum. By the end of the first semester, we should have our design completed and a prototype built.

At the end of Senior Design 2, our final project must be fully completed with all features as designed and ready to present. Having the printed circuit board designed as early as possible is going to be extremely important because it will require a couple weeks from the

time the board is ordered until it arrives, and we are able to test it in our device. If there are any errors or if the board needs to be redesigned or adjusted, it is important we have time to do that because the PCB is central to the design of the CFS. An exhaustive list of our deadlines is included in Table 1.

Table 1. Project deadlines

| Deadline Name | Due Date |
|---|----------------------|
| Divide and Conquer Project Document | September 20th, 2019 |
| Divide and Conquer Project Document v2 | October 4th, 2019 |
| 60-page Draft Senior I Design Document | November 1st, 2019 |
| 100-page Draft Senior Design I Document | November 15th, 2019 |
| Functioning Prototype with Microcontroller | November 30th, 2019 |
| Senior Design I Final Paper Deadline | December 2nd, 2019 |
| PCB Design Complete/Ordered | March 8th, 2020 |
| Final Project Complete | April 8th, 2020 |

4. Project Research

This section describes how the project will combine the design constraints and standards with the stated goals in order to meet the desired outcome. Hardware and software components are judged against the stated standards and comparisons are made.

4.1 Similar Products

Unsurprisingly, other companies understand the importance of chlorophyll fluorescence and have created products similar to the CFS. These products were observed by the design team and were used as starting points for the general idea of the CFS. The two main companies who have deployed chlorophyll fluorescence spectrometers in the past are NASA and Spectral Evolution.

NASA's CFIS (chlorophyll fluorescence imaging spectrometer) was built at the Jet Propulsion Laboratory (JPL). Its mission purpose is to monitor solar-induced fluorescence from the Orbiting Carbon Observatory-2 (OCO-2), specifically the O₂ A-band in the mid-700-800 nm waveband. Successful reports from the CFIS include showing that there are higher solar-induced fluorescence values in soy fields than there are in corn fields.

Another product is Spectral Evolution's SR-3500 full range UV/VIS/NIR field portable agricultural spectrometer. It is a handheld, wired device that is designed to test for nitrogen, phosphate, potassium, and chlorophyll content. The samples are excited with a 532 nm green laser and a full imaging system observes the spectrum from 350 to 2500 nm. The exact details of the internals of the device are not public knowledge, but it is expected that the imaging system is designed to be broadband. This contrasts with the CFS, which is designed to be shortband and is only focused on the fluorescence response found in exciting a chlorophyll sample at 430 nm.

4.2 Light Source

There are three possible processes that could occur when chlorophyll molecules absorb light energy: the energy could be used for photosynthesis to provide the plant with sustenance, the excess energy could dissipate as heat, or the plant could re-emit the light. This last process is known as chlorophyll fluorescence.

In general, fluorescence occurs when a material absorbs light of a certain wavelength and re-emits light at a longer wavelength than the original source. By studying and comparing the fluorescence emission spectrum of Chlorophyll *a* from various samples, it is possible to have a general understanding of the relative health of the samples.

Chlorophyll *a* fluoresces at a peak wavelength near 670nm when it has been excited by a light source emitting near 420nm. Figure 5 and Figure 6 each respectively display the absorption spectrum and the emission spectrum of Chlorophyll *a* samples in methanol. The

graphs of the spectra were created by Scott Prahl, PhD Professor at the Oregon Institute of Technology. Prahl obtained the data for the graphs from the PhotochemCAD package, version 2.1a which is a database containing the spectral information for various chemicals including Chlorophyll a. The absorption measurements were originally recorded by J. Li et al, Department of Chemistry at North Carolina State University, on December 11, 1997 using a Cary 3 and were later refined by J. Dixon et al from the same department in 2005. Similarly, the measurements for the emission of Chlorophyll a was obtained and refined by the same groups using a Spex FluoroMax.

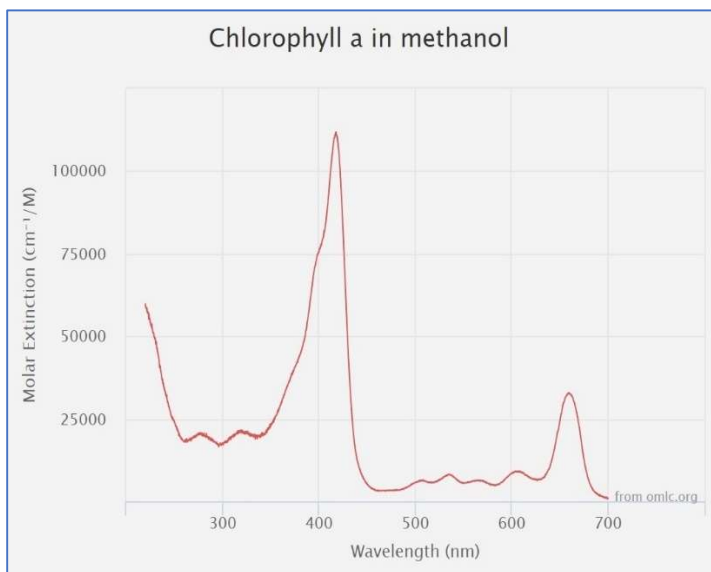


Figure 5. Absorption spectrum of Chlorophyll *a*
Reprinted with permission from Dr. Scott Prahl, OIT.

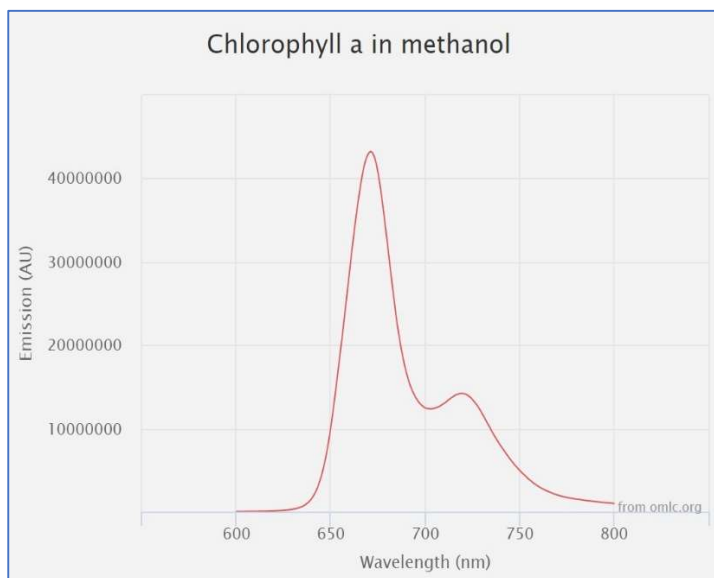


Figure 6. Emission Spectrum of Chlorophyll *a*
Reprinted with permission from Dr. Scott Prahl, OIT.

The light source needed for the CFS needs to have a small bandwidth with a high intensity around the 430nm wavelength. Common sources which fit these constraints and are cost-effective include a laser diode and an LED. These sources have various positive and negative characteristics. This section will discuss the differences in these characteristics and explain why a laser diode will be incorporated into the design of the CFS as opposed to the LED.

4.2.1 LED

A light-emitting diode (LED) is an active pn junction diode where the electron-hole pair (EHP) recombination results in the emission of a photon. An LED is usually made from a direct bandgap semiconductor in which the bandgap energy (E_g) is approximately equal to the energy of the emitted photon ($h\nu$) as displayed in Equation 1.

$$E_g \approx h\nu$$

Equation 1. Comparison of bandgap energy (E_g) to energy of a photon ($h\nu$)

The wavelength (λ) of the emitted light is directly related to the frequency (ν) by means of the speed of light constant (c) as displayed in Equation 2.

$$\lambda\nu = c$$

Equation 2. Relation between wavelength and frequency of a light wave

Injection luminescence is the means by which light is emitted as a result of EHP recombination. When a forward bias voltage (V) is applied, the built-in potential (V_0) decreases by V . This injects electrons from the n-side of the device into the p-side. As the electrons and holes recombine in the active region of the device, the photons are emitted in random directions known as spontaneous emission.

A direct recombination of electrons and holes results in the emission of photons because an electron has made a radiative transition from the foundation of the conduction band to the end of the valence band. This naturally occurs in direct bandgap semiconductors, but direct recombination can also occur in indirect bandgap semiconductors. The transition from the conduction band to the valence band in an indirect bandgap semiconductor usually generates a phonon or unit of heat.

However, there are some impurities which can be introduced into indirect semiconductors which enable radiative transitions resulting in photon emission. This allows for a wider variety of semiconductor materials to be used when designing or selecting an LED. The differences between the transition of an electron in a direct bandgap semiconductor and an indirect bandgap semiconductor are demonstrated in Figure 7.

An LED has a relatively narrow linewidth compared to a broadband source and can be centered around a peak wavelength. In order to fluoresce, the sample needs to receive efficient intensity from the light source. However, because the LED emits light in random directions, extra optics such as a focusing lens must be utilized to focus the emitted light onto the sample. This will increase the overall intensity of light the sample receives so it can properly fluoresce, but it also adds to the total cost of the project as optical lenses can be relatively expensive.

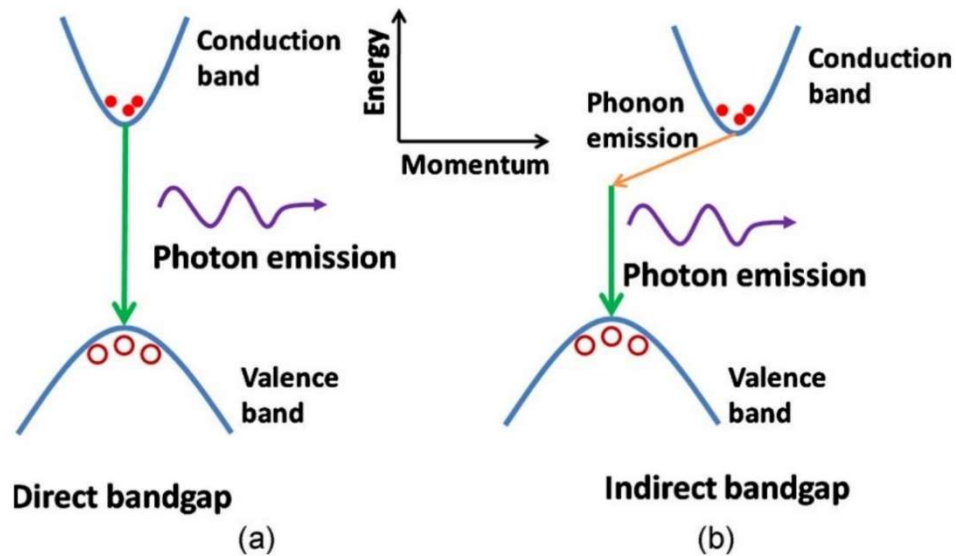


Figure 7. Electron transitions in direct and indirect bandgap semiconductors.
Reprinted with permission from Greg Sun, Professor of Physics, UMass Boston.

LEDs themselves are also cost effective due to their high external efficiency compared to traditional sources. They come in a variety of wavelength from UV-Infrared and many wavelengths are available for purchase. The wavelength of the LED should be centered near 420nm to properly match the peak of the Chlorophyll *a* absorption spectrum. It should be noted that Chlorophyll *a* also absorbs some wavelengths of red light.

A light source at a shorter wavelength was chosen instead of the longer wavelength because it there is a higher peak on the absorption spectrum at the shorter wavelength and the emitted light will be mostly red light. Therefore, the detector will more easily distinguish the excitation light of the source the further the wavelength is from the emitted light.

The LED was not chosen because compared to laser diodes, the light emitted from the LED has a lower intensity and is less tightly focused. While the LED may be less expensive on its own than the laser diode, the focusing optics which would be required in conjunction with the LED could easily make the device more expensive than it needs to be. Also, the broader spectrum of the LED is less appealing because we want our excitation source to be as monochromatic as possible, so we know we are exciting Chlorophyll *a* instead of other chemicals in the plants such as Chlorophyll *b* or Creatine.

4.2.2 Laser Diode

Lasers are available for purchase in many different forms with various dimensions and price tags associated with them. Gain mediums for lasers include liquids, gases, solid-state crystals, and semiconductors; however, all these lasers have similar properties. The light emitted from lasers has both spatial and temporal coherence. This means the emitted radiation will be highly monochromatic (has a narrow linewidth) and is also very directional. The laser being used for this CFS will be a semiconductor laser diode operating near a 420nm wavelength.

Lasing occurs when an environment allows for three processes to take place: photon absorption, spontaneous emission, and stimulated emission. These three processes are represented in Figure 8 by simple two-state energy diagrams where E_1 represents energy in the ground-state and E_2 represents the energy in the excited-state. Absorption occurs when a photon with energy $h\nu$ is introduced into the system. An electron in the ground-state can absorb this energy and transition to the excited-state.

However, electrons in the excited-state do not last there very long and eventually release the energy as a photon in a process called spontaneous emission, which was discussed in the previous section on LEDs. The light emitted from spontaneous emission appears as a narrowband gaussian output and is both isotropic and randomly polarized.

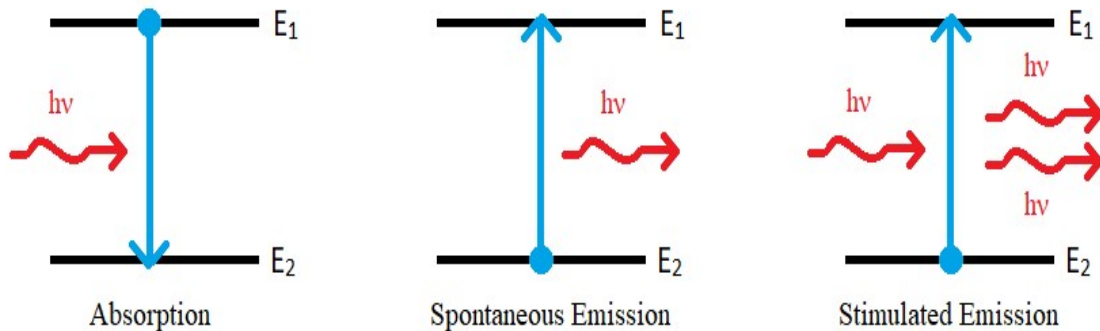


Figure 8. Energy diagrams of absorption, spontaneous emission, and stimulated emission.
Made by Robert Bernson.

After an electron has transitioned to the excited-state E_2 , it is also possible for an incident photon to induce the electron's transition back to the ground-state E_1 . The electron releases its energy as a photon in phase with the incident photon and with the same wavelength. This is the key process known as stimulated emission. When the semiconductor is at thermal equilibrium, there is a relatively small density of electrons in the excited-state so it is very unlikely for stimulated emission to occur and if it does occur the emission can be considered negligible.

In a semiconductor laser diode, the radiation needed to begin the optical transitions between the excited-state and ground-state is produced inside a Fabry-Perot resonator cavity such as the one seen in Figure 9. The length, width, and thickness of the cavity are referred to as its longitudinal, lateral, and transverse dimensions. A Fabry-Perot resonator cavity in a semiconductor is made by making two parallel clefts along natural cleavage planes in the longitudinal direction. These clefts act as partially reflecting mirror facets which allow for strong optical feedback in the longitudinal direction.

The feedback allows for light with wavelengths that are integer multiples of the cavity length to resonant within and be emitted from the cavity. Spontaneously emitted light at these wavelengths sees constructive interference and therefore gain; all other light sees destructive interference. This allows for a highly selective control for the radiation frequency of the laser. To ensure the emission from the laser is mainly in the longitudinal direction, the sides of the cavity are usually roughed. This limits the amount of light emitted in the lateral directions.

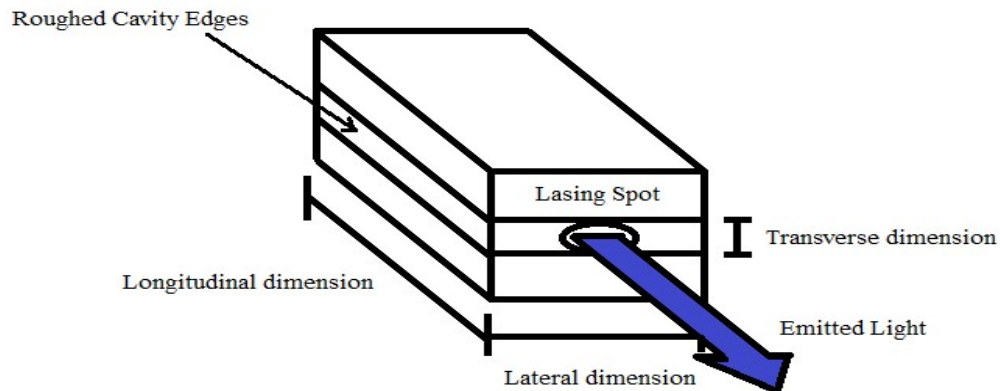


Figure 9. Fabry-Perot resonator cavity for a laser diode.
Made by Robert Bernson.

For lasing to occur, stimulated emission must exceed absorption, and this will only happen if there is a population inversion. It should be noted that population inversion does not occur naturally and therefore all lasers require a “pump” to ensure a higher density of electrons in the excited-state. For semiconductor laser diodes, the pump will simply be a connection to a power source which injects electrons into the diode near its contacts.

Laser diodes have some inherent disadvantages when compared to LEDs: they have a more complicated design, generally more expensive, and have a greater temperature dependence. However, regarding chlorophyll fluorescence spectroscopy, the advantages in using a laser diode over an LED outweigh the disadvantages. While LEDs have a narrow bandwidth when compared to traditional sources like a halogen bulb, the laser diode’s bandwidth is much narrower making the source more monochromatic than an LED.

The laser diode has a tighter beam and therefore smaller spot size than the LED, it will be easier to focus the laser onto the sample. The intensity of the focused light on the sample will also have a much greater intensity than the LED allowing the Chlorophyll *a* to yield higher fluorescence. The emitted light from the sample will also be tighter allowing it to be passed through the focusing optics and onto the detector more easily.

If we wished to measure the full emission spectrum based on various source wavelengths than an LED or a lamp would be more suitable for fluorescence spectroscopy, but since we only care about a single excitation wavelength and a narrow emission bandwidth, the monochromaticity of the laser diode makes it the most suitable light source for this CFS. Several different diodes were considered and are shown in Table 2.

Table 2. Laser diode comparison

| Laser Model | Manufacturer | Price | Peak λ | Power |
|-------------------|-----------------------|---------|----------------|-------|
| FVLD-415-45S-AR | Frankfurt Laser Co. | ~\$5000 | 415nm | 65mW |
| TG430 | RPMC | \$500 | 430nm | 50mW |
| LD2008 | Power Technology Inc. | \$6310 | 420nm | 120mW |
| MZH8340550D-AL01A | MZLASER | \$12 | 405nm | 50mW |

The laser module chosen for this product will be a CW 50mW laser with a 405nm center wavelength. This laser can be operated between -10°C and $+50^{\circ}\text{C}$ and stored between -40°C and $+80^{\circ}\text{C}$ with a wavelength drift of $0.25\text{nm}/^{\circ}\text{C}$. The beam size at a distance of 10 m is about 5×8 mm. It requires an operating voltage between 2.8-5.5V and an operating current $< 160\text{MA}$. The drive type is ACC and the service life is given to be over 8,000 hours. The casing for the module is made from Aluminum and is approximately 32mm in length with an 8mm diameter.

Although the absorption spectrum for Chlorophyll *a* has a peak near the 430nm wavelength, we decided on the 405nm wavelength due to cost. Most lasers centered at 430nm were very expensive ranging from \$500-\$5,000; however, lasers centered at 405nm are much less expensive and more readily available. The MZH8340550D-AL01A laser we ordered from MZLASER only cost \$12.00 per unit including shipping which is over a 97% decrease in price. A schematic of the laser and its dimensions can be seen in Figure 10.

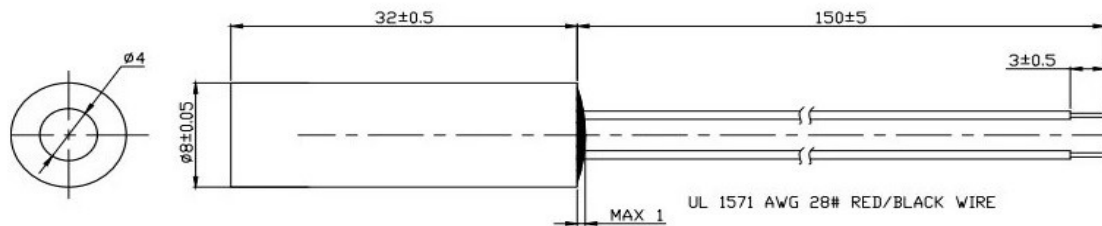


Figure 10. Schematic including dimensions for MZH8340550D-AL01A laser module.
Provided by Zhuhai MZLaser Technology Co. Ltd.

The main drawback to using the shorter wavelength is that we will have a lower intensity of emitted light. In order to ensure we still had enough light being emitted we created samples of Chlorophyll *a* diluted in Acetone until we reached an optical density <0.1. After our sample was deemed adequate, we placed it inside a Spectrofluorometer to see the emission spectrum of our sample based on different excitation wavelengths. We recorded our results and they are displayed in Figure 11.

From the following graph it can easily be seen that the 430nm excitation source provides the greatest amount of fluorescence intensity. The 420nm excitation wavelength shows about a 20% reduction in intensity, and the fluorescence intensity from the 405nm source has a very similar emission spectrum comparatively. In contrast, if the wavelength is increased to 440nm, there is a much more drastic reduction in peak fluorescence intensity by approximately 55%.

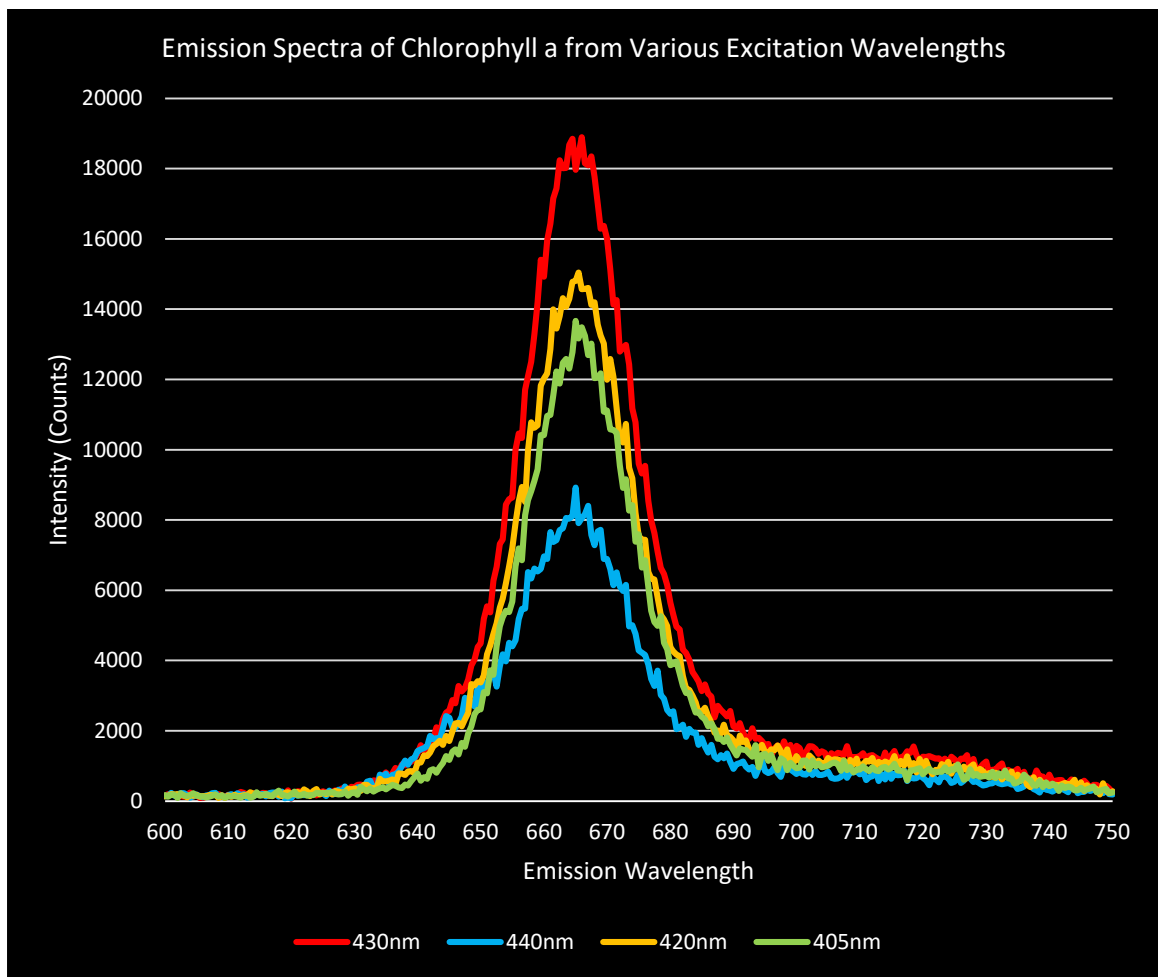


Figure 11. Measured emission spectra of Chlorophyll *a* in Acetone based on various excitation wavelengths from 405nm to 440nm.

The measurements were recorded by Samuel Knight and Robert Bernson on the spectrofluorometer at the College of Optics and Photonics at the University of Central Florida. The graph was reconstructed from the measurements by Robert Bernson.

These measurements make sense because they correspond to the absorption spectrum of Chlorophyll a seen previously in Figure 5. The peak of the absorption spectrum is at 430nm this excitation source can be expected to produce the greatest emission intensity. The 420nm and 405nm sources had similar absorption values, and both were slightly lower than the peak at 430nm. The absorption at 440nm was by far the lowest compared to the other sources so it should be expected to produce the least amount of fluorescence.

4.2.3 Cuvettes

The container holding the sample of Chlorophyll must also have the correct dimensions. If an LED were to be used, a lens would be utilized to focus the light emitted from the LED into a spot size which could illuminate as much of the sample as possible with a high enough intensity. However, we have decided to use a laser which simplifies this process. The beam from the laser should have enough intensity and focus without the use of a lens to make the sample inside the container fluoresce with a great enough intensity to be detected.

The use of the laser diode places fewer constraints on the kind of cuvette used in the CFS. Spectrophotometric cells come in different styles but there are three main categories: rectangular, cylindrical, and flow cells. Rectangular cells are the most basic and also the most common cuvette used in UV/VIS spectroscopy. Cylindrical cells are mainly used when the excitation source has a large circular beam and the volume of the sample is less important. Lastly, flow cells are used for which it is important to keep the samples constantly moving or flowing.

We are trying to incorporate the most basic design in our CFS to reduce costs and therefore will be using a screw top, micro rectangular cuvette which will have a volume between 1mm^3 and 6mm^3 . The spectrofluorometer which recorded the measurements held housing for cuvettes with a 1mm^2 base, but the cuvettes could have varying heights allowing for different volumes to be used if the base of the cuvette was the same. This idea could also be utilized in our design; however, a standard cuvette size could reduce the cost of the device and any replacement parts.

The material of the cuvette is also important. The fluorescing light needs to path through the cuvette as well so the material must have enough transmission for both the excitation wavelength and the emission spectrum. Most optical cuvettes sold are made of normal glass which is fine when analyzing the visible range especially near the infrared wavelengths. However, our laser excites the sample at 405nm which is near the UV range. In order to ensure the sample is excited with maximum intensity from the source we will be using a quartz cuvette which allows for adequate transmission between 300-800nm which completely cover the necessary range of wavelength to meet our design specifications.

We are currently borrowing a quartz cuvette from UCF as it is a very expensive piece of equipment. We are currently determining if we will order ourselves for the next phase of the design process.

4.2.4 Chlorophyll Sample Preparation

In order to obtain the measurements used to construct Figure 11, samples of chlorophyll *a* need to be obtained. Likewise, our device will make similar samples fluoresce and the preparation of these samples needs to be done in the same manner to ensure accuracy. The original samples can be used as a reference for a typical spectrum of Chlorophyll *a* which allows any new samples obtained to be compared to the reference. Also, if we compare the emission spectrum obtained with our device to the emission spectrum of the spectrofluorometer we can ensure our CFS is working properly.

In order to make our reference sample we followed a specific procedure:

1. Picked leaf from a *Tilia platyphyllos* plant (a healthy plant in Samuel Knight's yard)
2. The leaf was torn into smaller pieces and placed in a measuring cup
3. The cup was filled with 50mL of acetone
4. The pieces of leaf were grinded down inside the acetone
5. The solution was poured through a filter to remove the small pieces of leaf
6. The filtered solution contained a high concentration of extracted chlorophyll and had to be diluted further with acetone until it reached an optical density <0.1

Results of our sample preparation can be seen on Figure 12 below.



Figure 12. From left to right: Chlorophyll *a* sample diluted with 150mL (high concentration), Chlorophyll *a* sample after diluted until $OD < 0.1$, pure acetone.

The samples were prepared by Samuel Knight and the photograph taken by Robert Bernson

4.3 Optics

The optics in this device will be primarily utilized for the emitted light from the sample of Chlorophyll *a*. The light from the sample will pass through a vertical slit through a bandpass filter. The filter will serve only allow the excitation light through while blocking the shorter wavelengths from the excitation source. After passing through the filter the light will be projected onto a collimating lens which collects the light and transfers it onto a reflective diffraction grating or prism. The grating or prism will diffract the light so only the desired wavelengths reach the focusing lens. This lens then focuses the light onto the detector which passes the spectral information of the emitted light to a computer software program which can be interfaced by the user of the CFS. Optical components can be quite expensive, so it is necessary to research and plan which optics are required, and which are available within the project's economic constraints.

4.3.1 Filters

Optical filters are materials with frequency characteristics that can be engineered for specific needs. In fact, optical filters are completely defined by their frequency response and are used to allow only a specific range of frequencies to be transmitted through the filter. Shortpass, longpass, and bandpass filters are the most common types of optical filters.

The transmission of light through a of a longpass filter typically is 0 for a range of low wavelengths. After a threshold wavelength is surpassed, the gain spikes so the slope of the response drastically increases until it finally plateaus and remains near 0 for the rest of the range of wavelengths. This response means that the light transmitted through the filter will only be comprised of wavelengths greater than the threshold wavelength. An example of a longpass filter and its transmission based on wavelength can be seen in Figure 13.

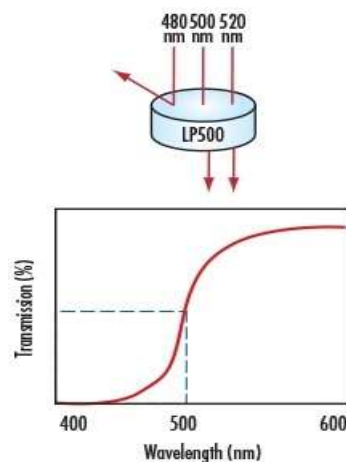


Figure 13. A longpass optical filter and its wavelength-dependent transmission curve.
Reprinted with permission from Edmund Optics.

A shortpass filter is basically the opposite of a long pass filter. The shortpass filter will transmit a range of wavelengths starting from 0 and up to a threshold wavelength. After the threshold wavelength is met, the gain drops so the slope of the response curve drastically decreases until the gain is fully diminished and the slope evens out again. This response means that the light transmitted through a shortpass filter will only be comprised of wavelengths less than the threshold wavelength. An example of a shortpass filter and its transmission based on wavelength can be seen in Figure 14.

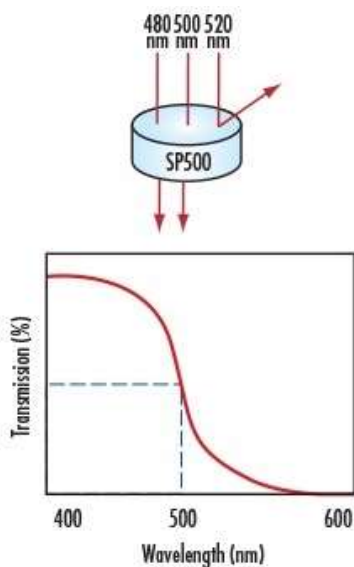


Figure 14. A shortpass optical filter and its wavelength-dependent transmission curve.
Reprinted with permission from Edmund Optics.

A bandpass filter allows the transmission of a certain range of wavelengths. Unlike the shortpass and the longpass filters which either have no lower limit or upper limit of wavelength, the bandpass filter has both. An example of an optical bandpass filter and its transmission based on wavelength can be seen in Figure 15. The bandpass filter is the most ideal choice for our CFS as we only wish to allow the transmission of the emitted light without any interference from the excitation source. An optical bandpass filter would allow us to target the specific range of wavelengths used for analysis and pass this light into the focusing lens of the device. This would reduce the amount of destructive interference from any amount of reflection inside the cavity of the device.

An optical longpass filter could also be used as the excitation source emits light at a shorter wavelength than the fluorescent light emitted by Chlorophyll *a*; however, there may be some excess light in longer wavelengths which would be unused by the CFS and possibly giving less overall accuracy. Filters can be very expensive pieces of equipment; further research is necessary before making the final selection between a bandpass filter or a highpass filter even though the bandpass filter is currently preferred.

We have currently decided to postpone ordering a filter to see if the device can function properly without one in order to reduce costs. If the fluorescence emission spectrum sees too much interference, then an appropriate filter will be ordered.

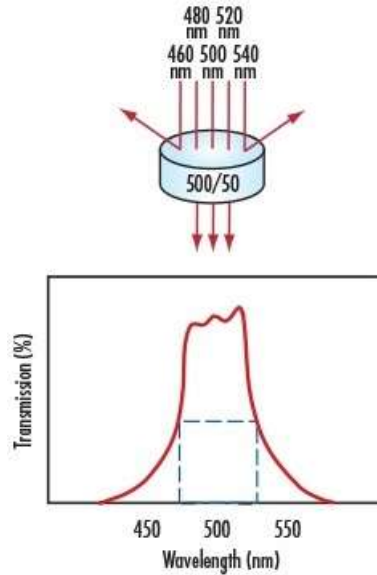


Figure 15. A bandpass optical filter and its wavelength-dependent transmission curve.
Reprinted with permission from Edmund Optics.

4.3.2 The Slit

Once the excitation source has interacted with the sample and fluorescence emission occurs, the light will exit the initial chamber through a narrow vertical slit. The width of the slit is an important factor when designing the resolution of the CFS. A larger width means more optical power which can reduce the amount of time required to obtain an accurate reading. However, the larger the slit, the narrower the resolvable bandwidth of the emission spectrum. There is a very wide width of range of possible slit widths to use ranging from $5\mu\text{m}$ up to $800\mu\text{m}$. For our design we are incorporating a $350\mu\text{m}$ slit width. This width was chosen from the ideal pinhole equation $d = 1.9\sqrt{t\lambda}$, where t is the distance from the slit to the image and λ is the wavelength of maximum transmittance (683nm for the CFS). As seen in 5.1.1 Optical Cavity Design, the collimating mirror is $t = 50\text{mm}$ from the slit.

The vertical size of the slit is less important as long as it is much larger than the slit width. Typical slit lengths range in between 1mm and 2mm with the typical length being 1mm . Our design will also incorporate a 1mm length slit. Our group has also started to research the possibility of using a slit with an adjustable width as we have seen in use on the CREOL spectrofluorometer when testing various samples. This would allow another degree of freedom for the user of the CFS.

4.3.2 Collecting & Focusing Optics

Lenses and mirrors are part of the hardware design of the system. They are tools which are picked while the system itself is being designed and require no intense or stringent research to be done except in the cases of F-# matching, effective focal length, and curvature. For

focusing, a concave mirror and a convex lens is used. For diverging, a convex mirror and a concave lens is used. The other characteristics such as focal length and diameter are all covered in the hardware design section 5.1.1 Optical Cavity Design. The collecting and focusing optics chosen for the project are itemized in Table 26. Bill of materials.

4.3.3 Monochromator

There are two possible monochromators that can be considered for the analysis of chlorophyll’s fluorescence spectrum: diffraction gratings and prisms. The chosen monochromator will need to be able to disperse the incoming optical signal to a resolution of at least 5 nm, a metric which this device shares with the sensor system. Both gratings and prisms will be briefly discussed, and a short comparison will be made between the two.

4.3.3.1 Prism

The prism is a solid piece of glass that directs light at a certain angle and splits it into its component wavelengths or frequencies. The good thing about a prism is that it can be cut to almost any dihedral angle and shape. This makes the deviation of light tunable from the manufacturing level, which simplifies the actual design process of the CFS. Since the deviation of light will be a known, “programmable” quantity, the rest of the system can be built around it almost arbitrarily.

A prism doesn’t have to be just an isosceles or right-angle triangle, either. There are many combinations of prisms that would fit into a spectrometer. For example, in Figure 16, the rightmost prism would work excellently with an incoming source at its left. This gets rid of a common problem with diffraction gratings—having to mechanically scan the grating to see an entire spectrum. With a prism or combination of prisms, the transmittable spectrum is shown without scanning or moving at all. It is entirely solid-state.

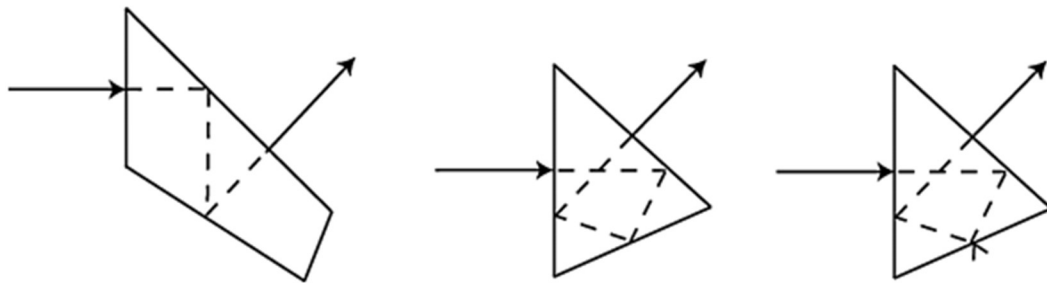


Figure 16. Example of deviating prisms.
Reprinted with permission from Dereniak [TgO.Dnk].

Deviating prisms take advantage of total internal reflection to capitalize on the fact that light can be displaced or deviated. Consider again the rightmost prism in Figure 16. The incident angle θ_1 is small enough such that its interaction at the second boundary—the left cleaved face—reflects the light completely back into the prism. The deviation is calculable

using Equation 3, where δ is the deviation, θ_1 is the incident angle, n_2 is the prism refractive index, n_1 is the refractive index of the medium the prism is in, and α is the dihedral angle between the principle plane and exit surface.

$$-\delta = \theta_1 + \sin^{-1} \left(\frac{n_2}{n_1} \sin \left(\alpha - \sin^{-1} \left(\frac{n_1 \sin \theta_1}{n_2} \right) \right) \right) - \alpha$$

Equation 3. Deviation angle for a prism

When the outermost inverse sine function is greater than or equal to 1, total internal reflection will occur. The deviation δ can be set to a desired angle relative to the incident light and the rest of Equation 3 can be used to solve for the missing unknowns. For example, the deviation in the rightmost prism of Figure 16 is 90 degrees, so $-\delta = -90^\circ$. The light incident at the rightmost prism's surface is 0 degrees, so $\theta_1 = 0$. Since $\sin \theta_1 = 0$, the innermost sine inverse term also becomes 0. Assume the prism is in air, so $n_1 = 1$. This leads to the reduced deviation formula $-90 = \sin^{-1}(n_2 \sin \alpha) - \alpha$ by plugging the known values into Equation 3.

From here, the values that can be manipulated for the designer are n_2 , which is the refractive index of the glass, and α , which is the dihedral angle of the prism's principle plane and the exit surface. Either one can be manipulated to the designer's specifications. The above formula is hard to solve analytically, but easily done with a graph.

The easiest solution for designers is to choose a known glass type with a known refractive index and design their prisms with a reduced formula like the one derived above. There will only be one unknown in the equation which makes it easy to solve.

For spectrometers, deviating prisms are atypical but not unused. A more common prism set-up for a spectrometer is a single dispersion prism, which is often nothing more than a piece of glass cut into an isosceles triangle. The same design requirements still apply, however, including deviation angle. The largest difference between the two prisms is that a dispersion prism aims to produce dispersion as a means of separating the spectrum of a light source. It is not uncommon for dispersion prisms to be used for other purposes, but their primary function, given their name, is to produce dispersive effects.

If a piece of glass has a great variation of effective refractive index, then it has great dispersion. Consider Figure 17. As light enters N-BK7 glass, it experiences a refractive index dependent on its wavelength. The refractive index of this glass varies from a peak at 1.55277 to a trough at 1.48602 across a 2300 nm waveband. This glass would therefore make great prism material, which is N-BK7's most common application.

The metric used to determine the effective dispersion of a prism is the *Abbe number*. It is a unitless number determined by Equation 4. *Abbe number* Equation 4 where n_d is the refractive index of the material at 587.6 nm (also called the "yellow index"), n_F is the refractive index of the material at 486.1 nm (also called the "blue index"), and n_C is the refractive index of the material at 656.3 nm (also called the "red index"). When the *Abbe number* is small, the prism is very dispersive. When the *Abbe number* is large, the prism

does not have a lot of dispersion.

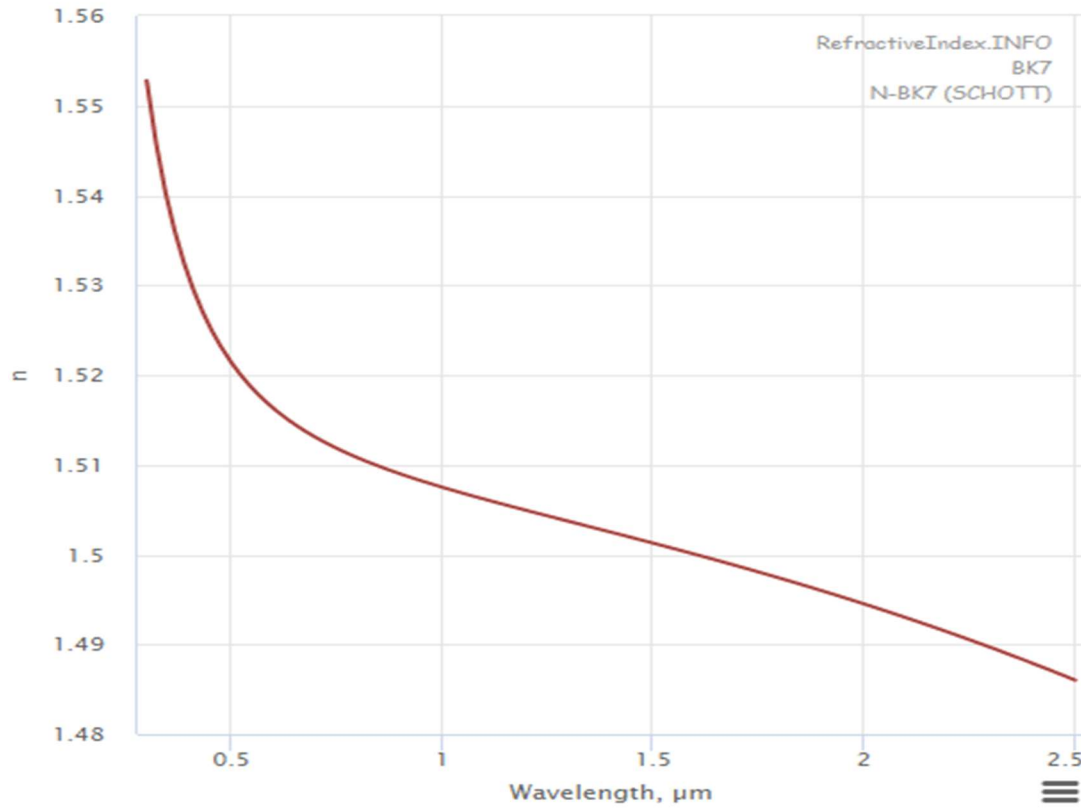


Figure 17. N-BK7 refractive index vs wavelength

Public domain via CC0 1.0.

$$V^{\#} = \frac{n_d - 1}{n_F - n_C}$$

Equation 4. Abbey number

When designing a spectrometer, it is important to pick a prism with a slightly smaller, but not miniscule, Abbey number. If the light is so dispersive that the angle at which it exists the prism cannot be collected by focusing optics or a sensor, then spectral information can be lost. Similarly, it is important to ensure the Abbey number does not become too large. If it is too large, the prism will not disperse the light effectively and some frequencies will overlap, leading to an incorrect spectrum.

Light which is totally internally reflected inside a prism experiences very little loss. Since refractive indices are complex numbers, there will be losses from the index. There will also be minor loss from back-reflection and propagation in the material, but those losses are negligible. Since the transmission of prisms is well over 95% for just about any material, reflection losses are ignorable. A prism's efficiency in splitting light makes it an incredible choice for the CFS.

When the light leaves the prism, it does not diffract in orders like it does with a diffraction grating. The light is merely separated into its spectral components and can be easily directed right to a sensor. This means that all refracted light is presented to the sensor; there is virtually no loss and the signal-to-noise ratio (SNR) is considerably higher than that of a diffraction grating.

However, there are some detracting considerations to be made when it comes to prisms. The primary factor is its design flexibility. As seen in Table 3, cost is not an issue, as the average dispersive prism costs about as much if not less than an average diffraction grating. The decision between prism and grating comes down to what design is finalized for the hardware and whether a grating or a prism fits that role better.

Table 3. Prism price comparison

| Prism Name | Manufacturer | Price | Peak Wavelength Range | Size |
|--------------|---------------------|-------|-----------------------|-------|
| BRAP19-AV | Newport Corporation | \$237 | 430 – 700 nm | 50 mm |
| BRAP13-AV | Newport Corporation | \$101 | 430 – 700 nm | 10 mm |
| F2 PS850 | ThorLabs | \$101 | 400 – 1250 nm | 15 mm |
| N-SF11 PS857 | ThorLabs | \$86 | 400 – 1400 nm | 15 mm |

4.3.3.2 Diffraction Grating

A diffraction grating is an optical component that splits light into its component frequencies. While this definition also fits a prism, the primary difference is how a diffraction grating splits the light as opposed to a prism. Diffraction gratings make use of the multi-slit configuration common in diffraction chapters of optics textbooks. The ruling or grating of a diffraction grating acts as a means of self-interference for incident light, causing light to interact with itself and diffract its spectrum appropriately.

Gratings are made by etching or ruling a piece of glass or reflective material in a periodic manner such that the light undergoes self-phase modulation. This type of grating is called “ruled.” Gratings can also be made using photolithography; these are called “holographic.” [TL.dfg] Traditionally, there are two types of diffraction gratings: reflective and transmissive. A reflective grating has a mirrored surface behind a reflective film that acts as a mirror in the geometric system. A transmissive grating allows light to pass through it and interact with its etchings, acting as a lens in the geometric system. [Hct]

The choice of what type of grating to use in a system comes down to the designer of an optical system. For some applications, a reflective grating is more useful, just as a lens is more useful than a mirror. For other applications, a transmissive grating is more useful, just as a mirror is more useful than a lens. It is important to remember that a grating diffracts light in orders, a notation marked with m in Equation 5 and Equation 6. Each order is more diffracted than the last, but also carries less intensity. For example, the 1st order diffraction from a transmissive grating is much more intense than the 13th order diffraction. Keeping orders in mind going forward will prove useful for quality analysis.

Generally, the equation for how strongly light diffracts from a diffraction grating is given by Equation 5. This equation works only for light at normal incidence and works for both reflective and transmissive gratings. When light enters a diffraction grating at an angle θ_i , the equation for its subsequent diffraction is given by Equation 6. In both equations, a is the diffraction grating groove or ruling spacing, m is the order number, λ is the wavelength of incident light, and θ_m is the light diffracted angle, signified by the order m in its subscript.

$$a \sin \theta_m = m\lambda$$

Equation 5. Diffraction angle for a grating with light at normal incidence

$$\sin \theta_m = \frac{m\lambda}{a} + \sin \theta_i$$

Equation 6. Diffraction angle for a grating with light inbound from non-normal angle θ_i

Equation 6 can be derived from Equation 5 by considering Young's double slit experiment. Additionally, Equation 5 can also be derived from Young's double slit experiment. Consider Figure 18. When light interferes with itself, it must diffract, and its diffraction will be at such an angle that it causes an optical path difference between two adjacent slits, which can be called two adjacent grooves for the grating example.

From Figure 18, it can be said that $r_1 > r_2$. The optical path length difference between them describes how strongly the light diffracts and is used to determine where the diffraction orders will fall after propagating some distance. This is a vital metric for choosing a proper diffraction grating. If the groove spacing a is too close to the peak wavelength λ , then there will hardly be any diffraction and wavelength separation will not be very large (since Equation 5 will basically become $\sin \theta_m = m$).

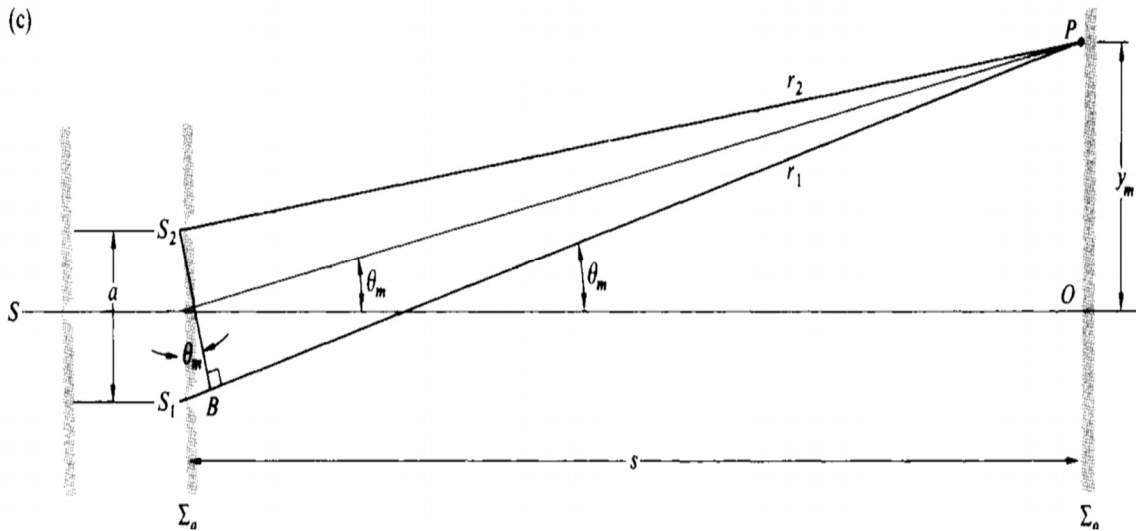


Figure 18. Young's double slit

Republished from [Hct].

So, by finding θ_m in Figure 18, the optical path length difference can be found. $\sin \theta_m = \frac{OPD}{a}$ since sine for a right triangle is the opposite angle leg divided by the hypotenuse leg. In this case, the opposite angle leg is the optical path difference. By rearranging, it is said that $OPD = a \sin \theta_m$. However, θ_m here is unknown. More information is needed.

According to the laws of constructive interference, the maxima for interference phenomenon occurs when $OPD = \frac{2\pi}{k} m$, or $OPD = m\lambda$. [Hct] Only the maxima are considered because the CFS will be built to observe the brightest light possible for maximizing SNR and minimizing losses from reflection, propagation, and dark noise. For any diffraction order m , therefore, m entire wavelengths should fit within the optical path difference. This can be stated as $a \sin \theta_m = m\lambda$, which is Equation 5. And, since there are now two optical path length formulas for the same situation, $OPD = OPD \Rightarrow a \sin \theta_m = m\lambda$, which again is just Equation 5.

Now, consider Figure 18 with light coming from an angle that is off the optical axis normal. If the light comes in from underneath the axis, the diffraction angle θ_m will increase to $+90^\circ$. Light that is angled going counterclockwise from the optical axis corresponds to a *positive* angle on the unit circle, so the change in angle must be positive. Add the positive angle. Conversely, if light comes in from above the optical axis normal, the diffraction angle θ_m will decrease to -90° . Light that is angled going clockwise from the optical axis corresponds to a *negative* angle on the unit circle, so the change in angle must be negative. To account for this, subtract the negative angle. Equation 6 is simply justified from here.

When designing the system, it is important to keep in mind the type of grating being used and why that grating should be selected over the other. Perhaps the most important thing to keep in mind is the blaze angle. The blaze angle is a property of a blazed diffraction grating which sets a maximum wavelength of efficiency for certain applications. Blazed diffraction gratings eliminate all but one selected diffraction order, including the zeroth order if it is not selected. These gratings seek to optimize grating efficiency, a metric given as $\eta = P/P_0$, where P is the diffracted power of light and P_0 is the incident power of light. Since gratings are not lossless devices, it is very important to have a high grating efficiency so that the system achieves maximum signal throughput.

The grating should be blazed at the angle of maximum efficiency for Chlorophyll *a*. To find this, use Equation 7 with the parameters $m = 1$ and $\lambda = 683\text{nm}$. m is the desired diffraction order, λ is the peak wavelength of incident light, and d is the line spacing of the diffraction grating (convertible from grooves per mm). Since d is typically a standardized number, this can be varied with those known quantities to produce a blaze angle that matches the m and λ values.

$$\theta_B = \sin^{-1} \frac{m\lambda}{2d}$$

Equation 7. Blazed grating equation

Typically, vendors will not list the blaze angle, but will instead list the wavelength of maximum efficiency. This, coupled with the grooves per mm, will narrow down the choices of diffraction gratings. Ideally, the CFS should use a diffraction grating that provides a significant angular dispersion without having such a large θ_m (Equation 6) that its diffractive order is impossible to calibrate with a focusing mirror. So, choosing a groove spacing that is close to the longest desired wavelength is not the ideal choice. Propagation of the light from the diffraction grating should spread the spectrum out a bit, preventing it from being so condensed that the sensor cannot differentiate between wavelengths.

There are a couple of known groove spacings: 300 gr/mm (3.33 μ m spacing), 600 gr/mm (1.66 μ m spacing), and 900 gr/mm (1111nm). Using Equation 6, light on the grating will diffract at the following angle: $\theta_m = \sin^{-1} \left(\frac{m\lambda}{a} + \sin \theta_i \right)$. Since only the first order of the grating is considered, $m = 1$. The wavelength of peak intensity for the CFS is $\lambda = 683 * 10^{-9}$ m. Now, consider a few groove spacings and their effect on the diffraction angle at various incidence angles θ_i in Table 4.

Table 4. Groove spacing vs incidence angle

| | 300 gr/mm | 600 gr/mm | 900 gr/mm |
|-----------------------------------|------------------|------------------|------------------|
| θ_m ($\theta_i = 15$) | 27.64° | 42.09° | 60.87° |
| θ_m ($\theta_i = 30$) | 44.84° | 65.70° | OoR* |
| θ_m ($\theta_i = 45$) | 65.81° | OoR | OoR |

*OoR = out of (calculable) range

While the incidence angle will affect how strongly the diffraction grating diffracts the light and at what angle, the groove spacing is what gives the incredible flexibility in diffraction angle. For the diffraction grating for the CFS, a groove spacing of 300 gr/mm is fine, but since the hardware can be designed so the diffraction grating can be at any angle, 600 gr/mm is also fine. 900 gr/mm diffracts strongly at the ideal wavelength and groove spacings in-between 600 and 900 are often custom-made and cost extra. Some considered diffraction gratings are shown in Table 5. The purchased grating is highlighted in green.

4.3.3.3 Monochromator Conclusions

According to Lightform Inc [LFI], a typical dispersion curve for a prism versus a diffraction grating can be seen in Figure 19. Included in that figure is a quantum efficiency curve for a Retiga-2000R CCD camera, but it has no significance to this project. According to Figure 19, prisms are generally more dispersive after 840 nm. This makes prisms ideal for separating out long wavelengths, but since the CFS is only concerned with the 600 nm to 700 nm bandwidth region, why bother considering prism?

As mentioned before, prisms are almost lossless solid-state devices with no diffraction orders and predictable angular dispersion. The lower dispersion for prisms, however, is considerable since the wavelengths in the 600 to 700 nm region will need to be dispersed enough that they are distinguishable from one another to a resolution of at least 5 nm. Table 5 displays a few gratings that have ideal groove spacing, physical size, and wavelength of closest maximum efficiency required for the CFS.

Table 5. Diffraction grating comparisons

| Name | Manufacturer | Grv/mm | Range | Max Efficiency | Size | Type | Price |
|-----------------|---------------------|--------|---------------|----------------|--------------|-------------------------|-------|
| 33009FL01-270R* | Newport Corporation | 300 | 300 – 1000 nm | 500 nm | 25 x 25 mm | Plane ruled, reflective | \$109 |
| 33066FL01-270R | Newport Corporation | 300 | 300 – 1000 nm | 500 nm | 12.5 x 25 mm | Plane ruled, reflective | \$89 |
| GR25-0305* | ThorLabs | 300 | 200 – 1100 nm | 500 nm | 25 x 25 mm | Plane ruled, reflective | \$117 |
| GR25-0605* | ThorLabs | 600 | 250 – 1300 nm | 500 nm | 25 x 25 mm | Plane ruled, reflective | \$117 |

*Different size available for lower cost.

However, of the two issues given above, lower than average resolution is by far the more acceptable choice. A system that cannot observe an incident signal due to internal power losses is useless, so if the decision to choose a diffraction grating is made, then it is likely that the lowest diffraction order possible will be chosen to maximize power throughput. For prisms, the major issue is the amount of dispersion. The 600-700 nm waveband passing through the prism may not be dispersed enough to resolve accurately on the CCD. This was the primary concern which led to the team deciding to discard prisms for consideration.

Ultimately, a decision was made based on efficiency, dispersive properties, angular dispersion, what fits into the hardware design, and what piece of hardware is the lowest price for the most acceptable quality. After reviewing the pluses and minuses of both, it was decided that a diffraction grating best fits the needs of the CFS. A grating is more dispersive in the desired waveband, is easier to integrate into the planned optical system, and offers more flexibility in design than a prism. Newport’s 33066FL01-270R was chosen from 4.3.3.3 Monochromator Conclusions.

According to Lightform, Inc [LFI], a typical dispersion curve for a prism versus a diffraction grating can be seen in Figure 19. Included in that figure is a quantum efficiency curve for a Retiga-200R CCD camera, but it has no significance to this project. According to Figure 19, prisms are generally more dispersive after 840nm. This makes prisms ideal for separating out long wavelengths, but since the CFS is only concerned with the 600nm to 700nm bandwidth region, why bother considering prisms?

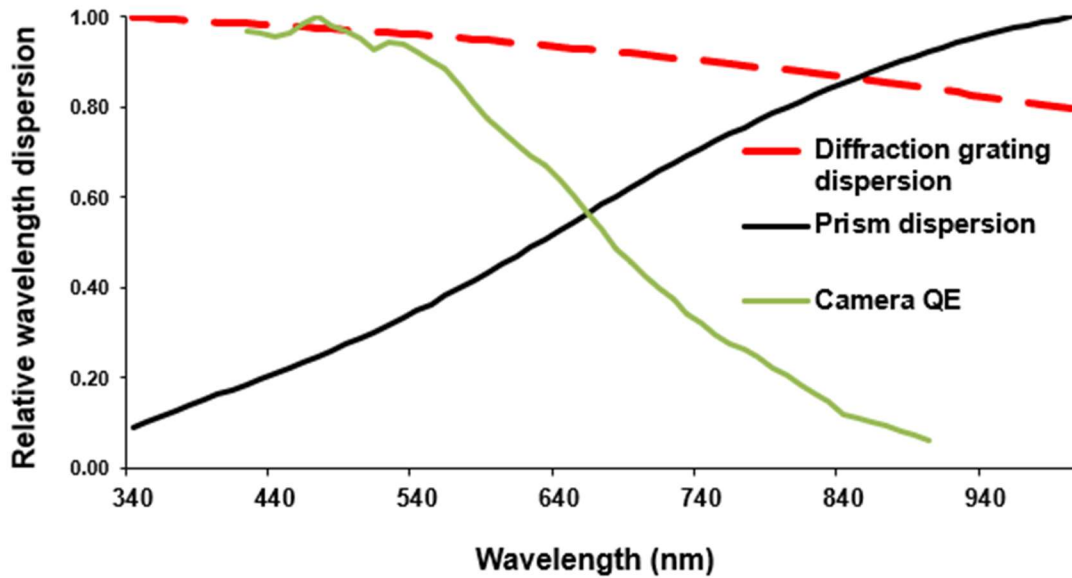


Figure 19. Dispersion comparison of a prism versus a diffraction grating

Republished with permission from Jeremy Lerner, LightForm, Inc.

Since the light from chlorophyll will be passing through a slit and will not diffract much in the vertical direction, there is no need to pay extra for the extra surface area. The horizontal area should be maximized without breaking the budget, hence the dimensions being 12.5 x 25 mm, which narrowed the choice to the 33066FL01-270R.

4.4 Sensor System

The sensor is arguably the most important optical device in a spectrometer. A sample can be illuminated, have its light transferred by collecting and focusing optics, and have its spectrum split up by a diffraction grating or prism, but if there is no system in place to analyze the incident light, the spectrometer is useless.

In this section, several sensors are analyzed for their effectiveness in the project. Some features examined are on-board ADC conversion, sensitivity, pixel pitch, supply voltage, and more. The primary metric used for choosing the sensor for the CFS is the sensor's ability to obtain 5 nm of resolution for an incident beam of light over the 600 to 700 nm waveband, a metric that this sensor shares with the dispersive optical element, or monochromator.

4.4.1 Linear Sensor Arrays

Sensors that only output analog signals are very common for linear arrays. A linear sensor may require an outside analog-to-digital converter (ADC) to convert the data from spectrometry into digital bits processable by computer programs. Many microcontrollers

and central processors have built-in ADCs in their hardware, making this design choice easy to implement, but comes with some costs, primarily issues with bit conversion since the data takes longer to transmit and convert, increasing the bit-error ratio.

Building an ADC is out of the scope of this project, so the ideal sensor should have a built-in ADC or be compatible with a microcontroller that has a built-in ADC. Therefore, it is imperative to put great consideration on linear array sensors with an on-board ADC. However, a sensor that does not have a built-in ADC is not automatically excluded from the project if its other metrics outperform other sensors in consideration.

4.4.1.1 AMS TSL1401CL

The TSL1401CL by Austria Mikro Systeme (AMS) is a linear sensor array with a sensitivity curve spanning 400nm to 1000nm with peak wavelength sensitivity around 780nm. The TSL class of sensor arrays offered by AMS consists of linear arrays, light-to-frequency converters, ambient light sensors, and proximity detectors.

In the specialty class of linear arrays, AMS offers only three product choices. The TSL1401CL was chosen for review for its low cost per unit, short length, and low supply voltage. The TSL1401CL matches three of the seven engineering requirement specifications for the CFS—cost, dimensions, and power delivery. This sensor is also RoHS compliant.

4.4.1.2 AMS TSL3301CL

The TSL3301CL by Austria Mikro Systeme (AMS) is a linear sensor array with a sensitivity curve spanning approximately 300nm to 1100nm with a normalized peak wavelength of 660nm. The TSL3301CL was chosen for review for its good rise time, low dark noise, high clock frequency, and on-board ADC converter. Additionally, due to its low cost per unit, short length, and low supply voltage, the TSL3301CL matches three of the seven engineering requirement specifications for the CFS—cost, dimensions, and power delivery. This sensor is also RoHS compliant.

4.4.1.3 Melexis MLX75306 3rd Generation

The MLX75306 3rd Generation linear sensory array by Melexis is the third linear sensor array that is being considered for observing the spectrum of the chlorophyll fluorescence. The sensor has an operating wavelength of 400 to 1000 nm. It has a peak wavelength sensitivity at 880nm, which is longer than the ideal sensitivity of 683 nm for chlorophyll fluorescence. The MLX75306 was chosen because it has an on-board ADC, a very small active length, low dark noise, and a small supply voltage. The device is also RoHS compliant.

4.4.2 Square CCD Sensors

Square sensors offer a few attractive advantages over their linear array counterparts. Square sensors are thoroughly documented, have a very large market which makes for a diverse variety of products to choose from, are easily integrable with common microcontrollers and processors, typically operate at low power, and offer more room for a margin of error in vertical dispersion smearing. For example, if a pixel's dimensions are 10-by-10 μm and the dispersed light has a real width of 1 mm, the pixel is losing over 30dB of information.

To retain all this information and boost signal strength, it would be better practice to have a large square sensor which can retain all the information from the dispersed light. From here, the back-end software of the system can vertically sum all the pixels to create a pseudo-linear array where there is very little signal loss from the pixels being too small. There, of course, will be some losses from the pixel pitch being a non-zero number, but that is the nature of every marketed sensor. It is an un-mitigatable characteristic if the designer wants to use pixel arrays to solve a problem.

Square sensor arrays are typically not used in commercial spectrometers. Those devices use linear arrays which have been carefully engineered to match the full waveband of a fan of incident light. Ideally, the CFS would mimic the exact design of a commercial spectrometer, including the linear array, but as research was done on the effectiveness of linear arrays in previous projects, it was learned that many groups struggled to implement the linear array into their own projects. Some of these projects were spectrometers operating in a very wide waveband, effecting the capability of their budget linear arrays to produce a spectrum. With this known pitfall in mind, research was conducted on square sensor arrays of interest and their metrics were compiled into the following sections for review by the designers.

4.4.2.1 Renesas ISL29147

The Renesas ISL29147 is a square sensor array with a peak spectral sensitivity at 575 nm. This sensor offers some very promising metrics that are attractive to the chlorophyll fluorescence spectrometer. It has a minimum supply voltage of 2.25 V and a maximum of 3.63 V. The device has a 12-bit resolution for its on-board ADC. It has a very low price per unit. Its minimum lux range is 56.25 lux, which puts it roughly in the area for sensing the low light of fluorescence. It has a dark noise coding error of 1 LSB and interfaces with I²C outputs. The device is approximately 2.04 x 4 mm in size, making it easy to fit into the device but a little challenging to image on to.

4.4.2.2 Texas Instruments OPT3002

The Texas Instruments OPT3002 (shown in Figure 20) is a low-cost, dynamic light-to-digital sensor with an effective wavelength range of 300 to 1000 nm. It has a peak sensitivity at 505 nm and varies between 60% to 80% quantum efficiency in the 600 to 700 nm waveband—the imaging waveband for the chlorophyll fluorescence spectrometer. It is

compatible with I²C and SMBus, can be operated in continuous or single-shot mode, and has a less than 1 μ W power consumption from a 1.8V power supply.

The OPT3002 has an automatic full-scale range setting that dynamically adapts the device's sensitivity to the lighting conditions that it encounters. This is particularly useful for the CFS since the ideal low-level light conditions inside the closed, dark optical cavity could vary during testing. The capability for a device to automatically adjust its sensitivity to the ambient light conditions means that the quality of any test runs without the chlorophyll fluorescence spectrometer closed and sealed will be just as valid as the quality of a run with a fully closed chlorophyll fluorescence spectrometer. The range is also completely adaptive—that is, the new range for each measurement is set according to the range recorded from the previous measurement. If the measurement is on the lower end of the full-scale capacity, then the device will automatically adjust the range so that the new measurement is scaled down one or two settings to account for the previous one.



Figure 20. OPT3002 picture by TI (insert)

The OPT3002 has a normalized response curve for incidence angle with a standard deviation of approximately 14%. Consider Figure 21. This response curve is very important with regards to the function of the OPT3002 in the device hardware. It could be the case that the hardware design will require the square sensor array to be set at an angle in order to satisfy the dimensions engineering requirement. If this is the case, then it is important to know how much signal will be lost by angling the device. It should be noted that the device doesn't post more than a 3dB loss of incoming light information until it has been angled almost 60 degrees with respect to the incoming light. As long as the engineering hardware design has been designed appropriately, particularly the optical cavity that houses the mirrors and monochromators, then there will be no need for the designers to consider how Figure 21 effects the power properties of the signal.

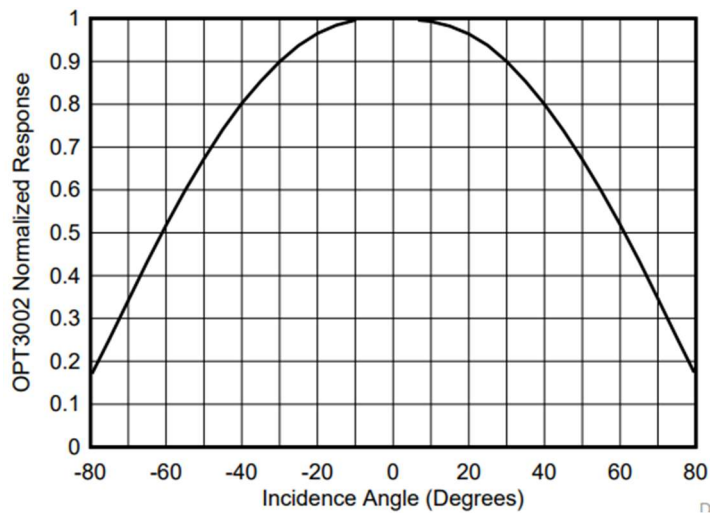


Figure 21. OPT3002 incidence angle vs normalized response curve

What is most impressive about the OPT3002 is the dark response of the device versus temperature. Until the device reaches operating temperatures of 100 degrees Celsius, the dark output response of the device never clears 7 nW/cm². In fact, for operating temperatures below 30 degrees Celsius, the dark output response of the OPT3002 is zero. This means that the average thermal noise that can be expected from this device is almost zero in every case, even normal outdoor operation in Florida during the summer.

The fastest rise-fall time for the OPT3002 is 40 ns. This is perfectly fast for a device that has the purpose of imaging the slow-to-fluoresce and slow-to-decay response of chlorophyll fluorescence. The device has a measured resolution of 1.2 nW/cm² at 505 nm, a metric which can comparatively be said to be excellent. The device doesn't need to be able to detect single photons, so any resolution remotely close to the above stated range is acceptable for the CFS's purpose. It should be noted that there is an infrared drop-off in efficiency beginning at 850 nm. Here, the efficiency is 20% of its peak at 505 nm.

The OPT3002 has a maximum operational supply voltage of 3.6 V. This is roughly typical of those found in the linear array category and can be considered meeting, but not exceeding, generally accepted specifications. Its power supply rejection ratio (PSRR) is roughly 0.1% per Volt. If the device is operated at 2 V, it rejects approximately 200µV, so the actual operating voltage of the device is between 2.0002 V and 1.9998 V.

The device has stock in three of the seven engineering requirement specifications—cost, dimensions, and power delivery—and meets them all. The cost per unit is less than \$3 and thus the device can be easily picked up by even the most miserly team. The device has a physical body size of 2.00 x 2.00 mm, which makes it easily integrable into the system. The one obvious issue for such a small active area will be compressing the light from the monochromator such that it fits on to the active area.

To solve this problem, simply choose a focusing mirror with a certain effective optical power such that the imaged beam width fits on to the sensor's active area. As mentioned previously, the OPT3002 requires very low operation power and has an operating power supply voltage that rivals or exceeds that of all the linear sensor arrays previously listed. This makes it an incredibly attractive choice for the project.

4.4.2.3 ON Semiconductor AR0130CS Series

The ON Semiconductor AR0130CS Series is a line of CMOS image sensors that come in monochromatic and RGB color scales. Depending on the exact model of the AR0130CS, the color scale may change. All sensors in the AR0130CS line shares the same electrical and optical characteristics, namely spectral efficiency, on-board ADC, supply voltage, and RoHS compliance. The main differences are pixel array dimensions, pixel size, and cost.

The primary sensor reviewed is the AR0130CSSC00SPBA0-DR, or ARDR for short, shown in Figure 22. The ARDR is a monochromatic CMOS image sensor with an active pixel array area of 4.86 x 3.66 mm². It comes with an on-board 12-bit ADC, peak spectral efficiency at 570nm, a required supply voltage of 1.8 or 2.8 V depending on the application,

automatic dark current and shot noise correction, and a responsivity of 6.5 V/lux-s. A monochromatic sensor was chosen for review since it makes the creation of an intensity profile easier. The idea with the ARDR sensor, as mentioned before, is to sum up the pixels vertically to produce a 1-D intensity profile. This will be used to create the spectrum of the fluorescing chlorophyll.

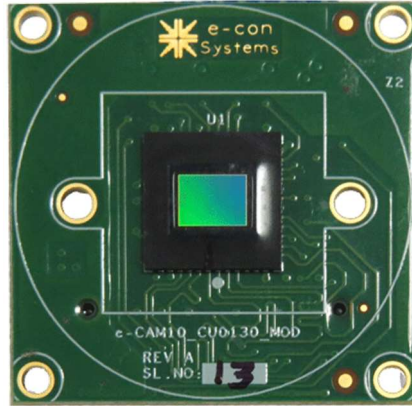


Figure 22. AR0130CS (ARDR) imaging sensor on a PCB

4.4.3 Sensor Comparisons

The biggest issue with comparing the sensors to each other is the non-standard responsivity metric. Each sensor's datasheet had its own metrics, reference source, units, and in many cases, the responsivity of the detector isn't even listed. Converting any or all of the responsivities to a single standard proved too difficult, so it was decided that the responsivity metric should not be considered when comparing the sensors to each other. Another issue that was considered was the physical size of the sensor. The sensor must not be so small that imaging the entrance slit of the device on to the sensor becomes a problem. If this becomes the case, the sensor will begin losing a lot of light information. For this reason, the physical size of the sensor was limited such that it could be no less than 2 mm in any dimension. The metrics for comparison are listed in Table 6.

To start, consider the TSL1401CL. Its small active length of 8.12 mm makes it ideal for integration into a system that seeks to meet the dimensions requirement. It also has low cost per unit at \$9.22, meeting the cost requirement, and does not require much voltage to power it at 3 to 5 Volts, meeting the power delivery requirement. The problem with the TSL1401CL is the lack of an ADC. This introduces a source of bit error which could propagate into the software and cause inaccurate readings at the output. The linear array is also a bit noisy, having 84 mV of inherent readout dark noise in the system. Regardless, the TSL1401CL was kept under consideration since it met the cost, power delivery, and dimensions requirements.

For the TSL3301CL, the datasheet did not show the sensitivity or responsivity. Compared to the TSL1401CL, this was a big detriment to the device. However, that detriment was quickly bolstered by the fact that the TSL3301CL has a built-in ADC. The cost per unit of the TSL3301CL is a little more than that of the TSL1401CL, but both are well within the budget of the project and are within a dollar's range of each other.

The TSL3301CL sensor is small enough at 8.64 mm active length that it easily meets the dimensions requirement of the CFS. The low voltage operation requirements of the sensor at 3 to 5 Volts make it attractive as well since it matches that of the TSL1401CL. The dark noise is incredibly low for this sensor: 0 to 2 least-significant bits root-mean squared. That low noise level can be easily accounted for in the software's error control and correction algorithms.

What really set the TSL3301CL apart from the TSL1401CL was the inclusion of a built-in ADC. Going forward, it was decided that every sensor should have a built-in ADC before being considered for inclusion in the project. For this reason, it was decided that the TSL3301 was simply the better sensor compared to the TSL1401CL, so the TSL1401CL was discarded from consideration for the project's sensor.

The MLX75306 meets three of the seven engineering specifications—cost, dimensions, and power delivery. The cost of this Melexis linear array is well within the budget at \$13.65 per unit. The MLX75306 is more expensive than the TSL3301CL, so to make up for the increase in cost, it must have metrics that the TSL3301CL does not share or cannot meet. The Melexis array is smaller than the TSL3301CL, satisfying the dimensions requirement. However, it is right on the specified threshold for sensor size at 7 mm, a metric which was carefully noted for the concern mentioned previously. The required voltage supply for the array is 3 to 3.3 V which, on average, is less than the TSL3301CL. This is a nice plus for the MLX75306 since the sensor is a device that should not be consuming much power in the system. Their bit depths and dark noise are the same. The MLX75306 has a reading for sensitivity, but the TSL3301CL does not.

So, what sets the MLX75306 apart from the TSL3301CL? The MLX75306 is smaller and requires less power. This meets two of the three engineering requirement specifications pertinent to the sensor: power delivery and dimension. The MLX75306 is a little more expensive and its spectral bandwidth is 100 nm shorter, but since the desired waveband is 600 to 700 nm, this shorter bandwidth doesn't matter. Its low power requirement was also attractive for operation, so the TSL3301CL was discarded in favor of the MLX75306.

After finally deciding on what felt like the perfect sensor, it was discovered that previous groups performing work with linear arrays suffered certain setbacks. Some groups were unable to complete any spectral analysis with a linear array due to timing problems and difficulty coupling on to the small area. Those groups defaulted to using photodiodes and power meters tuned to a known wavelength instead of observing the full spectrum of their samples.

After reviewing the linear arrays and consulting with faculty advisors, it was decided that the group should expand and review CMOS and CCD sensors before making a final decision. CCD and CMOS devices are compatible with any number of computing systems, are easily understood by most users, are well-documented, robust, and can be adapted to perform imaging work if necessary. This makes them attractive to the project. The first square sensor array to be reviewed was the Renesas ISL29147. The ISL29147 has the major plus of being a CMOS sensor in a decision matrix dominated by linear arrays. It has a low

supply voltage of 2.25 to 3.63 Volts, 12-bit ADC conversion, and its active area is approximately 9.6 mm², giving the sensor plenty of room to image a scene. It looked to be a good sensor capable of replacing the MLX75306.

However, while reviewing the sensor more closely, the spectral efficiency curve of Renesas's ISL29147 square sensor array has less than 10% quantum efficiency in the 650 to 700 nm waveband, the area where Chlorophyll *a* fluoresces the strongest. A drop of that size in quantum efficiency at that range is too poor for the CFS to consider. Reviewing the physical price of the device also brought up some concerns. Though the price per unit is slightly below \$2, the minimum purchasable quantity is 1000, meaning the team would have to spend over \$2000 just to get one device worth using, severely violating the cost engineering requirement. These reasons made the ISL29147 too unattractive for integration and it was discarded from consideration for the project's sensor. The OPT3002 by Texas Instruments was then considered for review.

As expressed in section 4.4.2.2 Texas Instruments OPT3002, the team was very excited about the TI OPT3002. It has low price of \$1.60 per unit, a single low-power operating supply voltage at 3.6 Volts, and a wide waveband from 200 to 1000 nm. It has slightly more variance in its dark noise at 0 to 3 LSB compared to the MLX75306, but it makes up for that with tremendous ADC bit depth at 23. Its main detriment is the small active area of 4 mm², a dimension which scrapes the boundary of the previously mentioned limiting size of a considered sensor. While it doesn't have a responsivity or sensitivity listed in its data sheet, the OPT3002 excels in so many categories that it was considered a no-brainer for the project. As such, the OPT3002 was purchased and marked as the sensor of choice for the CFS.

However, almost immediately after ordering the part, it was discovered that the TI OPT3002 is merely a power sensor; it cannot measure spectrum, defeating the purpose of the CFS. For this reason, the TI OPT3002 was discarded from the project and reserved as a back-up in case the new sensor failed to meet spec. The TI OPT3002 was relegated to testing for emitted power from chlorophyll fluorescence only, but its purchase was included in the budget as a test device. With all sensors in the CMOS and CCD category failing to meet spec and deadlines beginning to choke the testing phase of the project, the last sensor reviewed became the final one for the project. If ON Semiconductor's ARDR could not meet spec, then the project would revert to the MLX75306 linear array and choose that as the sensor of choice.

The price of the ARDR is \$8.38 per unit, which is cheaper than the MLX75306. The active area is 17.78 mm², which is plenty of space to image the chlorophyll spectrum. Its supply voltage can be 1.8 or 2.8 Volts, depending whether the device operates in I/O (either), digital (1.8 V), or analog mode (2.8 V); all of these are lower than MLX75306's lowest supply voltage. Its operating wavelength is 300 to 950 nm, which is shorter than MLX75306's, but it still covers the 600 to 700 nm waveband. The ARDR has an on-board ADC with a bit depth of 12 bits, exceeding that of MLX75306's 8 bits.

Table 6. Sensor Electro-Optic Specifications

| Specification | TSL1401CL | TSL3301CL | MLX75306 | ISL29147 | OPT3002 | ARDR |
|---------------------------|-----------------------|-----------------------|------------|--------------------|---------------------|------------------|
| Manufacturer | Austria Mikro Systeme | Austria Mikro Systeme | Melexis | Renesas | Texas Instruments | ON Semiconductor |
| Price per unit | \$9.22 | \$9.80 | \$13.65 | \$2 (min: 1000) | \$1.60 (min: 20) | \$8.38 |
| Active Area | 8.12 mm | 8.64 mm | 7.1 mm | 2.4 x 4 mm | 2 x 2 mm | 4.86 x 3.66 mm |
| Supply voltage (V) | 3 – 5 | 3 – 5 | 3 – 3.3 | 2.25 – 3.63 | 3.6 | 1.8 or 2.8 |
| Operating wavelength (nm) | 400 – 1000 | 300 – 1100 | 400 – 1000 | 475 – 650 | 200 – 1000 | 300 – 950 |
| Dark Noise | 84 mV | 0 – 2 LSB | 0 – 2 LSB | - | 0 – 3 LSB | - |
| ADC Depth (bits) | N/A | 8 | 8 | 8 or 12 | 23 | 12 |

*The notation “-” means a spec was not listed on any datasheet, website, or white paper.

The ARDR matches or excels in all areas when compared to the only remaining viable sensor, the MLX75306. The ARDR beats it in price per unit, active area, supply voltage, and ADC depth. The slightly smaller operating wavelength is not a major concern since the operating waveband is well-confined for both sensors. ARDR matches all the relevant engineering requirement standards in cost, dimensions, and power delivery. Moreover, it beats its best competitor in four of five metrics and has the plus of being a square CMOS sensor as opposed to a linear array. This made the device very attractive to the group at large.

4.4.4 Conclusion

The group ultimately chose ON Semiconductor’s ARDR for its monochromatic response, great power supply requirements, wide operating waveband, excellent responsivity, cost, effectiveness, and built-in ADC. The ADC in particular eliminates a lot of potential sources of bit error from occurring at the digital processing stage. Since the plan is to take the spectrum of the fluorescing chlorophyll source, the output of the pixels will be summed vertically to produce an intensity graph. What really set the ARDR apart from the other sensors was that it is simply an imaging pixel array with no lens. From the start of the project, this should have been the focus of sensor review instead of considering linear arrays and accidentally considering power meter devices.

The ARDR is also the only sensor that didn’t disappoint after further research was accomplished on it. It wasn’t listed as a challenge to overcome in other group’s projects like linear arrays, it didn’t turn out to be a power detector like the OPT3002, and it isn’t necessary to purchase the device in quantities of thousands from a foreign manufacturer like the Renesas ISL29147. The ARDR is everything the CFS needs for an image sensor and fits the role perfectly.

4.5 Electronics

Our electronics design includes our processor, memory, storage, sensors, light source, power supply, battery, charging circuit and wireless networking hardware. These will all be integrated onto a single printed circuit board. Integrating each of these components together will require a collaboration of photonics, electrical, and computer engineering. With further research, our design may also include a data and power transfer via USB cable.

4.5.1 Printed Circuit Board

A printed circuit board is the primary technique for connecting electronic components in an electronic device. A printed circuit board (PCB) is made using a substrate such as paper combined with resin, or fiberglass with copper traces to connect the components. A PCB can be made from one or more layers depending on the complexity of the system. Copper traces allow power and signal to propagate across the board, connecting systems together in order for the components to function as designed. The resistance of a copper trace is calculated by multiplying the resistivity which is a parameter of the material used multiplied by the length of the conductor and divided by the cross sectional area. A PCB can be populated by hand or for more complicated designs with a CNC machine called a pick and place machine.

For components with large enough contacts to solder by hand, a soldering iron is used. 805 and 603 size components are ideal for this project because they are large enough to be easy enough to solder by hand and small enough that they will not have a very large footprint on the printed circuit board. A soldering iron can produce high quality connections that provide a low resistance electrical connection as well as a strong structural joint. Surface mount components which are too small, delicate or complicated to solder by hand will require the use of a pick and place machine. Surface mount components are generally smaller than their through hole counterparts and so have seen increased use as devices tend to get smaller and more densely packed with electronics. Another advantage of surface mount technology is that components may be placed on both sides of the printed circuit board.

Smaller connections on surface mount components mean lower resistances and reactances which can produce noise and voltage attenuation. Drilling holes in the PCB is an expensive process, which makes through hole mounting of components more expensive. A pick and place machine is the fastest way to populate a PCB with components. Both techniques can be used on the same product with larger power diodes, op-amps and transistors still being installed as through hole components. A printed circuit board that is designed to be populated with surface mount parts will usually have solder pads which are flat contacts made of tin, lead-tin or copper.

Solder paste, which is a mixture of flux and solder particles, is applied to the contacts to be soldered. There are two ways that this can be done, either applied with a stencil or a CNC applicator which is similar to the operation of an inkjet printer. The components are then

placed in the correct orientation by the pick and place machine before the part is put in a solder reflow oven. It is the heat of the oven which causes the solder to melt, simultaneously soldering all of the components on the printed circuit board.

It is common practice to wash the printed circuit boards with a solvent after soldering to remove flux residue. There are vendors available which are capable of building a printed circuit board as well as populating the boards with surface mount components based on our designs. We will order 2 or 3 PCBs providing for the event that we fail in assembly. Having a PCB made for us should cost somewhere in the range of \$20-\$30. The lead time for producing a PCB varies from vendor to vendor and can vary from 2 weeks to 24 hours. Getting a printed circuit board made in a hurry has a higher cost than if you are willing to wait a little longer.

When soldering it is important that the device not exceed its maximum soldering temperature. This value can be found on the product datasheet and is different from the operating temperature. Exceeding the rated temperature while soldering can result in a device which no longer works or no longer works as intended. This can result in a cascading failure and damage other parts in the circuit, even if they were originally unaffected.

A printed circuit board provides electrical connections for data and power transmission as well as providing structural rigidity, keeping the components in a precise orientation. Since we are building a portable electronic device, it is important that it maintains structural integrity. The basic components mounted on printed circuit boards are resistors, inductors, capacitors, transistors, diodes, op-amps and integrated circuits built using networks of these components on a single silicon wafer using photolithography, often becoming very complicated. A printed circuit board will often be treated with a conformal coating after soldering.

The function of conformal coating is to protect sensitive electronics from dust, moisture, heat and corrosion and is particularly important in electronics which will be in service for a prolonged period of years. Conformal coating can be composed of acrylic, parlyene, silicone or urethane. There are multiple methods of application for conformal coating, being brushing, dipping or spraying.

4.5.2 PCB Design Software

There are several software tools available to aid in the design of embedded circuits. One such application is Kicad. Kicad is an open source free software platform distributed under a GPL v3+ license. Kicad allows for the design of complex electronic circuits and facilitates the conversion to a PCB layout. Kicad also has tools for creating bill of materials, gerber files, 3D views and component diagrams. Being built on C++, Kicad will run on essentially any modern computer architecture and operating system. The PCB design utility PCBNew allows for up to 32 layers and stores dimensions in nanometers as a 32-bit integer which allows for a PCB up to 2.14 meters which is far more than we require for this project.

Another Electronic Design Automation (EDA) software which we can use to design our PCB is Autodesk EAGLE. Autodesk EAGLE is a commercial engineering software sold on a subscription model. Autodesk EAGLE will run on Windows, Linux and Mac. Autodesk EAGLE consists of a schematic editor, a PCB layout editor, gerber file support and a graphical user interface for project management.

We have chosen to use Kicad because its free and open source nature makes it more accessible as well as it being easy to use. Since we already have some experience modelling using Kicad, there are fewer new skills needed in order to complete this project. Being available for free is an advantage over most commercial software for this purpose because it helps us keep the project's budget under the limit.

4.5.3 CPU

The Central Processing unit, or CPU is one of the most important components of an embedded device. The CPU is responsible for performing arithmetic, executing programs which include logic, interacting with memory, storage and managing inputs and outputs. Modern processors include a cache which is a faster form of memory that will store data from memory which gets used most often, in order to speed up processing. The CPU will generally be much faster than the memory which is in turn much faster than the storage.

Some processors are packaged as a “system on a chip” or SoC, this includes the system memory with the processor, integrated graphics hardware as well as some non-volatile secondary flash storage. An SoC design would simplify the design for this project by reducing the number of components which need to be included on our printed circuit board. The advantage of not using an SoC is that we can meet each of our requirements more precisely without including hardware that we will not need.

The important metrics of a processor are its frequency, architecture, core count, cache capacity and configuration, thermal design power (TDP), coprocessors included and features supported. Many modern processors include dedicated graphics hardware, floating point arithmetic units, analog to digital conversion, and audio/video codecs and encoding. ARM7 is a family of low power 32-bit RISC microprocessors released from 1993 to 2001. Intended for microcontroller use, these devices are no longer recommended for new integrated circuit designs. (p) A more modern approach would be to use an ARM Cortex-M processor. ARM Cortex-M is a family of microprocessors intended for microcontrollers and based on a 32-bit RISC architecture.

4.5.2 ARM7

The first processor that we researched for this project was the AT91SAM7SE512B. The reason this part was attractive was because it is affordable, and at 55 MHz 32 bit processor it should be more than powerful enough for our application. Other attractive features of this device are EBI/EMI implementation, I2C, SPI, four independent 16-bit PWM controllers, three 16-bit timers, an RTT, SSC, UART/USART and USB support.

This arm7 SoC also provides pulse width modulation which may be required for our light source. This is a surface mount device available in either a 128 or 144 pin package. There are 512 KB of flash storage which can be used to store our program and 32 KB of RAM which may be a limitation for our project, depending on what the user interface becomes.

The direction we are going for the user interface is to use an app which will allow a smartphone to pair with our device over Bluetooth and then doing most of the processing on the smartphone. This gives us the ability to use lower power hardware. The AT91SAM7SE512B operates with an input from 1.65 to 3.6 Volts and draws 80 mA peak power supply current, for a maximum power draw of 288 mW.

4.5.4 ARM Cortex-M

The ARM Cortex-M family of processors is designed to be a low cost, low power processor for microcontrollers. ARM Cortex-M processors are based on a 32-bit RISC ARM instruction set architecture (ISA). One ARM Cortex-M processor that we think is an excellent candidate for inclusion in our senior design project is the FS32K144, which can be purchased for \$5.00 manufactured by NXP USA Inc. The FS32K144 is powered by an ARM Cortex-M4F core running at 80 or 112 MHz depending on the configuration.

The FS32K144 comes equipped with an IEEE-754 single precision FPU for processing floating point data as well as a Cryptographic Services Engine which may be useful if encryption is required for the communications of this device. Cycle Redundancy Check (CRC) is also present on this chip for error detection to ensure our data is uncorrupted. The FS32K144 has an integrated digital signal processor (DSP) and 7 separate clocks. 5 power management states are available to allow this system to consume less power depending on which features, peripherals and processing power are currently needed.

2 MB of flash memory with error correcting memory (ECC) are available for program storage on the FS32K144. 2 12-bit analog to digital converters (ADC) are built in to this SoC. For communication protocols, the FS32K144 supports up to 3 modules connected over UART, 3 low power SPI modules, up to 2 low power I2C modules, a 10/100 Mbps ethernet with IEEE1588 (precision time protocol) support. The FS32K144 will accept voltage from 2.7-5.5 Volts and draw between 29.8 μ A and 61.3 mA depending on which features are currently enabled and in use. This provides a maximum power consumption of 337.17 mW.

Another important factor to consider for the cost of the project is the cost of a development board. While the FS32K144 would be a fitting product for use in the CFS and can be had for less than \$5.00 per piece, the development board that we would be using to prototype for this processor can not be had for less than \$65.00. The STM32F407VE is a 32-Bit ARM M-4 processor which can be acquired for \$4.41 or less and is more than powerful enough for our project and has the GPIO we will need for parallel communication with our sensor, UART capabilities for interfacing with our Bluetooth module. The development board which we will be needing in order to prototype with this processor is available for \$9.00 or less which removes a large burden that would otherwise strain our budget.

Below is Table 7, comparing processors by features supported and cost. Since each processor included has enough computing power by clockrate, that is not included in the table. Memory will be an important benchmark for the device we choose because it limits the resolution of data that we can process and send. Since we have decided to use an image sensor with a built in ADC to simplify our design, we are no longer considering ADC implementation in a processor. Because of the favorability of the STM32F407VE, we have chosen to include this processor into our project.

Table 7. Processor table of comparison

| Processor | Power Consumed | RAM | Component Cost | Development Board cost |
|----------------|----------------|----------|----------------|------------------------|
| AT91SAM7SE512B | 300 mW | 32 KB | \$10.00 | N/A |
| FS32K144 | 337.17 mW | 64 KB | \$5.00 | \$65.00 |
| STM32F407VE | 58.5 mW | 192+4 KB | \$4.41 | \$9.00 |

4.5.5 Power Delivery

To be useful, a power supply must be able to provide power at a constant specified voltage, regardless of the load and the power being drawn from it. Every design is going to have limitations and compromises, there will be a very slight drop in voltage as current being drawn increases, the number of components being used and the complexity of the power supply all need to be balanced.

There are two obvious approaches to powering an electronic device, we can use power from a 120 VAC outlet or we can use battery power. The advantage of powering the CFS with the plugin approach is that the device has a theoretically unlimited runtime and never needs to be charged. Disadvantages are that the device must always be plugged in and receiving power from the electrical grid in order to function. The advantage of using battery power is that the CFS will operate for a time even if the power grid is not functioning and allows the device to be portable and analyze samples in the field.

The utility of a portable chlorophyll fluorescence spectrometer is an attractive feature, for this reason we have elected to power our device with a battery. The output voltage needs to remain within an acceptable range even as the battery's voltage decreases with discharge. When the battery is discharged, the battery needs to be disconnected because being discharged completely is damaging to the battery.

In order for every component of our device to operate as designed, each must be supplied with the necessary power within the rated voltage, usually 3.3 or 5 Volts. When a battery is used to provide power for a device, the voltage is going to attenuate based on the charge level of the battery. Because electronic components are sensitive to fluctuations in voltage, our design must account for inconsistent sources.

There are various tools available to aid the electrical engineer in designing a power supply circuit. One such tool is Texas Instruments WEBENCH Power Designer. Webench is a web-based utility that will aid in design by providing a circuit based on input parameters which is tunable, including recommendations for components. Emphasis can be placed on optimizing cost, efficiency or footprint. Alternatively, a balanced approach can be used which will compromise between the three.

Webench supports designing for a DC or AC supply. For the CFS, we have decided to provide power from a lithium-ion cell. For this reason, we will develop our designs using the DC/DC Power Design environment. There are components designed just for regulating power at these voltages such as the 7805 linear regulator, typically packaged as a 3 pin component. The 7805 has an input voltage pin, a common (ground) pin as well as an output voltage pin. A boost converter or other form of switching regulator can be used to convert 3.7 DC Volts provided by a lithium ion battery to 5 Volts ("Boost Converter Operation".

LT1070 Design Manual, Carl Nelson & Jim Williams). The 7805 can provide up to 1.5 Amps at 5 Volts (7.5 Watts) as long as sufficient heat dissipation is allowed and the input voltage is in the range of 7 and 25 volts. This integrated circuit utilizes a network of transistors and resistors as shown in Figure 23 with voltage reference Zener diodes, switching to adjust the resistance in order to provide the correct voltage for a range of current being drawn.

Another approach to voltage regulation is a switching regulator. A switching regulator is a device which uses pulse width modulation to produce an output which is lower than its input. The output voltage is going to be equal to the magnitude of the peak output voltage multiplied by the duty cycle. The limitation of this technology is that the input must be higher than the desired output, or a different type regulator is required. An example of a discrete component used for a switching regulator is the LM2576 Step down voltage regulator.

This device is capable of delivering 3 Amps of power and can be adjustable. The LM 2576 comes as a 3.3, 5, 12, or 15 Volt regulator, as well as an adjustable version. The LM2576 offers fault protection built in as well as a fixed frequency oscillator. The advantage of an LM2576 over a linear regulator is higher efficiency. This translates into less power consumption as well as less heat production in our device. The efficiency of the switching regulator is highly dependent on the input voltage as well as the output voltage. The greater differential present between input and output voltage, the lower the efficiency of the switching regulator.

For the CFS, we will be required to increase the voltage from the 3.7 Volts of our lithium ion cell to the 5 Volts, 3.3 Volts and 4.6 Volts required by our electronics. In order to do this a boost converter can be used. A boost converter is a type of switching regulator which is used to produce a DC output which is greater than its DC input. The simplest boost converter that can be made contains a single transistor and diode, used with an energy storage component. The energy storage component can be a capacitor, an inductor or a combination of both.

The transistor can be a MOSFET or a bipolar junction transistor and operates as a switch, charging the energy storage device in the closed state and then discharging the energy storage device in series with the source voltage and the load when the switch is in the open position. As the device is rapidly switched on and off, the energy storage device does not fully discharge, and the supply current is sufficient to meet the demands of the load.

Using a capacitor in parallel with the load helps to maintain the required voltage across the load in both switching states. The higher the capacitance and the higher the equivalent load resistance, the lower the voltage ripple will be. The equation governing the discharge of a capacitor is $V = V_{Max} * e^{-t/RC}$ where V is the output voltage, V_{Max} is the peak voltage, t is the time in seconds, R is the load resistance measured in ohms, and C is the capacitance value of the capacitor in parallel with the load, measured in Farads.

There are commercially available boost-buck converters which can provide what we need for the power supply in this device, however by integrating this part onto our printed circuit board with the battery cell charging and voltage regulation circuit, we can reduce the volume of the device. By implementing every part of the power supply, charging circuit, battery, sensors, Bluetooth module, and light source we can include all the electronics on the device onto a single PCB.

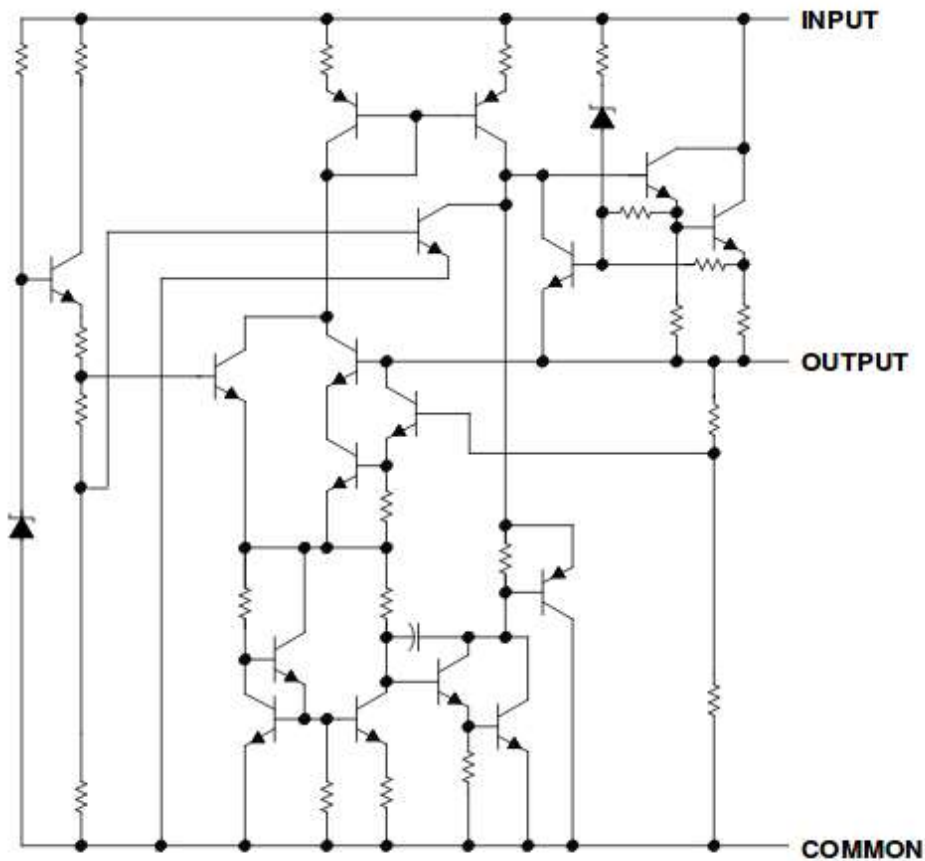


Figure 23. Internal Functioning of a 7805 linear regulator

The first step in designing a power supply for an electronic device is determining the power and voltages required. The total power required for our system is going to be the sum of the power required for each individual component, as shown in Table 8. Estimate of power consumption. Since we have not yet determined the components we will use with certainty, I will look at all the options we are currently considering for a single component and consider the power requirement that is larger. This does not account for all losses that will be present on the device, however it will function as a minimum value and rough estimate of the power that this device will need.

Sources of power loss can be found due to the internal resistance of the battery, and losses in the power supply itself, resistances in the printed circuit board, soldered connections and so on, all producing heat. However, not every component will be functioning continuously. The radio antenna will not always be activated, the processor has low power modes which will be used whenever the requirements for the processor allow, the light source and sensor will only be active when taking a measurement and not run continuously.

Table 8. Estimate of power consumption

| | |
|---------------------------------|--|
| CPU [STM32F407VET] | 1.95 V 30mA (Assuming 30MHz operation) |
| Laser Diode [MZH8340550D-AL01A] | 3.00 V 160 mA |
| CMOS Sensor [AR0130] | 1.8 V 82 mA + 2.8 V 40 mA |
| Bluetooth Module [RN4020] | 1.95 V 16 mA |
| Total | 829.3 mW |

Calculating the power draw for a component can be done when a datasheet lists nominal values for voltage and current. To do this we use Equation 8. For the MLX75306, the datasheet specifies 7 mA during operation. Multiplied by the power supply voltage of 3.3 V, this yields a power draw of 23.1 mW.

Similarly, for the TSL3301CL, 17 mA is specified in the data sheet for the supply current during operation. Multiplied by the power supply voltage of 5 V, this component will draw 85 mW of power during operation. The TSL1401CL draws 4.5 mA from the power supply at a nominal 5 V, consuming 22.5 mW. The TSL3301CL requires the most power, 85 mW maximum so we will use that figure for our design.

$$P(\text{Watts}) = I(\text{Amps}) \times V(\text{Volts})$$

Equation 8. Calculating Power from Current and Voltage

The FS32K144, which is an ARM Cortex-M processor which we are considering requires between 2.7-5.5 Volts and draws between 29.8 μ A and 61.3 mA depending on which features are currently enabled and in use as well as the clock frequency. This provides a maximum power consumption of 337.17 mW. The ARM7 processor we are looking at is the AT91SAM7SE512B which draws a peak of 80 mA at a maximum supply voltage of 3.6 Volts resulting in a maximum power consumption of 288 mW. Because the FS32K144 has a higher power consumption we will use this figure for our calculations.

The light source we are currently considering is the NDVA416T 45mW violet laser diode. Despite being a 45mW laser, the NDVA416T does not consume 45mW of electrical power. The actual power requirement will be higher due to losses. The NDVA416T draws 75 mA at 4.6 V, consuming 345mW.

The components which we will be using are the STM32F407VET ARM processor, the MZH8340550D-AL01A laser diode, the AR0130 CMOS sensor and the RN4020 Bluetooth module. The device will be powered with the Samsung 25R single cell lithium ion battery. For our battery charging circuit, we have decided to use the AP5056. Using TI Webench, 4 voltage regulation integrated circuits were found which would be most suitable for use in this project to meet these loads given the single cell lithium ion battery.

The 4 ICs we will be using are the TPS62231DRY, the TLV71328PDBV, the TPS62233DRY and the TPS799195. The TPS62231DRY was selected to provide 82 mA at 1.8 Volts which is required for the AR0130 CMOS sensor. The TLV71328PDBV was selected to provide the 40 mA at 2.8 Volts for the AR0130 sensor. The TPS62233DRY was selected to provide 160 mA at 3.0 Volts which is required for our MZH8340550D-AL01A laser diode. The TPS799195 was selected to provide 30 mA for the STM32F407VET ARM processor as well as 16 mA for our RN4020 Bluetooth module, each at 1.95 Volts.

4.5.6 Battery

The battery is an important component for any portable electronic device. Battery weight, capacity, maximum power output, and longevity must be taken into consideration. The choice of one of several competing battery technologies will have a large impact on the final form of the senior design project. A lead acid battery would be low cost and therefore helpful for keeping the budget as low as possible. However, lead acid batteries are heavier and have lower energy densities than some competing technologies, resulting in a more cumbersome final product.

A lithium battery has higher energy density and thus a lower weight for a given energy capacity and power capacity, however this comes at a higher cost. For this project, the weight savings absolutely justifies using a lithium battery to power our instrument. The capacity we require is enough to sustain the maximum power draw of our device for a continuous 6 hours of operation. To find the desired capacity of our battery, we use Equation 9 which tells us the relation between power and energy. Rearranging for energy, we get energy is equal to the maximum power draw multiplied by the duration of discharge.

$$P(\text{Watts}) = \frac{\text{Energy}(\text{Joules})}{\text{Time}(\text{Seconds})}$$

Equation 9. Calculating Power from Energy and Time

Computing Energy capacity for power equal to 0.83 Watts times 21,600 seconds which comes from our 6 hour battery life constraint results in a battery capacity of 17.9 kJ or 4.98 Wh which is equal to 1,350 mAh at 3.7 Volts. Another important operating parameter for a battery is the maximum current supplied. There are many batteries available which meet or exceed these requirements such as the Panasonic NCR 18650B which has a capacity of 3400 mAh, delivers 3.7 Volts and can supply up to 4.65 Amps.

The Panasonic battery can be found online for around \$5.00. An alternative would be the Samsung 25R which is also a 18650 size battery and operates at 3.6 Volts. The Samsung 25R has a capacity of 2500 mAh and can supply 20 Amps. The Samsung 25R is available online for around \$4.00. Both batteries meet our technical requirements and are low cost enough to not have a profound impact on our budget. Both of these batteries are compact enough that they can be soldered to our printed circuit board resulting in further space savings. When designing a circuit involving a lithium battery, special care must be taken not to damage the battery. We have decided to use the Samsung battery because it balances performance, cost and footprint favorably.

4.5.7 Battery Charging Circuit

If not designed correctly, a lithium battery can become very dangerous, getting hot and even catching fire. A lithium ion battery cell can safely be charged up to 4.1-4.2 Volts but never higher. A lithium ion battery cell can also not be discharged below 2.5 Volts and operating a battery at the extreme thresholds reduces the battery's service lifetime. A lithium ion battery will also have a maximum discharge current rating, and this is very important because a battery can fail destructively if this is exceeded. If the load current is too high then the battery should be isolated from the circuit. Dedicated integrated circuits exist specifically to ensure that lithium batteries operate safely and correctly. One such integrated circuit is the Texas Instruments bq2970 voltage and current protection integrated circuit for single cell lithium-ion and lithium-polymer batteries.

The bq2970 uses MOSFET transistors to remove the battery cell from the circuit when the charge parameters are no longer within the safe range. As shown in Figure 24, the transistor labelled CHG has a diode bridging the source with the drain. The effect of this is to shut off the charging if the voltage applied is too high, preventing the maximum charging current from being exceeded. The lithium cell can still be discharged even if the CHG circuit is disabled.

The DSG diode will shut off the DSG NMOS in exactly the same way if the voltage of the lithium ion cell becomes too low or if the discharge current is too high. The ion cell can still be charged even when the DSG circuit is disabled. Lithium cells can share a protection circuit if they are connected in parallel. The bq2970 is a very low cost component and can be purchased for \$0.55 per piece. The Hipera AP5056 battery charge management circuit is an 8 pin device that provides 1 Amp of charging current, has a 4.2 Volt charging voltage and a 2.9 Volt trickle charging threshold.

The Chipera AP5056 is a constant voltage and constant current linear battery charge management circuit. This 8 pin device provides 1 Amp of charging current, has a 4.2 Volt charging voltage and a 2.9 Volt trickle charging threshold. The AP5056 is designed specifically to incorporate charging via USB cable. If we decide to implement data transfer over USB as well, that would make this component a good candidate to charge the battery at the same time with the same cable.

The AP5056 is fully programmable, is capable of taking input from an NTC temperature sensor to open the circuit in the event that the battery gets too hot. Connecting the temperature input pin to ground will cause the management circuit to function normally without taking temperature into account. Ensuring the battery stays within a safe temperature range is important not only for prolonging the life of the battery but also for safety. A battery which gets too hot potentially becomes very dangerous.

Simplified Schematic

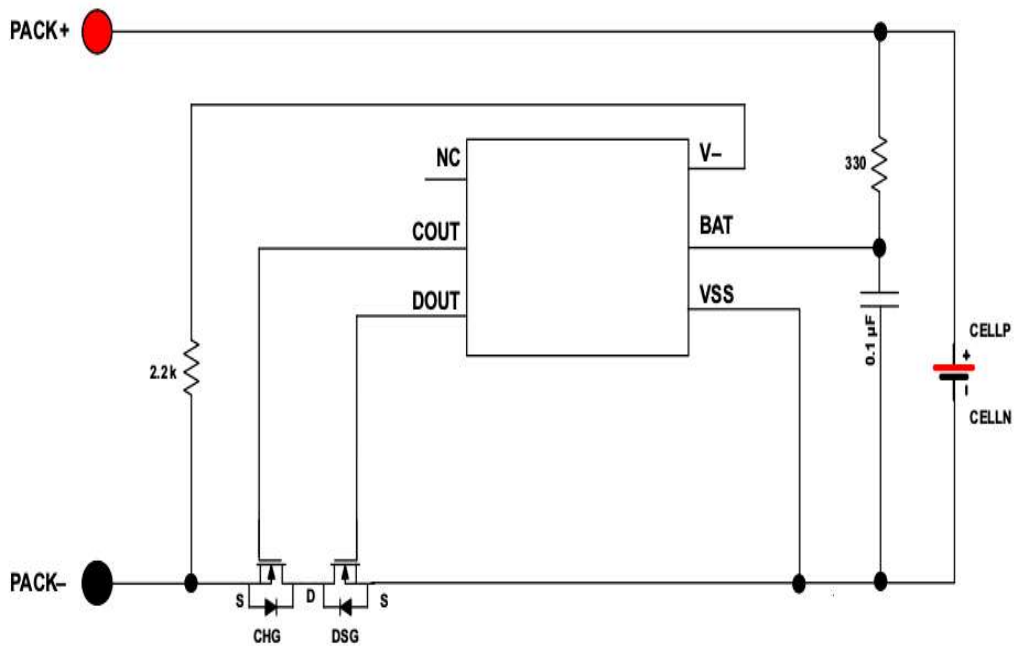


Figure 24. Simplified schematic for the bq2970

4.6 User Interface

The User Interface is a pivotal part of any product design, due to how deeply entangled the user interface and user experience are with the cost, ease of use, and durability of a product. When deciding how our customers will interact and experience our product, we considered both on-board and off-board interface methods and prioritized analyzing how each option would affect the usability and portability of our product. The level of complexity for each user interface method was also taken account throughout our analysis.

4.6.1 Smartphone Application (Wireless)

The advantage of using a wireless communication paired with a smartphone is that it reduces the amount of hardware required. A relatively cheap Bluetooth module would eliminate the need for SD storage or wired communication. The drawback to this approach is that it requires the user to have a smartphone and it requires us to write an app to interface with the device. Research on the wireless communication protocols and hardware modules considered for this user interface method are included in sections 4.7 and 4.8 of this paper.

4.6.2 Desktop Application (Wired)

It is possible to connect our device to a PC over USB. This could reduce the overall cost of product and be simpler to implement, but it has its disadvantages as well. The drawback to this approach is the device either becomes stationary (not portable at all) or requires the integration of storage for the data to be recorded. This would probably be implemented as a microSD card connected over I²C, or possibly SPI or UART.

4.6.3 On-Board Touch Screen

An onboard touch screen has the advantage of one device for both user input and data output. The touchscreen can be a simple and intuitive way to interact with electronics. The main drawback we saw with an on-board touch screen is that it would increase the price of our product and be a large single point of failure. If the on-board touch screen ever malfunctioned, the device would be rendered totally unusable and would require an expensive and possibly destructive repair process. This is a big drawback because large touch screens are commonly fragile and can crack easily or become water damaged; given that our device is likely to be used outdoors, on-board touchscreen malfunctions are something that we can expect to be common on our device if we were to go with this user interface method.

Furthermore, an on-board touch screen would greatly increase the power consumption of our device, which would complicate the design of our power source circuit and reduce the battery life of our device. Because of these reasons, we felt that an on-board touch screen was more of a hindrance to the overall usability of our product, and we have decided to not research it further.

4.6.4 On-Board Display with Mechanical Buttons

Due to the large amount of touchscreen-specific issues identified with the onboard touch screen user interface method that was researched, our team decided to research a physical screen with mechanical buttons as an alternative method of providing an onboard user interface. When compared to a large touch screen, this user interface has many benefits such as being less expensive to replace, and not being as susceptible to water damage.

Although it has some benefits, having an onboard screen with mechanical buttons still has some of the drawbacks that we found with the onboard touch screen option. The main drawbacks of this user interface method are increased power consumption, increased cost, and increased software development and hardware design complexity. Having all the processing done onboard the device would also require a much stronger microcontroller, raising the cost of the device even more. Due to these issues, our team decided to not have an onboard user interface method at all.

4.6.5 User Interface Comparison and Final Selection

After finishing initial research for possible user interface styles, the team decided that we would not be implementing any on-board user interface. This was due to the fact that an on-board user interface would increase the cost of our device and would increase the complexity of the chassis and software design. Although we had decided to stick to an off-board user interface early on in our research phase, we still needed to decide whether we would use wireless or wired communication between the off-board client device and our measurement device.

We want our device to be portable, so we opted to make mobile phones the main supported client for our device, which led us to choosing a wireless user interface as the main user interface method. We also plan on supporting wired communication for a wired off-board user interface; This interface will serve mainly as a backup user interface for debugging and in the case that the wireless communication is no longer working and will be designed with desktop and laptop computers in mind.

Table 9. User Interface Method Comparison

| User Interface | Cost | Notes |
|---------------------------|--------|--|
| On-board Touch Screen | High | Not chosen due to cost, durability, and implementation complexity |
| On-board Screen + Buttons | Medium | Not chosen due to cost and implementation complexity |
| Off-board – Wireless | Low | Will be used as main user interface method |
| Off-board – Wired | Low | Will be used as a backup user interface method, due to its reliability |

4.7 Wireless Communication

In this section, we analyze different wireless communication methods that may be used to provide a wireless off-board user interface for our product. Wireless communication will allow for a convenient way to transmit and receive data between the user and the device. When analyzing different wireless communication technologies, we took note of how each method affected the cost and ease of use of our product. Specifically, we compared the maximum range, device compatibility, latency, power consumption, data rate, and implementation complexity of each of the technologies.

4.7.1 Bluetooth Classic

The first wireless communication technology that was assessed was Bluetooth, which is a wireless communication technology designed for secure device-to-device communications, mainly geared towards devices that are near each other. In this section, we outline our research related specifically to Bluetooth Classic, which is a term referring to the classic operating mode of the current Bluetooth standard. A summary of our technical findings can be found in Table 10.

Table 10. Traditional Bluetooth Specifications

| Specification | Value | Notes/Pertinency |
|---------------------------|----------|---|
| Range | 30 m | Comparatively low, but sufficient for use in our product |
| Device Compatibility | High | Compatible with almost all mobile devices |
| Latency | ~100 ms | Comparatively high, but sufficient for use in our product. |
| Power Consumption | Low | |
| Data Rate | 2-3 Mbps | Comparatively high, more than enough the data our product will transfer |
| Implementation Complexity | Low | Easily available software libraries and sample code |

Bluetooth seems to excel in almost all the technical specifications that we were judging wireless communication standards by. The specifications in which Bluetooth stands out the most area power consumption, device compatibility, and implementation complexity. Bluetooth was designed primarily for low power consumption, which is necessary to provide our users with a product that can survive on battery power for a long enough time for them to perform many analyses.

Due to Bluetooth being the industry standard for short range low power device communication for the last few years, there is a large amount of resources available for the development of applications based on Bluetooth communication; this increased availability for development examples and research greatly reduces the implementation complexity for this protocol. The ubiquity of Bluetooth in industry today also increases the number of devices that will have Bluetooth modules built in, which increases the compatibility of our product with products that our customers may already own.

Although Bluetooth excelled in most of the categories researched, there were some worrying results. When compared to the other wireless technologies considered, Bluetooth had by far the greatest average latency; while latency is not the most important specification we will be taking into account, we still want to ensure that our customers can get their analysis data to their devices as quickly as possible to improve the user experience.

4.7.2 Bluetooth Low Energy

Since the release of Bluetooth 4.0 in 2010, Bluetooth has had two versions: Bluetooth Classic, and Bluetooth Low Energy. While researching Bluetooth Classic, we came across Bluetooth Low Energy and decided to research it as another possible wireless communication technology that we could use to send data between our device and the customer devices if we implemented an off-board user interface. A summary of our technical findings can be found in Table 11. Bluetooth Low Energy Specifications.

Bluetooth Low Energy shares many of the core features of Bluetooth Classic. Like Bluetooth Classic, Bluetooth Low Energy, or BLE, is a wireless communication technology designed for secure device-to-device communication at short ranges. While it shares many similarities to Bluetooth Classic, BLE is designed specifically for low power sensors and phone accessories which do not require continuous connection.

Bluetooth Low Energy has many of the same benefits as Bluetooth Classic regarding the specifications we were analyzing, and even has improved performance on some. BLE has much lower power consumption than Bluetooth Classic and all the other wireless communication technologies analyzed, usually anywhere from 1%-50% of the power consumption of Bluetooth Classic.

Table 11. Bluetooth Low Energy Specifications

| Specification | Value | Notes/Pertinency |
|---------------------------|----------|--|
| Range | 50 m | Comparatively medium range, more than enough for our product |
| Device Compatibility | Medium | Compatible with most mobile devices from the last 4 years |
| Latency | ~6 ms | Comparatively medium, sufficient for our product |
| Power Consumption | Very Low | 50% or less of Bluetooth Classic |
| Data Rate | 2 Mbps | Comparatively medium, sufficient for our product |
| Implementation Complexity | Low | Less software libraries and sample code than Bluetooth Classic, but similar implementation |

In addition to lower power consumption, BLE has a higher range than Bluetooth Classic, a similar maximum data rate, and even has greatly reduced latency, which was one of the main concerns we had with Bluetooth Classic. Although our findings were mostly positive, some concerns did arise throughout our research. The main drawback to using BLE would be the reduced compatibility, this is because BLE is not backwards compatible, so it requires the hardware Bluetooth module to support the Bluetooth Low Energy standard.

Since BLE is a newer standard, compared to Bluetooth Classic and some of the other technologies analyzed, less devices have Bluetooth modules which support BLE. This could cause issues for our customers, especially in the case that we only provide Bluetooth connectivity between the off-board user interface (application), and the actual product.

4.7.3 Wi-Fi

Wi-Fi is the common name for the set of standards defining wireless network communication. Our team briefly researched Wi-Fi to see if it would be a good fit for the wireless communication that may be required between our device and an off-board user interface device. A summary of our technical findings can be found in Table 12.

Table 12. Wi-Fi Specifications

| Specification | Value | Notes/Pertinency |
|---------------------------|---------|--|
| Range | 100 m | Comparatively high, more than enough for our product |
| Device Compatibility | High | Compatible with almost all mobile devices and laptop computers |
| Latency | 1.5 ms | Comparatively low, more than enough for our product |
| Power Consumption | High | Can use up to 40 times more power than Bluetooth Classic |
| Data Rate | ~1 Gbps | Comparatively very high, more than enough for our product |
| Implementation Complexity | High | Highly complex communication protocol to implement |

While Wi-Fi is widely used for wireless communication, our research led us to believe that it will not be a good fit for our project due to their being many drawbacks to this technology that greatly outweigh the few benefits it has. The main benefits of Wi-Fi include extremely fast data transfer speeds, especially compared with the other wireless communication technologies, as well as more range and lower latency.

These benefits are outweighed by the drawbacks which include much higher power usage than the other wireless communication technologies, and a much higher implementation complexity. For our project, range and data transfer speeds are not as important as power consumption and implementation complexity, so we have decided not to consider Wi-Fi communication as a final candidate for our wireless communication technology.

4.7.3 ZigBee Wireless Technology

ZigBee is a wireless technology developed to address the needs of low-power wireless Internet of Things networks which have become more common in the recent years. Our team briefly researched ZigBee to see if it would be a good fit for the wireless communication that may be required between our device and an off-board user interface device. A summary of our technical findings can be found in Table 13.

The main reason ZigBee was researched was due to the fact that ZigBee was designed with low-cost, low-power IoT networks in mind, but upon further research it was found that it would not be a good fit for our project because our product does not fully match the intended use-case of this communication technology. ZigBee excels at providing connectivity for networks of multiple interconnected sensors and devices, due to their custom “digiMesh” technology; digiMesh is allows for the implementation of mesh networks without single points of failures.

Table 13. ZigBee Specifications

| Specification | Value | Notes/Pertinency |
|---------------------------|----------|---|
| Range | ~300 m | Comparatively high, more than enough |
| Device Compatibility | Low | Not compatible with many mobile phones |
| Latency | 20 ms | Comparatively medium, meets standards |
| Power Consumption | Low | Similar power consumption to BLE |
| Data Rate | 250 Kbps | Comparatively low, but may be enough |
| Implementation Complexity | High | Not as many guides or software examples due to being a newer protocol |

Our product will not require a mesh network, given the fact that there will only be two products involved in the wireless communication at any given time, which would be the CFS and the customer’s mobile device or computer. Because we will be unable to take advantage of the digiMesh technology, ZigBee has little benefits over the other wireless technologies that were analyzed. On top of having few benefits, ZigBee also has some drawbacks such as lower compatibility, due to mobile phones commonly not having ZigBee compatible modules, higher implementation complexity due to our members not having experience with the ZigBee protocol, and a lower average data rate.

4.7.4 Wireless Communication Comparison and Final Selection

Throughout our research we found that, out of the wireless communication technologies analyzed, Bluetooth stood out due to its overall low power consumption, low implementation difficulty, and high device compatibility. This left us needing to decide between Bluetooth Low Energy and Bluetooth Classic; after analyzing the two communication technologies further, the team decided to choose Bluetooth Low Energy for this product.

The main deciding factor was the significant reduction in power consumption for Bluetooth Low Energy. Although Bluetooth Low Energy is compatible with slightly less devices, there are still enough mobile phones which support Bluetooth Low Energy to make it a viable choice. Table 14 below shows the comparisons between various wireless communication technologies which were researched and compared.

Table 14. Wireless Communication Comparison

| Technology | Power Consumption | Client Compatibility | Implementation Complexity |
|----------------------|--------------------------|-----------------------------|----------------------------------|
| Bluetooth Classic | Low | High | Low |
| Bluetooth Low Energy | Very Low | Medium | Medium |
| Wi-Fi | High | High | High |
| ZigBee | Very Low | Very Low | High |

4.8 Wired Communication

In this section, we analyze different wired communication methods that may be used in our product, both within our circuit for communication between sensors and the microcontroller, and between the product and an external user interface device. Choosing the right communication protocols for the communication within the circuit is essential to increasing the efficiency of the circuit and reducing the PCB design complexity. Wired communication technologies are also important because having wired communication as a method for an off-board user interface device to communicate with our measurement device will allow for a convenient way to transmit and receive data between the user and the measurement device.

To narrow our search, we only analyzed serial communication technologies for our project. Serial communication is any wired communication that transmits single bits at a time, as opposed to parallel communication technologies which send multiple bits at the same time. Parallel and serial technologies each have their benefits, but we felt that serial technologies best suited our project so that we could minimize the amount of wires to minimize the complexity of our PCB design.

When analyzing the different serial communication technologies, we took note of how each method could be leveraged in our project. Because of the many different places where wired communication can be used within our project, our research was more focused on finding the strengths of each technology and where it would best fit within our project, instead of trying to find a single communication technology that solved every problem. When analyzing the strengths and weaknesses of each technology, we took note of the use cases in which the technology is most commonly used, as well as the technology's latency, data-rate, overall compatibility, and cost.

4.8.1 UART

UART, or Universal Asynchronous Reception and Transmission, is a serial communication protocol. As seen in Figure 25, UART only requires the use of 3 wires for communication: Tx (transmit), Rx (receive), and Ground. Unlike SPI and I2C, the other serial communication protocols we researched, UART communication does not require a shared clock signal. This is because in UART communication both the receiver and the transmitter have their own clock signals that are synchronized based on the configuration of the device.

The fact that no shared clock is required makes UART a great option for transmitting data between two devices, which is why this is one of the common uses for the UART protocol. For this reason, we will be using the UART protocol to transmit data between our measurement device and an off-board user interface device, to provide for a wired communication alternative to our main wireless off-board user interface.

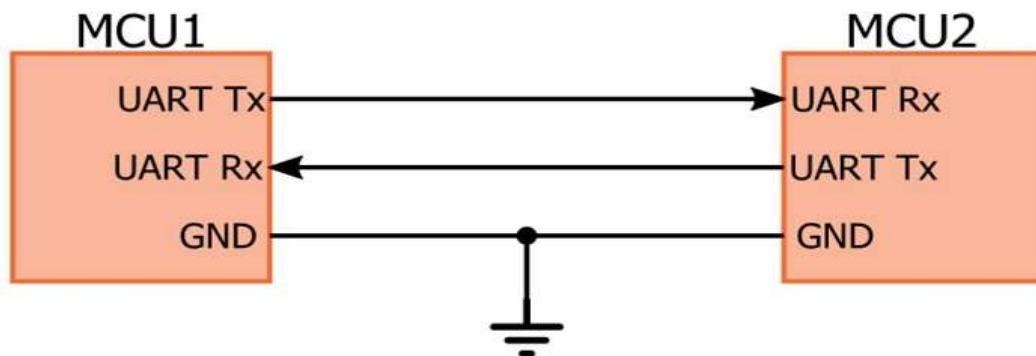


Figure 25. UART Device Configuration
Reprinted with permission from EETech Media, LLC [EET.UART].

We will be using UART over USB, also known as Serial over USB, for this communication. UART over USB was also chosen due to the experience that some of the team members had with the technology. Figure 26 shows an example of how the operating system of the user interface device could communicate with the measurement device via Serial over USB by using a Communication Class Driver.

4.8.2 I2C

I2C, or inter-integrated circuit, is a serial communication protocol which is designed specifically for microcontrollers. As seen in Figure 27, I2C only uses 2 wires for communication and uses a shared bus with master and slave devices, allowing you to connect up to 128 different devices to communicate with each other over the same set of busses. The two wires used in I2C communication are the SDA line (data), and the SCL line (clock). Like SPI, I2C is a synchronous communication protocol which is why a shared clock line is required between the devices.

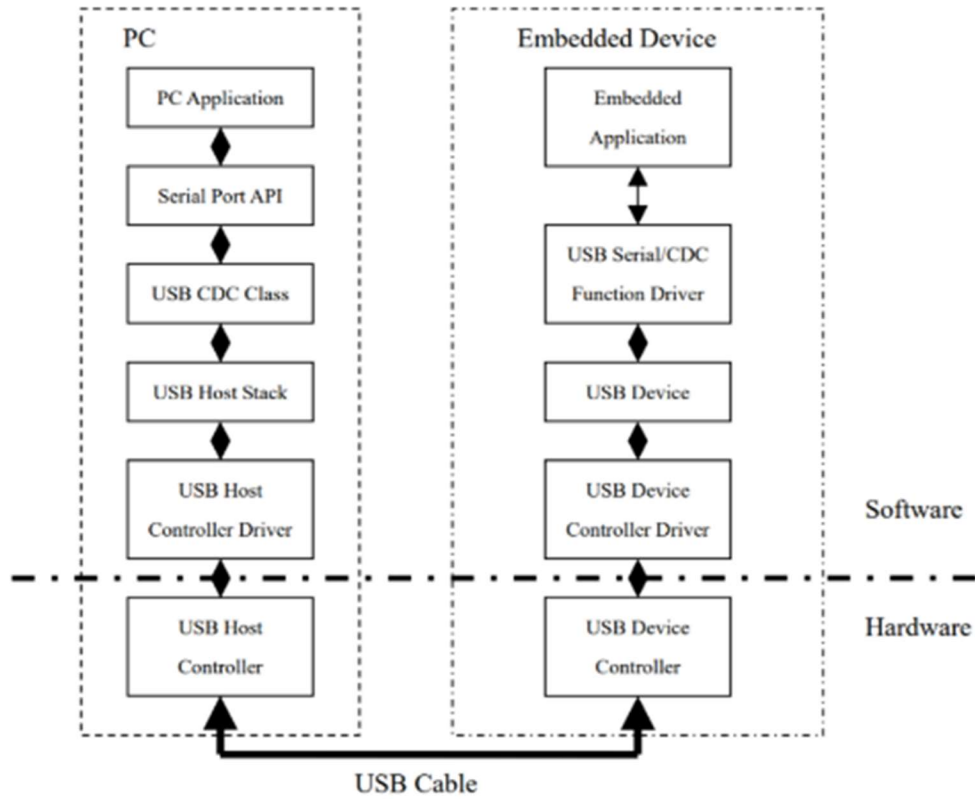


Figure 26. Serial over USB Communication

Reprinted with permission from Micro Digital [MD.WUUES].

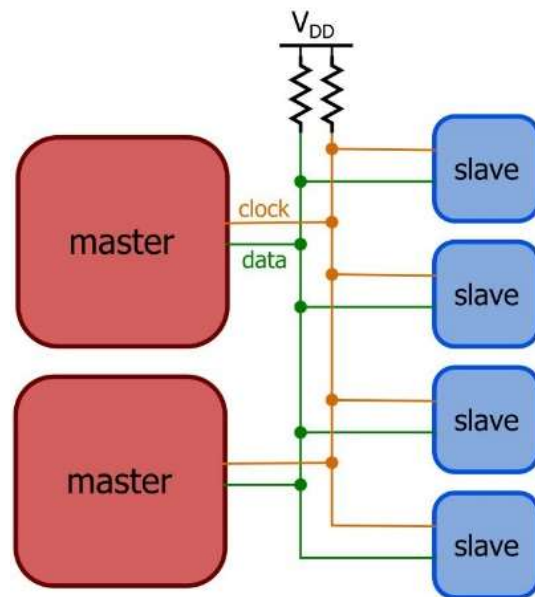


Figure 27. I2C Device Configuration

Reprinted with permission from EETech Media, LLC [EET.I2C].

The fact that there is only one data line means that I2C is only half-duplex, unlike UART which is full duplex, which means that when using I2C only one device can transmit data at a time on the I2C bus. To be able to handle that many devices on a single data line, I2C uses a master-slave architecture where there can be many masters and many slaves. In the master-slave architecture, the master devices get to control all reads and writes on the wire; this makes it so that I2C can use a bus topology while avoiding the chaos of having multiple devices trying to communicate at the same time.

One of the main benefits of I2C is the ability to maintain a low signal count even with many devices on the wire, due to the fact that it only requires 2 signals compared to SPI which requires more. Another big benefit of I2C is the option for multiple masters, but this benefit is not one that we would take advantage of, as we do not see a need for multiple masters in our design.

While the need for less signals and wires would simplify our PCB design, this benefit is countered by the need for pull-up resistors. These resistors consume space on the PCB and complicate the layout, as well as increase the power dissipation in our circuit. Another drawback to using I2C is that firmware development for I2C communication is usually more complex than UART or SPI. The largest drawback for I2C is that when compared to SPI, the speeds are much lower.

Even though I2C has many drawbacks when compared to SPI, it is very commonly used to configure sensors. This is the case with many of the Bluetooth and Camera sensors we have researched. While we may use SPI to transfer data between our sensors and our MCU, we will likely incorporate I2C into our design for the purpose of sensor configuration.

4.8.3 SPI

SPI, or Serial Peripheral Interface, is a serial communication protocol designed to allow multiple microcontrollers to communicate with each other, much like I2C. As seen in Figure 28 and Figure 29, SPI also uses a shared bus with a master and multiple slave devices, but SPI uses three main wires for communication: the CLK line (for the shared clock signal), the MOSI line (master output line), and the MISO line (master input line). In addition to the three main lines, SPI will also have one extra wire for each slave, used by the master for selecting which slave is being communicated with at a given time.

The shared clock signal means that SPI is a synchronous communication protocol, unlike UART. The fact that there is two data lines means that SPI is full duplex, unlike I2C which is only half-duplex, which means that when using SPI two devices can transmit data at a time. Even though SPI is full duplex, it still uses busses to support multiple devices on the same two data lines. To be able to handle that many devices on the shared lines, SPI uses a master-slave architecture where there can only be one master and many slaves. In the master-slave architecture, the master device gets to control all reads and writes on the wires; this makes it so that SPI can use a bus topology while avoiding the chaos of having multiple devices trying to communicate at the same time.

Master and slave devices can be configured in two possible ways: Multiple-Slave-Select configuration and Daisy-Chain configuration. Examples of both configurations can be found in the figures below. Multiple-Slave-Select configuration is the standard SPI configuration. Even though it requires more data lines than the daisy-chain configuration, after conducting our research we have decided that the Multiple-Slave-Select configuration is the configuration we will use when implementing SPI communication in our device due to the increased simplicity and greater sensor support.

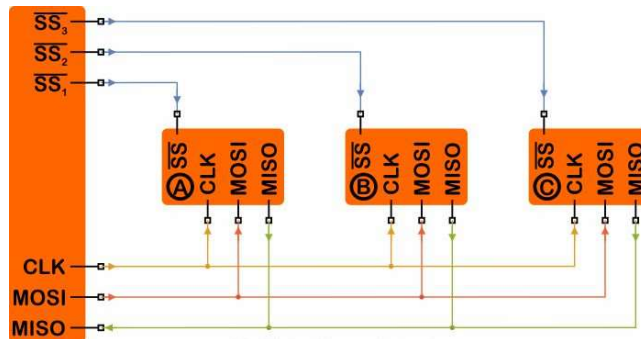


Figure 28. Multiple-Slave-Select SPI Configuration

Reprinted with permission from EETech Media, LLC [EET.SPI].

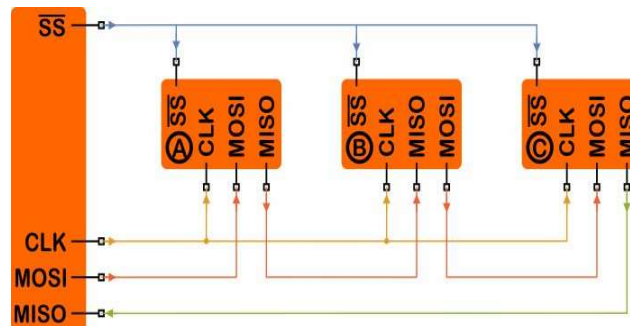


Figure 29. Daisy Chain SPI Configuration

Reprinted with permission from EETech Media, LLC [EET.SPI].

The main benefit of SPI is the data rate; SPI is known to be much faster than I2C on average. This is because the SPI protocol is much simpler which minimizes overhead and the fact that the protocol supports higher clock frequencies. The simplicity of the SPI protocol not only increases the data transfer rate, it also makes firmware development and low-level hardware design for SPI communication much easier.

The main drawback of using SPI is the higher pin-count due to the requirement for each slave to have a separate slave-select signal. SPI also only supports a maximum of four slave devices, which is much smaller than I2C's 128 possible slaves. This reduction in maximum slave amount reduces the number of sensors that you can connect to a single MCU using the SPI protocol. Another slight drawback to SPI is that there is no central SPI standard. Without a central standard, many sensors and devices have slightly different definitions of how SPI communication should be conducted. This increases the amount of research that has to be done when using parts that communicate of SPI.

Throughout our research we found that SPI is much less common than I2C, even though it has many benefits. A common use for SPI in circuits is for data transfers that require higher speeds, such as SD card readers, display modules, and camera modules. This has been the case with many of the SD card readers and camera modules we have researched, and we will implement SPI for use in these cases.

4.8.4 Wired Communication Comparison and Final Selections

Throughout our research we discovered that no wired communication technology is perfect, and that they are each best suited for very specific tasks. For this reason, we have chosen to implement all wired communication technologies that we researched, as they each meet a certain need that we have for our project. Table 15 below shows what we will be using each wired communication technology for.

Table 15. Wired Communication Technology Uses

| Wired Communication Technology | Use in Project |
|---------------------------------------|--|
| UART | Debugging, Wired User Interface |
| I2C | Component Configuration: Camera Sensor, Bluetooth Module |
| SPI | High-Speed Data Transfer: Flash Memory |

4.9 Bluetooth Module

In this section, we analyze different Bluetooth modules that may be used to provide our measurement device with the capabilities needed to communicate with a wireless off-board user interface device. Wireless communication will allow for a convenient way to transmit and receive data between the user and the device; these modules have been researched for use in the event that we choose Bluetooth or Bluetooth Low Energy as the wireless communication method for our off-board user interface.

When analyzing the different modules, we took note of how each method affected the cost, development complexity, and ease of use of our product. Specifically, we compared the maximum range, device compatibility, Bluetooth version, latency, power consumption, maximum data rate, size, and implementation complexity of each of the modules.

4.9.1 HC-05

The HC-05 Bluetooth module is a popular module amongst hobbyists due to its affordability and simplicity; you'll find this module in the majority of Bluetooth compatible beginner Arduino projects. Due to the ubiquity of this module, our team researched it to

see if it would be a good fit to provide our measurement device with the wireless communication capabilities that may be required between our device and an off-board user interface device. Table 16 contains a summary of the technical specifications of this device.

As mentioned previously, the main benefits of the HC-05 module are its affordability and low implementation complexity. HC-05 modules can be found online for less than \$10 per part, which would help us maintain a low cost for our device and offset some of the higher than expected costs of the optical equipment. The implementation complexity for this module is so low due to the fact that it is extremely popular amongst the hobbyist community. This means that there are a wide variety of existing projects that include this module, giving us an almost endless source of tips and other good information regarding how to properly integrate this module into a design; the ubiquity of this module also means that there are well-developed software libraries written to interface with the API of this device, making the software development significantly easier.

Table 16. HC-05 Technical Specifications

| Specification | Value | Notes/Pertinency |
|------------------------|-------------|--|
| Bluetooth Version | V2.0+EDR | Outdated Bluetooth version, missing key features |
| Max Data Transfer Rate | 3 Mbps | Average among modules researched |
| Minimum Footprint | 12.7mmx27mm | Average among modules analyzed |
| Sensitivity | -80dBm | Same as the RN42 |
| Transmit Power | +4dBm | Same as the RN42 |
| Supply Voltage | 3.3 V | Average among modules researched |
| Current Draw | N/A | Unavailable |
| Communication Protocol | UART | ASCII Command Line Interface over UART |

The main drawback of this device is the fact that it only supports Bluetooth V2.0. This is the lowest supported version of Bluetooth out of the Bluetooth modules that we researched, which leaves this module at a great disadvantage. When compared to the Bluetooth V2.1 supported by the RN42 module, a comparable module which we analyzed, Bluetooth V2.0 is missing important features such as the Bluetooth Simple Pairing Protocol (SPP).

Having a Bluetooth module which supports SPP is important to us because SPP reduces the pairing complexity and would improve the usability and overall user experience for our product and having an easy to use product is important to our team. Another feature missing in Bluetooth V2.0 is Bluetooth Low Energy support. During our research of Wireless Communication technologies, we found that the qualities of Bluetooth Low Energy were in-line with our goals for the project, and we would prefer to have a Bluetooth module which supported this technology, which was introduced in Bluetooth V4.0.

4.9.2 RN42

The RN45 Bluetooth module is an affordable Bluetooth module which is very similar to the HC-05 module. Because this module has been used in many other Senior Design projects, our team researched it to see if it would be a good fit to provide our measurement device with the wireless communication capabilities that may be required between our device and an off-board user interface device. A summary of the technical specifications of this device can be found in Table 17.

Throughout our research of this module we found that the RN42 is highly like the HC-05 module, especially in terms of the technical specifications. The main technical difference between the two modules is the fact that the RN42 module supports a higher version of Bluetooth. The RN42 supports Bluetooth V2.1, compared to the HC-05 which only supports Bluetooth V2.0. As mentioned in the previous section, this is an important difference due to the fact that Bluetooth V2.1 comes with support for the Simple Pairing Protocol, which is a feature we would like to have so that we can provide our customers with the best user experience possible.

Table 17. RN42 Technical Specifications

| Specification | Value | Notes/Pertinency |
|------------------------|----------------------|---|
| Bluetooth Version | V2.1+EDR | Contains more features than the HC-05, but still does not support BLE |
| Max Data Transfer Rate | 3 Mbps | Average among modules researched |
| Minimum Footprint | 13.4 x 25.8 x 2.4 mm | Average among modules researched |
| Sensitivity | -80 dbM | Same as HC-05 |
| Transmit Power | +4 dBm | Same as HC-05 |
| Supply Voltage | 3 V – 3.6 V | Average among modules researched |
| Current Draw | 2 uA, 3 mA, 30 mA | Comparatively medium |
| Communication Protocol | UART, PIO, AIO, SPI | ASCII Command line interface over UART |

Although it is very similar in terms of technical specifications, the RN42 is missing some of the key benefits that the HC-05 had. The RN42 costs upwards of \$30, almost 3 times as much as the HC-05 module. Although this is still a small amount compared to our overall budget, we did not find that the 300% increase in price is justified, especially because the module has almost the exact same technical specifications as the HC-05. The RN42 also does not share the same ubiquity of the HC-05 module, meaning that there are not as many software libraries that exist for this module. Another drawback of the RN42 is that, although it supports a newer version of Bluetooth than the HC-05, it still does not have support for Bluetooth Low Energy, which was introduced in Bluetooth V4.0.

4.9.3 RN4020

The RN4020 Bluetooth Low Energy RF module is a Bluetooth communication module that supports Bluetooth 4.1 and includes an MCU, digital analog I/O capabilities, an on-board stack, and an ASCII command API. In our initial research, we found that this module is one of the most common modules for Bluetooth Low Energy communication. Therefore, our team researched to see if it would be an adequate measurement device and appropriately interface with wireless communication capabilities.

A summary of the technical specifications of this device can be found in Table 18. This module differs greatly from the two Bluetooth Classic modules that we researched for this portion of our design. Compared to the first to modules researched, the RN4020 has a much smaller footprint, uses a fraction of the power, has a stronger signal, and is more sensitive. While it is not cheaper than the HC-05, the RN4020 is still very affordable, especially when its technical specifications are taken into account. The RN4020 can be found for under \$20, placing it between the HC-05 and the RN42.

Table 18. RN4020 Technical Specifications

| Specification | Value | Notes/Pertinency |
|------------------------|-----------------------|---|
| Bluetooth Version | V4.1+BLE | Supports Bluetooth Low Energy |
| Max Data Transfer Rate | 1 Mbps | Comparatively low, sufficient for our product |
| Minimum Footprint | 11.5 x 19.5 x 2.5 mm | Small compared to other modules researched |
| Sensitivity | -92.5 dBm | Higher than most modules researched |
| Transmit Power | +7.5 dBm | Higher than most modules researched |
| Supply Voltage | 3.3 V | Average for modules researched |
| Current Draw | 900 nA, 1.5 mA, 16 mA | Comparatively low, since BLE uses low power consumption |
| Communication Protocol | UART, PIO, AIO, SPI | ASCII Command line interface over UART |

Aside from besting the other modules in most of the technical specifications analyzed, the main advantage that the RN4020 has is that it supports Bluetooth 4.1 and Bluetooth Low Energy. This capability is important because the Bluetooth Low Energy would be the best fit for our project as far as wireless communication technologies go.

The only drawbacks that the RN4020 has are the data transfer rate and ease of implementation. These drawbacks are not unique to the RN4020; lower data transfer rate and slightly higher implementation difficulty are characteristics that will come with most Bluetooth Low Energy sensors.

4.9.4 ESP32

ESP32 is a low-cost, low-power chip series with Wi-Fi & dual-mode Bluetooth capabilities built in. In our initial research, we found that this chip is commonly used in amateur Bluetooth Low Energy projects. Because of this, our team researched it to see if it would be a good fit to provide our measurement device with the wireless communication capabilities that may be required between our device and an off-board user interface device. A summary of the technical specifications of this device can be found in Table 19.

Upon further research our team found that, although an ESP32 chip can be used as a separate Bluetooth or Wi-Fi module, the chip is more commonly used as a full microcontroller because of the large amount of capabilities that are built into this chip. ESP32 chips support peripherals such as touch sensors, temperature sensors, CAN 2.0, and more. Because the ESP32 is a full system on a chip, as opposed to a dedicated Bluetooth module, we found that this device would be overkill for this project. Even though this chip is extremely low cost, it would have higher PCB design complexity, and much higher power usage compared to the other modules researched.

Table 19. ESP32 Technical Specifications

| Specification | Value | Notes/Pertinency |
|------------------------|--------------------------|---|
| Bluetooth Version | V4.2+BLE,EDR | Highest supported Bluetooth version of modules researched |
| Max Data Transfer Rate | 4 Mbps | Comparatively high |
| Minimum Footprint | 25.5 mm × 18 mm × 3.1 mm | Average for modules researched |
| Sensitivity | -97 dBm | Highest among modules researched |
| Transmit Power | +12 dBm | Highest among modules researched |
| Supply Voltage | 3.3 V | Average for modules researched |
| Current Draw | 100 uA, 30 mA, 100 mA | High for a BLE module due to unnecessary components |
| Communication Protocol | UART, PCM, SDIO, SPI | ASCII Command line interface over UART |

4.9.5 Bluetooth Module Comparison and Final Selection

After analyzing the results of the research, the team decided to choose the RN4020 RF module for our Bluetooth communication. This decision was mainly due to the RN4020's support for Bluetooth Low Energy, its low power consumption, and low cost. Out of the 4 modules analyzed, only the RN4020 and the ESP32 supported Bluetooth Low Energy, which is preferred for this project to keep the battery life as long as possible.

Between the RN4020 and the ESP32, the RN4020 had lower power consumption and would be easier to integrate into our PCB design, both were due to the inclusion of many unnecessary modules in the ESP32 board. Table 20 on the next page compares the modules that were researched and highlights the RN4020 as our choice.

Table 20. Bluetooth Module Comparison

| Module | HC-05 | RN42 | RN4020 | ESP32 |
|---------------------------|---------------|----------------------|----------------------|--------------------------|
| Cost | <\$10 | <\$35 | <\$20 | <\$20 |
| Size | 12.7mm x 27mm | 13.4 x 25.8 x 2.4 mm | 11.5 x 19.5 x 2.5 mm | 25.5 mm × 18 mm × 3.1 mm |
| Power Consumption | Medium | Medium | Very Low | Low |
| Bluetooth Version Support | V2.0 | V2.1 | V4.1, BLE | V4.2, BLE+EDR |

5. Project Design

This section will describe the hardware designs which the project for the chlorophyll fluorescence spectrometer went through in order to achieve its constraints, standards, and research goals.

5.1 Hardware Design

This section will describe the hardware design of the chlorophyll fluorescence spectrometer. Previous hardware designs will be briefly reviewed so that there will be no confusion about the particulars of the final design. This section includes the optics design, the electronics design, and the joining of the two.

5.1.1 Optical Cavity Design

The final system design is shown Figure 30.

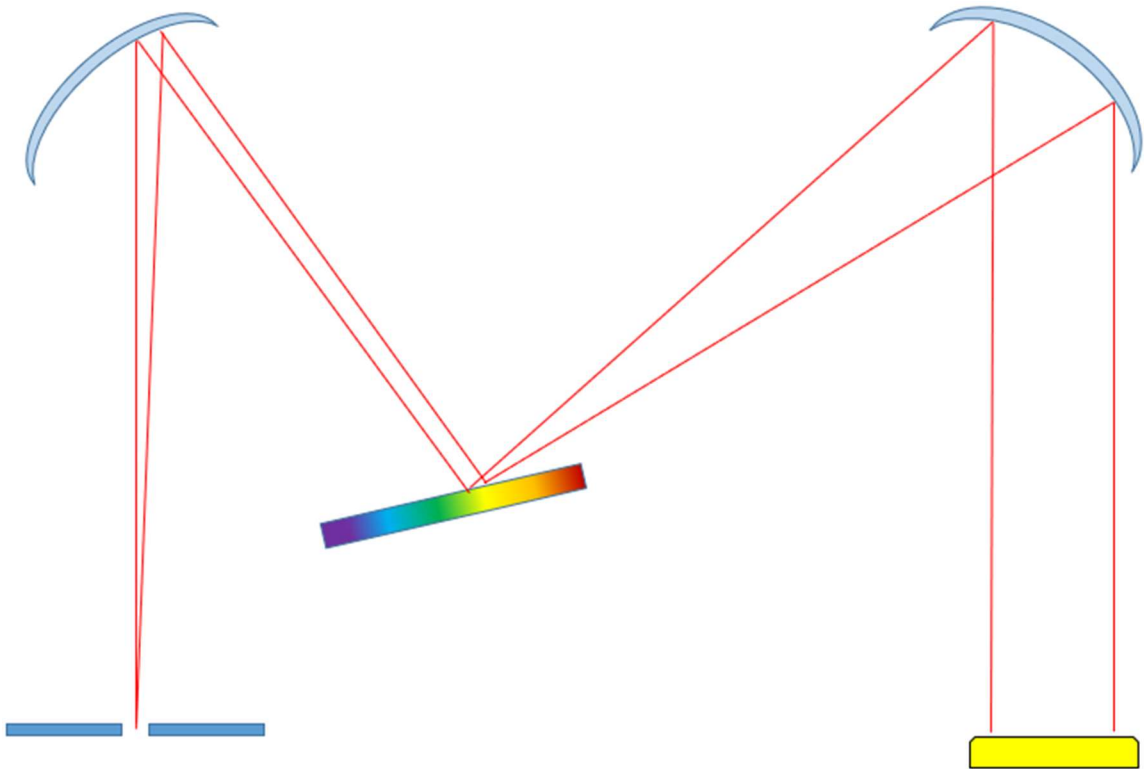


Figure 30. Dimensionless optical system design.

First, the question must be raised about the monochromator: why were only reflective gratings chosen when transmissive gratings would simplify the optical system? The reason a reflective grating was chosen over a transmissive grating is due to the popular blaze angle for transmissive gratings being at 14.7 degrees, which correlates to a peak wavelength

efficiency of 300 nm. Despite thorough searches, few transmissive gratings could be found with a blaze angle closer to 4.3 degrees, and those that had blaze angles around the ideal wavelength were too expensive for the project's budget. From here, transmissive gratings were discarded for reflective gratings.

Originally, the system had a lens in front of the entrance slit, but after discussing with faculty, it was decided that the lens could be safely discarded. This design change saved the team some money and cut down the dimensions of the optical cavity.

There are two systems to the optics design: the system before the grating and the system after it. It is prudent to design this system backwards, starting with the sensor array at the end. If it is not done this way and the system is designed from the start forwards, the variables will compound on each other and the system will be much more difficult to solve.

The ideal case for this system is to have the light from the vertical entrance pupil (which will spread horizontally) be spread completely across the active horizontal dimension of the image sensor. In order to give a margin of error in the design process, say that the light from the entrance slit will cover 90% of the active horizontal dimension. This covers the case where the optics may spread out the spectrum a little wider than anticipated, which will prevent the loss of waveband information. According to the ARDR image sensor's data sheet, the active horizontal dimension is 4.83 mm. 90% of this is 4.347 mm, so say that the entrance slit light must be smaller than 4.34 mm in length by the time it reaches the image sensor.

This decision, shown in Figure 31, discards the use of 5% of the pixels on either side of the image sensor, which will hurt the resolution of the spectrum. However, consider the following: the sensor has 1288 active pixels in the horizontal dimension. 90% of these active pixels will be illuminated by light—approximately 1159 pixels. Since the imaged waveband will be from 600 to 700 nm, which is 100 nm, the resolution will be the waveband divided by the number of pixels over which it spreads. That is, $100/1159 = 0.086$ nm will be the spectrometer's effective resolution. Given some smearing on the optics side, losses, and spreading, it is likely that the resolution of the spectrometer will be closer to 0.1 nm. However, this still exceeds the resolution requirement specification of 5 nm by 5000% in the ideal case.

The light that hits the diffraction grating will have an angular dispersion which will de-collimate it from the front half of the optical system. To re-collimate it for the detector, place a focusing mirror at a distance equal to the mirror's focal length away from the grating. To find this focal length, the angular dispersion of the waveband from the diffraction grating and the angle of the light incident on the grating from the front half of the optical system must be known.

Consider again Equation 6. The longest λ is 700 nm and the shortest λ is 600 nm. $a = \frac{1 \cdot 10^{-3} \text{ m}}{300} = 3.33 \text{ } \mu\text{m}$, where a is the spacing between the grooves of our grating. The grating that was purchased is blazed for the first order, so $m = 1$. The only variable constraint is the angle of light incident on the grating θ_i , which is a metric that can be manually

controlled. For the long end of the waveband, $\frac{m\lambda}{a} = 0.21$. For the short end of the waveband, $\frac{m\lambda}{a} = 0.18$. These numbers will be used in place of their variable fraction counterparts from here on out.

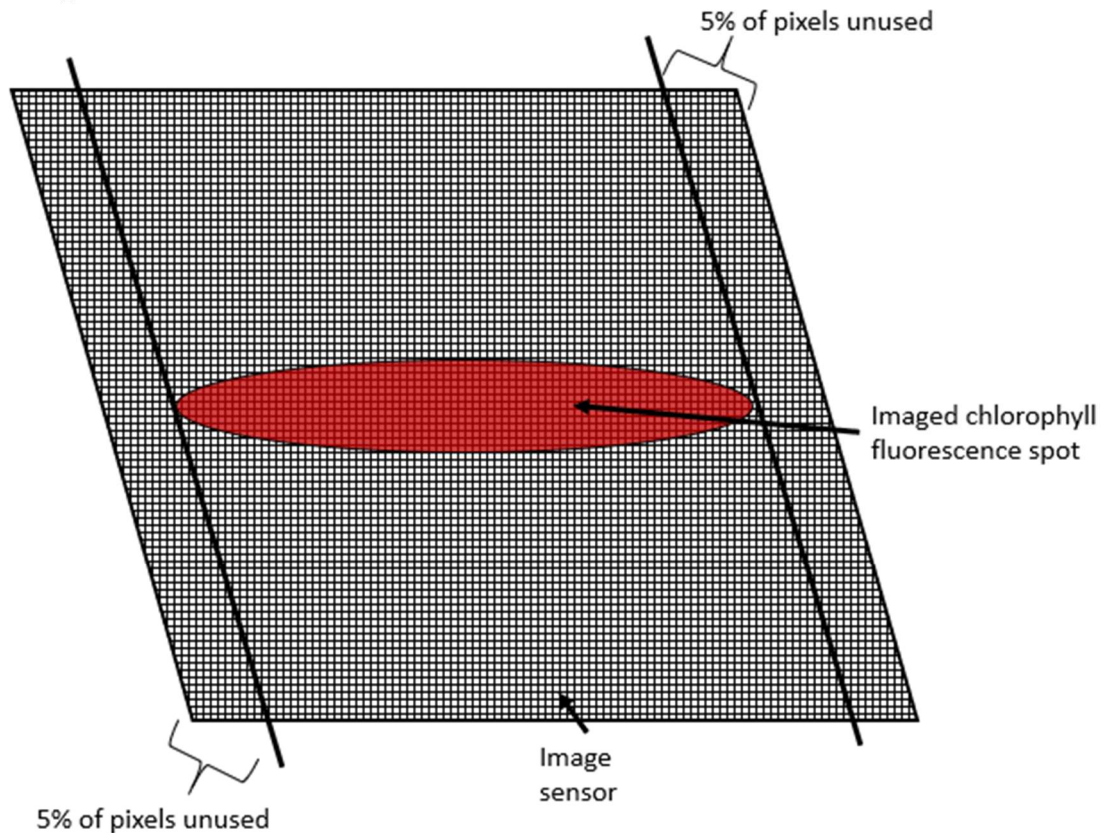


Figure 31. 90% sensor fill using the chlorophyll fluorescence spot.

The grating angular dispersion is the longest wavelength's dispersion minus the shortest wavelength's dispersion, or $\sin^{-1}(0.21 + \sin \theta_i) - \sin^{-1}(0.18 + \sin \theta_i)$. Since θ_i is a mechanical, controllable variable that can be chosen by the designers, this function will act as a tool to produce the angular separation the designer's desire. The plot relationship between incidence angle and grating angular dispersion is shown in Figure 32. There is a cut-off at $\theta_i = 51.84^\circ$, so as long as the incidence angle does not exceed this value, the grating angular dispersion will be real.

The reason the angular separation is so important is its effect on the effective slit size when the light reaches the image sensor. The tangent relationship will give the exact distance from the grating to the final mirror required for the light to spread to its ideal size, which the mirror will then collimate on to the image sensor. Again, the final mirror will be placed at its focal length's distance from the grating to collimate the light such that it appears to have come from infinity at the sensor, so it is important to find the angular separation first before choosing a mirror.

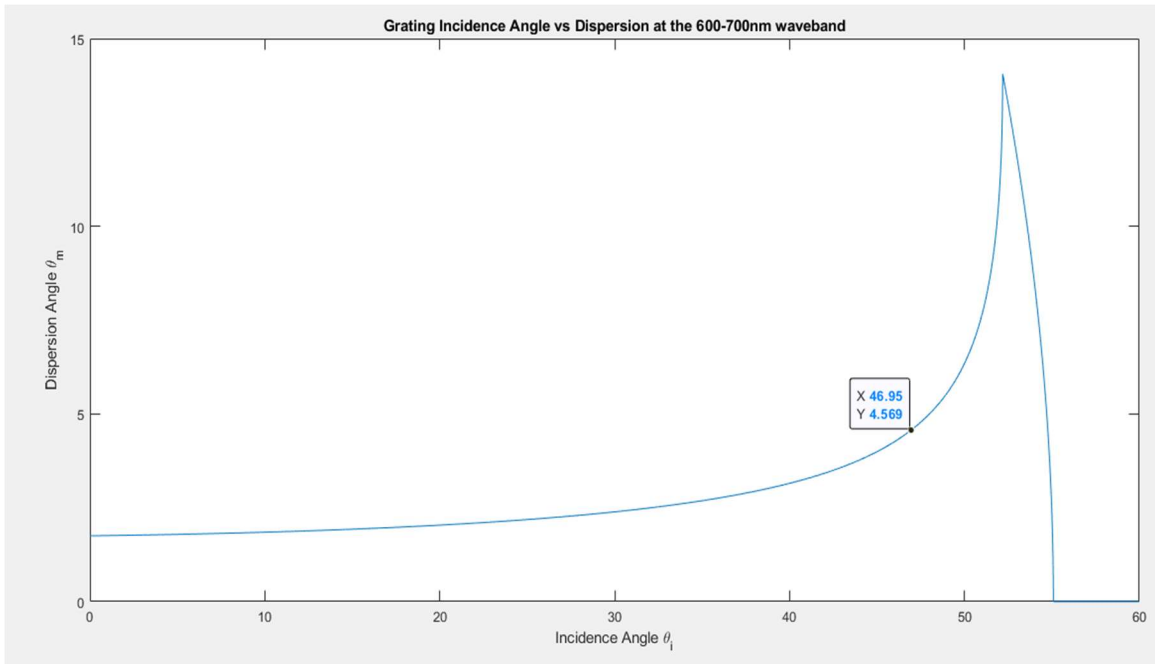


Figure 32. Diffraction grating incidence angle vs angular dispersion at 600-700nm waveband

However, it is important to note that the size of the slit imaged through the system will affect the focal length of the focusing mirror. Consider Figure 33. The angular dispersion θ_m is divided between the shortband dispersion at one end of the grating and the longband dispersion at the other.

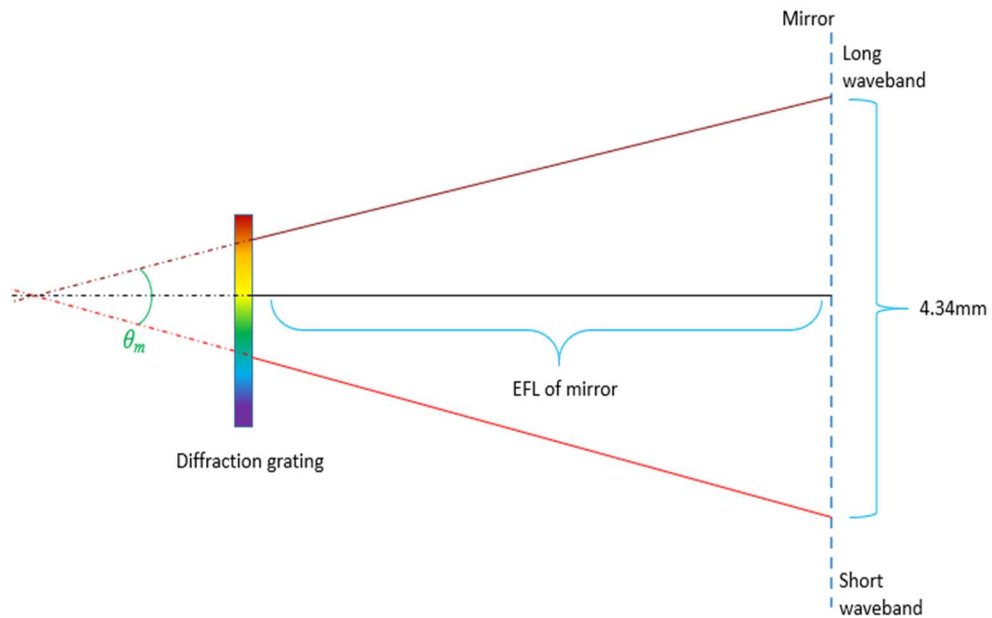


Figure 33. Illustration of the geometric system between the diffraction grating and the focusing mirror (simplified)

However, geometric analysis cannot be made from the grating to the mirror since the object to be analyzed would be a rhombus, not a right triangle. By tracing the geometric triangle back to the virtual space behind the grating, a true right triangle is made. The base of this full triangle can be solved for using the known trigonometric tangent identity, the angular dispersion θ_m , and the ideal image size of less than 4.34mm. Then, to find the effective focal length of the mirror, subtract the base of the triangle behind the grating from the base of the full triangle.

In equation form, the effective focal length that the focusing mirror should have is shown in Equation 10. This equation can be equalized to any focal length and the controllable parameters can be matched appropriately. A common focal length used in spectrometers is 40mm, and since cheap mirrors usually come in multiples of 25mm, the design team elected to go with a focusing mirror that has a 50mm effective focal length.

$$efl = \frac{4.34 - slit}{2 * \tan\left(\frac{\theta_m}{2}\right)}$$

Equation 10. Effective focal length of focusing mirror using slit size and angular dispersion

Using Equation 10 and a slit size of 350 μ m and aiming for an efl around 50mm, it was found that the angular dispersion $\theta_m = 4.6^\circ$, which corresponds to an incidence angle $\theta_i = 47^\circ$. The actual efl of this system is 50.008 mm which creates a focusing error of 0.016%. A percentage this low is generally ignorable and will be ignored going forward.

The incidence angle, a controllable factor required for the hardware design of the system before the diffraction grating, is now known. The system after the grating has thus been solved and it includes a 10% error buffer at the imaging plane just in case calculations were not perfectly accurate or there are optical misalignments.

Consider the optical system before the diffraction grating. The incidence angle is 47° , an angle which will easily expand the size of the system if one of the dimensions isn't controlled properly. The controllable dimension in this case is the distance from the entrance slit to the collimating mirror. The distance from the slit to the grating is also controllable, but it will make coordinating the optics a little more challenging. This should be kept in mind as the next discussion is made since it will affect the cost requirement specification of the mirrors in the system.

Now, consider the task of matching the F-number of the two mirrors. The F-number is a unitless ratio of the focal length to the diameter of the aperture. In this case, the aperture of a mirror is its physical diameter. Two considerations have to be made: the size of the F-number and the effect of that F-number on cost. Generally, as the F-number's absolute magnitude increases (1, 2, 5, 10, 20, etc.), the aperture lets in less light but has a greater depth of field. And, conversely, as the F-number's absolute magnitude decreases (10, 5, 2, 1, 0.75, 0.5, etc.), the aperture lets in more light but loses depth of field.

Since this a spectrometer, depth of field is not immensely important in the design process. Gaining as much light as possible to maximize signal, however, is a primary design concern. As such, the F-number of both optics should be chosen such that they all match and are relatively low in absolute magnitude. Anywhere from $f/1$ to $f/4$ is a safe range, but a specific F-number should be chosen. This is where the requirement specifications help narrow the search.

Interestingly, as F-number decreases in absolute magnitude, the price generally goes up for mirrors. $f/4$ mirrors cost between \$35 to \$50. $f/4$ systems offer large effective system sizes (here meaning the size of the distance from the entrance slit to the collimating mirror), but this correlates to an increase in the dimension specification, which is not advisable. $f/4$ systems also take in a little less light than their lower magnitude counterparts. $f/1$ systems are very, very expensive, usually reaching \$150 per mirror or more, heavily constraining the cost requirement. However, their effective system size is generally small. $f/1$ systems also take in the most amount of light, a plus for the chlorophyll fluorescence spectrometer.

In the end, a happy medium at $f/2$ was decided since this F-number offers a great amount of light transmission, generally acceptable price ranges, and reasonable system size. Considered focusing mirrors are shown in Table 21. That which was highlighted in green was chosen for integration into the CFS.

Table 21. Mirror prices and other metrics

| Part name | Manufacturer | Price | EFL (mm) | Diameter (mm) | F# |
|---------------|--------------|----------|----------|---------------|-------|
| CM127-050-P01 | ThorLabs | \$39.50 | 50 | 12.7 | 3.937 |
| CM254-050-P01 | ThorLabs | \$60.34 | 50 | 25.4 | 1.968 |
| CM508-050-P01 | ThorLabs | \$90.63 | 50 | 50.8 | 0.984 |
| 10DC100ER.1 | Newport | \$141.00 | 50 | 25.4 | 1.968 |

The collimating mirror's F-number must be matched. There are only a few collimating mirrors that have a small efl at the standardized diameter. As such, it was decided that the same mirror should be used for both focusing and collimating. Thus, the mirror highlighted in green in Table 21 will be purchased twice, eliminating any F-number matching concerns and providing no need for extraneous calculations.

The mirrors will be coated with silver. According to ThorLabs, their silver-coated mirrors offer an average of 97.5% reflectance in the 450 nm to 2 μ m waveband as opposed to the aluminum-coated mirrors offering only 90% reflectance in the same waveband. Both mirrors cost the same and have the same dimensions, but to minimize loss from reflection, silver-coated mirrors were chosen for the CFS.

And so, with all the optics chosen, the original optical system can be updated with numerals to produce the final optical system shown in Figure 34. This figure is not to scale in an angular or geometric sense, but the numbers are accurate and provide a good base for the creation of the housing. The housing will secure the optics and align them perfectly so that no mistakes are made during alignment procedures. A misalignment on the optics side will severely cripple the project's capabilities.

The one thing of note is the two major dimensions: 50mm in length and 91mm in width. The width was rounded from 90.4mm (the distance from between the two mirrors) to give the designers some extra room to account for the size of the optics, housing design, and other mechanical margins of error.

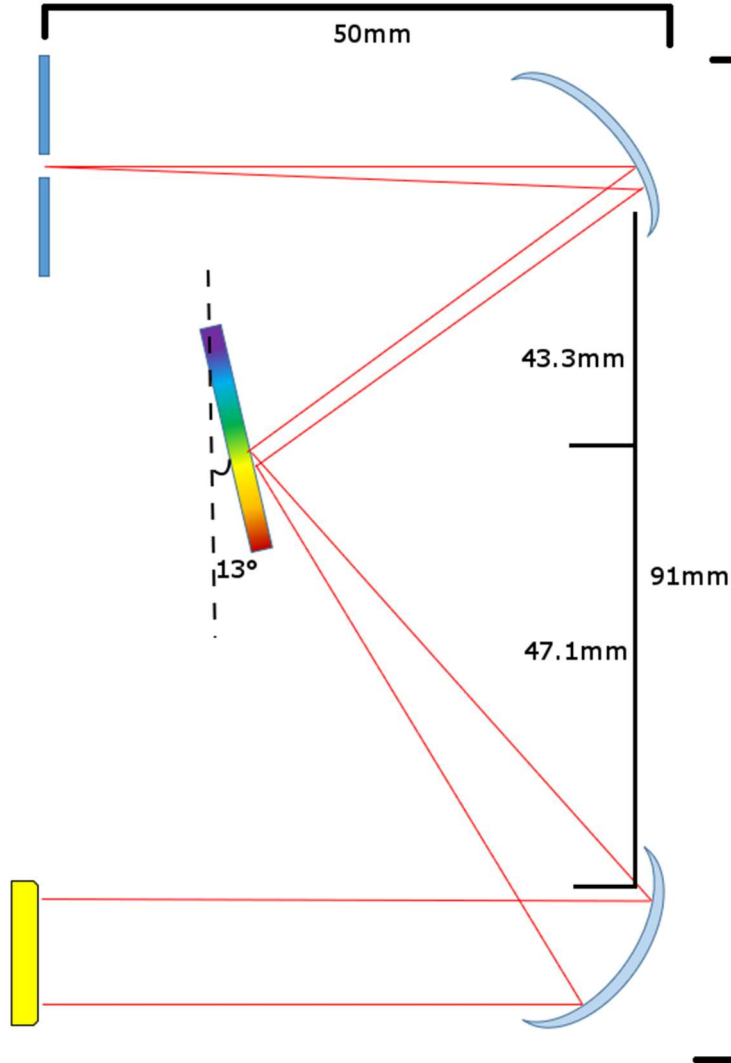


Figure 34. Final optical system design with major angles and dimensions

Also, note that the design in is only for the optics housing area. It does not include the dimensions of the power system, Bluetooth module, or light cavity from which chlorophyll will be emitting. It does not contain minor dimensions such as the location of the mirrors and grating with respect to the slit and image sensor, nor does it contain the angles of the mirrors, their dimensions, or their focal lengths (and thus the distances from their surface to any other surface). These dimensions are covered in-detail in 5.1.5 Housing Design.

5.1.2 Optical Cavity Loss Calculations

As light moves from the source to the receiver, it will undergo many levels of power loss from propagation, reflection, transmission, and imperfect efficiency at the grating and sensor. A loss calculation is important because it describes how much signal the source will lose by the time the light reaches the sensor.

There are five primary optical components: two concave mirrors, one entrance slit, one diffraction grating, and one sensor array. The light will also have to propagate from the chlorophyll sample through a cuvette and through the system to reach the sensor. These sources of loss can be calculated using ideal equations, tweaking them slightly to account for real-world variations, and summing them all up at the end.

For the geometric system, propagation losses were considered negligible and were not included in the calculation. The total loss incurred by the fluorescence from when it enters the spectrometer to when it reaches the sensor is included below in Table 22. The numbers used for each calculation is included in Appendix C, Table 37.

Table 22. Table of expected interface losses

| | 600nm | 683nm | 700nm |
|---|---------------|---------------|---------------|
| Reflection loss from collimating mirror (dB) | 0.1323 | 0.0877 | 0.0877 |
| Reflection loss from diffraction grating (dB) | 1.3668 | 2.0066 | 2.0761 |
| Reflection loss from focusing mirror (dB) | 0.1323 | 0.0877 | 0.0877 |
| Sensor quantum efficiency loss (dB) | 1.0790 | 1.6115 | 1.6749 |
| Total Losses (dB) | 2.7104 | 3.7935 | 3.9264 |

Considering the table above, in an ideal situation without calculating the losses incurred from fluorescence passing through the slit, the system will see over half the power lost from propagation from slit to sensor. Most of the power loss comes from the diffraction grating since its efficiency curve peaks around 500nm, shown in Figure 35. There is also power loss at the sensor's interface due to the quantum efficiency of the sensor, shown in Figure 36.

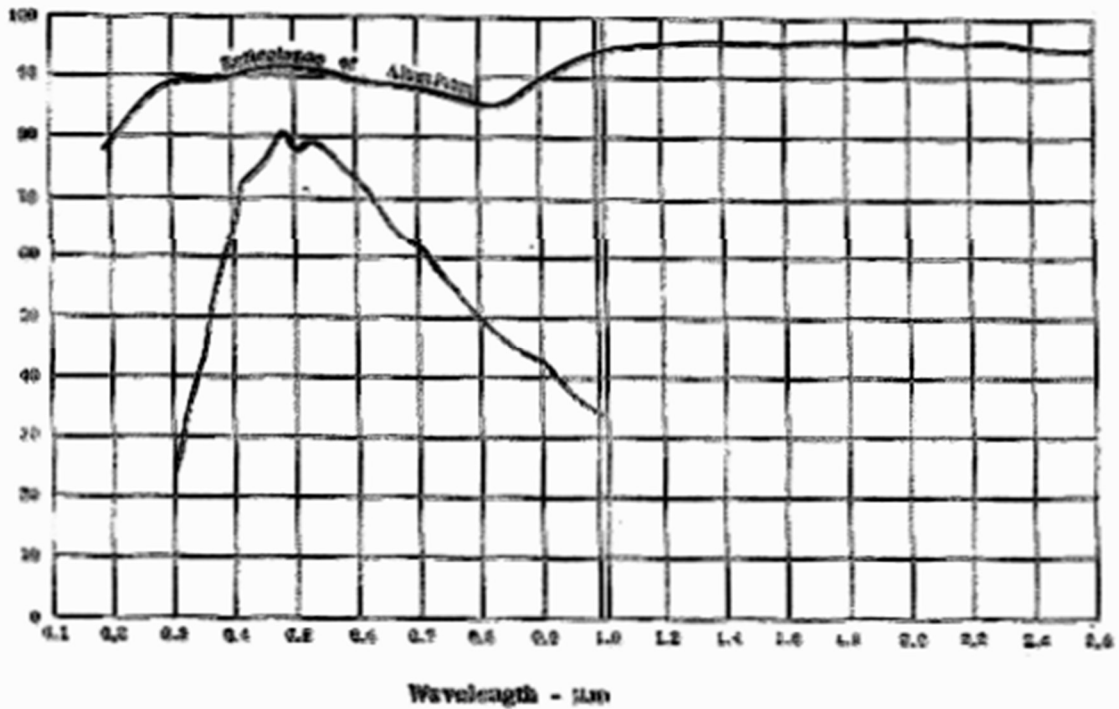


Figure 35. Diffraction grating efficiency curve (source quality)

*Republished from Richardson Gratings' data sheet for 53-*270R gratings.*

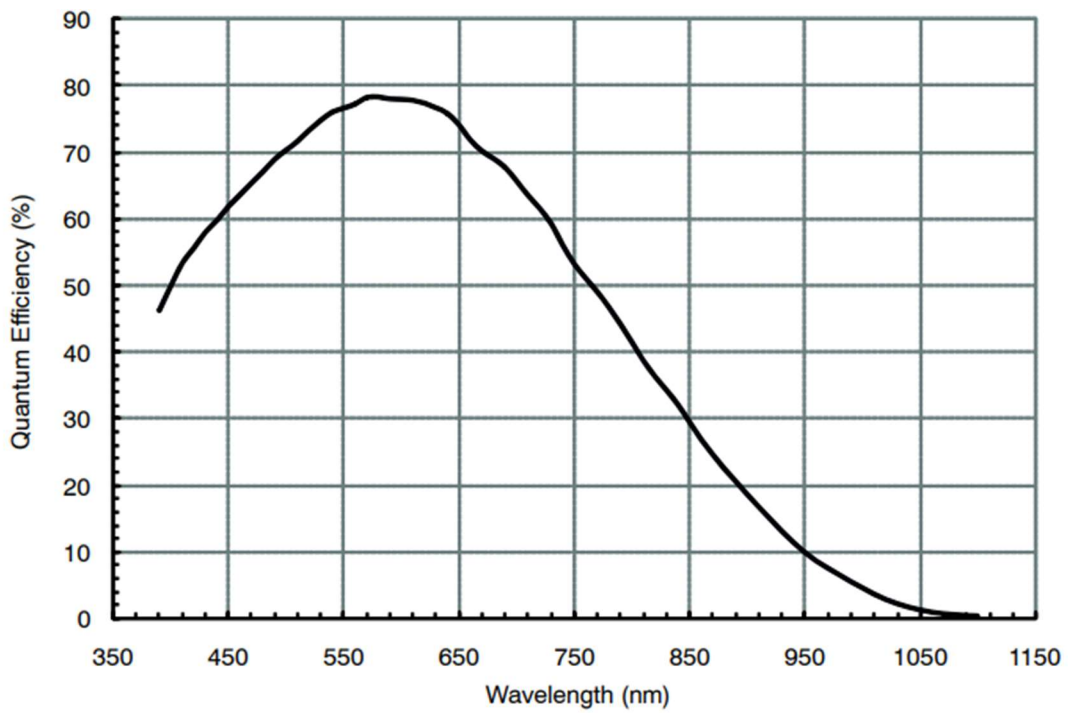


Figure 36. ARDR Monochrome Sensor quantum efficiency curve vs wavelength

Republished from ON Semiconductor's AR0130CS data sheet.

To account for these losses, special consideration will be made to two specific things: power output from the sample and fluorescence isolation. The darker it is inside the cavity, the lower chance there will be of scattered light effecting the signal received at the sensor end, so the fluorescence effect must be perfectly isolated within the source cavity and the optics cavity. The power output from the sample must also be maximized, hence its low optical density to prevent re-absorption and the intense power of the laser light source.

Unfortunately, loss mitigation is regulated to just these two considerations—that is, they are the only way to prevent the fluorescing light from losing so much power that it appears as noise at the sensor side. The one saving grace of chlorophyll fluorescence is that the process to reach peak fluorescence is comparatively slow (about 1 second) and the intensity lasts for a long time, maintaining about 85% max intensity for at least 20 seconds [Qck.Htn].

With this in mind, if losses prove too great for the sensor to operate in capture mode where not enough signal will be obtained, the sensor's integration time can be increase to a very long timescale to absorb as many photons as possible. This will help the sensor create an ideal intensity plot after normalization for fluorophore dimming. This mode of operation will increase the amount of time it takes to produce a plot for the user, but it will guarantee that the most amount of signal is present at the sensor's interface.

5.1.3 Electronics Design

Texas Instruments WeBench was useful in the design of the power supply for the Chlorophyll Fluorescence Spectrometer. The design parameters used include the range in voltage that the lithium ion cell will fluctuate during operation. This is going to range from 4.2 Volts down to 3.7 Volts. Across this range, each component will continue to be supplied the necessary voltage and current to operate normally. The reason specialized integrated circuits are used is because as the source voltage changes and as the current drawn from each component changes, the output voltages need to stay constant.

From the datasheet for each component, we learn how to connect and configure each regulator. From the datasheet for the TPS62233DRY, we learn that the TPS62233DRY can output up to 500 mA and that the efficiency will vary depending on the current draw. Efficiency is also affected by the input voltage, output voltage and inductor/capacitor values.

The voltage regulation is accomplished with pulse width regulation in a switching circuit at 3 MHz. 4 ICs we will be using are the TPS62231DRY, the TLV71328PDBV, the TPS62233DRY and the TPS799195. The TPS62231DRY was selected to provide 82 mA at 1.8 Volts which is required for the AR0130 CMOS sensor. The TLV71328PDBV was selected to provide the 40 mA at 2.8 Volts for the AR0130 sensor. The TPS62233DRY was selected to provide 160 mA at 3.0 Volts which is required for our MZH8340550D-AL01A laser diode. The TPS799195 was selected to provide 30 mA for the STM32F407VET ARM processor as well as 16 mA for our RN4020 Bluetooth module, each at 1.95 Volts.

To protect the Samsung INR18650-25R single cell lithium ion battery during charging, we are using the AP5056 battery charger. This integrated circuit has the function of safely limiting the charge which can flow to the battery during charging. It will also limit the voltage placed on the battery to 4.2 Volts for safety and longevity of the component. The charge rate is programmable using a resistor on pin 2. From the data sheet we have decided to use a 1 k Ω resistor for a charging rate of 1 Amp since this is a safe charging rate for our lithium cell.

The battery charger has an optional input for a temperature sensor which disconnects the battery any time the temperature exceeds the safe operating limit for the lithium ion cell. The lithium ion cell acts as the input voltage for each of the 4 voltage regulation circuits. Our ARM processor and Bluetooth module share a voltage regulator because they are able to operate at the same voltage and the supply can provide enough current for both.

The charging circuit includes indicator LEDs for the purpose of indicating charge state. The integrated circuit is programmable in the sense that the charging current can be specified by setting a resistor value Figure 37. Shows the implementation of these devices to provide power to each load in the CFS. Figures 37-41 comprise the complete power schematic for our device.

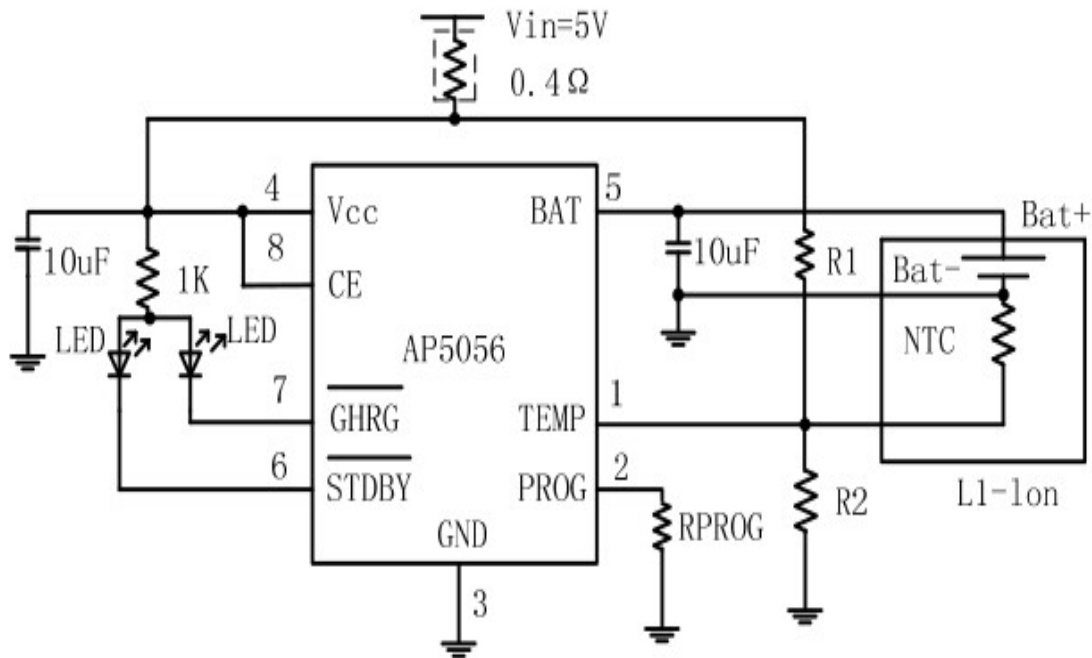


Figure 37. Battery Charging Management Circuit

Made by Luke Preston using AP5056 Datasheet.

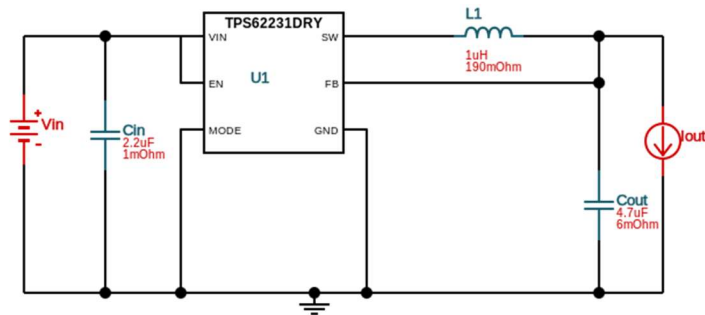


Figure 38. CMOS sensor 1.8 Volt supply
Made by Luke Preston using TI WeBench.

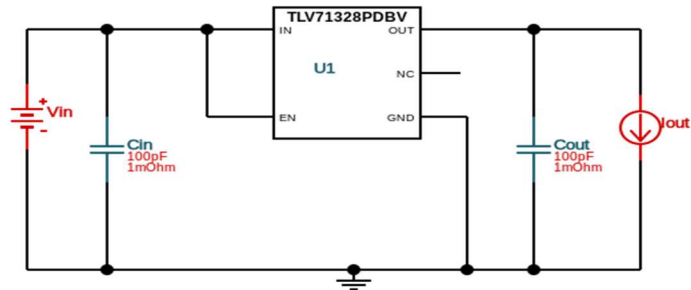


Figure 39. CMOS sensor 2.8 Volt supply
Made by Luke Preston using TI WeBench.

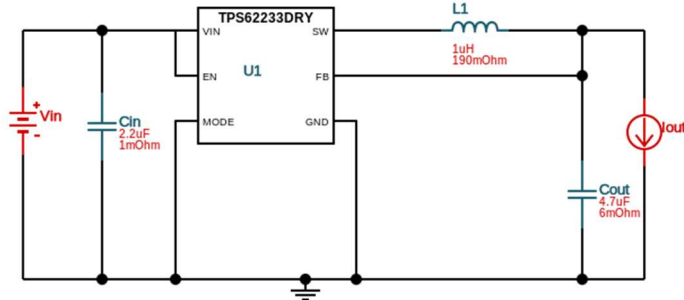


Figure 40. Laser Diode 3.0 Volt Supply
Made by Luke Preston using TI WeBench.

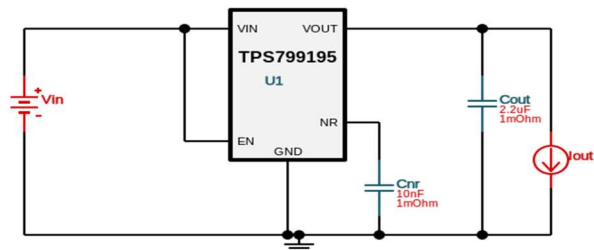


Figure 41. ARM M-Processor and Bluetooth module power supply
Made by Luke Preston using TI WeBench.

The first step in building a PCB is to design a schematic for the device. We have chosen to use Eeschema for this purpose. Below we have integrated each component to one circuit diagram for our design, removing the features which we will not need. An example of a feature which was not needed was the temperature sensor for the lithium ion cell. Because our current draw is going to be so small, the additional circuit for monitoring the temperature is not necessary and was removed.

An important consideration for components with high frequency switching is the impedance. Because transient voltages in a high frequency switching circuit will deviate from their desired values and because the length between PCB traces are sometimes large, using capacitors near the voltage inputs for some of the inputs is necessary in order to isolate the inputs. It is important that the effective series resistance be small on these isolating capacitors in order for them to be effective. The placement of these capacitors is also important. The closer they are to the input they are buffering the better. When designing the printed circuit board this will be an important consideration. The capacitors may need to be placed on the other side of the PCB to get as close as possible, to minimize the inductance due to the PCB traces.

Figure 41 shows the complete schematic for the Fluorescence spectrometer. The largest component in the circuit is the stm32f407ve processor. This integrated circuit will be located in the center of the board to reduce total trace distance because it has the largest number of connections. There are four integrated circuits dedicated to voltage regulation and one integrated circuit that facilitates charging the lithium ion cell.

The charging input will be implemented using a MicroUSB connector supplying 5 Volts to the input of the AP5056. The trigger for activating the laser will be controlled by the GPIO pin PE12 which is pin 43 on the LQFP100 package. This is connected to the enable pin of the TPS62233DRY voltage regulator. An earlier concept for this design would have used a MOSFET transistor to control the activation of the MZH8340550D-AL01A 405 mm laser diode. We realized that this complicated the design unnecessarily and would introduce losses as well as power wasted as heat dissipation.

The light source is a two-pin device, only passing power. However, it has its own dedicated voltage regulator and the regulator has an enable pin. The slew rate for our voltage regulator is high enough that the latency is negligible. Our laser will be powered on for one or more seconds to take measurements from our CMOS sensor. The data connections required to connect our processor with the Bluetooth module are shown in Table 23. Two additional pins will provide power from our voltage regulator at 1.95 Volts and a connection to ground.

Our CMOS sensor interfaces with the ARM processor via a 12-bit parallel connection. In order to control the device, other connections are necessary including the master clock input, pixel clock output, and trigger input. The CMOS sensor requires 5 power connections, with a separate ground for analog and digital connections as a result of the high frequency switching of the component.

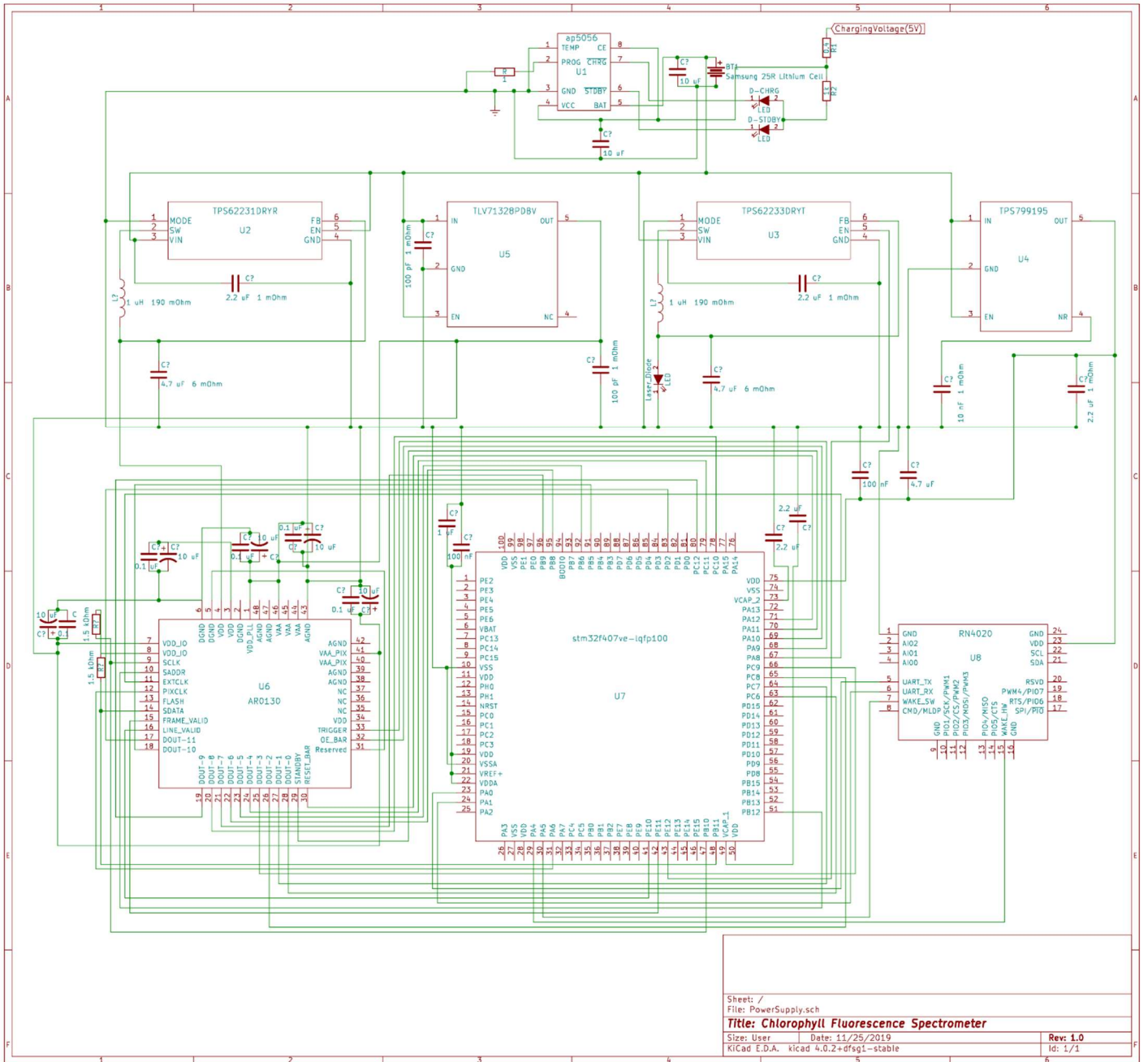


Figure 42. Circuit schematic for the CFS

Made by Luke Preston using Eeschema

There are two pins to the CPU which will be used for programming the device, SWDIO and SWCLK which are pins 72 and 76 respectively. Another two pins are required for debugging, USART2_TX and USART2_RX which are pins 25 and 26 respectively. These will be implemented on the PCB using 4 pinouts, labelled with the silkscreen.

Table 23. Bluetooth Module IO Connectors

| Description | Bluetooth Module Pin Number | Microcontroller Pin Name | Pin Number (LQFP100) |
|------------------------|------------------------------------|---------------------------------|-----------------------------|
| Generic GPIO (Wake HW) | 15 | PA4 | 29 |
| Generic GPIO (Wake SW) | 7 | PA5 | 30 |
| UART4 TX | 5 | PA0 | 23 |
| UART4 RX | 6 | PA1 | 24 |

The AR0130 requires voltages at 2.8 and 1.8 volts and each supply connection needs to be decoupled using two capacitors in parallel. The maximum allowable effective series resistance for these capacitors in parallel is 2Ω as per the AR0130 datasheet. The capacitors should be $0.1 \mu\text{F}$ and $10 \mu\text{F}$ in parallel and placed as physically close to the contact on the processor as possible to minimize inductances in the trace and provide a true voltage value. The data and control connections required to connect our processor with the CMOS Sensor module are shown in Table 24.

Using this electronic schematic, the printed circuit will be developed during winter break and refined in the first week or two of senior design two. The plan for our group is to design the printed circuit board using our schematic, laying out the physical location and footprint of each component and connection, and then send the designs to an external supplier who will fabricate the boards for us. We will be ordering two or three boards as an assurance in case we have a manufacturing defect and need to start over. The cost of the board is an important factor, but not nearly as important as the time it would take for us to order and receive another part.

We will be populating the boards ourselves using 0805 components when possible. The reason for this selection is that 0805 components are very easy to solder by hand and will not result in soldering defects. The circuit board will be a two layer design, which allows our circuit board to be more compact than it would be if we only placed components on one side of the board. Limiting our design to two layers simplifies design and fabrication, keeping the cost of the CFS low. As discussed in the research portion of this document, we will be using KiCad Pcbnew and PCB footprint editor to complete the design of our printed circuit board. KiCad has the ability to export a design as a series of GERBER files, an industry standard which we can send to our board manufacturer.

These GERBER files will instruct the board manufacturer on how the board is to be constructed, including the necessary information about all contacts, connections, vias, and traces. Two files will be used to describe the copper top and bottom, which map out the topology of all the conductor traces and solder contacts on the printed circuit board. Another two files will be used to specify the top and bottom solder mask, which is a nonconductive polymer layer used to prevent short circuits. The solder mask is usually green but can be any other color as well.

Additionally, two files will be used to communicate the top and bottom silkscreen. The silkscreen is the layer which is used to label and mark the printed circuit board. Reference designators are applied to components and a logo may also be added. The silkscreen is generally white ink, but other colors are possible. Finally, one GERBER file will be used for the drill legend. Drilled holes are used for mounting the board rigidly to the housing of the device as well as placing electrical connections from one layer of the board to another, which are called a vias. Drilled holes are expensive and vias do not provide as good an electrical connection as a copper trace, so the use of drilled holes on our printed circuit board should be minimized.

Table 24. CMOS Sensor IO Connections

| Description | CMOS Sensor Pin Number | Microcontroller Pin Name | Pin Number (LQFP100) |
|----------------------------|-------------------------------|---------------------------------|-----------------------------|
| Master Clock (MC01) | 11 | PA8 | 67 |
| I2C_SDA | 14 | PB11 | 48 |
| I2C_SCL | 9 | PB10 | 47 |
| Generic GPIO (SADDR) | 10 | PB12 | 51 |
| Generic GPIO (TRIGGER) | 33 | PA9 | 68 |
| Generic GPIO (OE_BAR) | 32 | PA10 | 69 |
| Generic GPIO (STANDBY) | 29 | PA11 | 70 |
| Generic GPIO (RESET_BAR) | 30 | PA12 | 71 |
| Generic GPIO (LINE_VALID) | 16 | PE10 | 41 |
| Generic GPIO (FRAME_VALID) | 15 | PE11 | 42 |
| DCMI_D0 | 28 | PC6 | 63 |
| DCMI_D1 | 27 | PC7 | 64 |
| DCMI_D2 | 26 | PC8 | 65 |
| DCMI_D3 | 25 | PC9 | 66 |
| DCMI_D4 | 24 | PC11 | 79 |
| DCMI_D5 | 23 | PB6 | 92 |
| DCMI_D6 | 22 | PB8 | 95 |
| DCMI_D7 | 21 | PB9 | 96 |
| DCMI_D8 | 20 | PC10 | 78 |
| DCMI_D9 | 19 | PC12 | 80 |
| DCMI_D10 | 18 | PB5 | 91 |
| DCMI_D11 | 17 | PD2 | 83 |
| DCMI_PIXCLK | 12 | PA6 | 31 |

5.1.4 Laser Cavity Design

The Laser Cavity in our device contains the elements which allow our chlorophyll to fluoresce and emit light at the desired range of wavelengths. This includes the laser module, a quartz cuvette, and an optical slit. The cavity will be manufactured so it can hold the laser and cuvette in place while allowing enough light to pass through the slit and into the main optical cavity. A layout of the laser cavity and its dimensions can be seen in Figure 43.

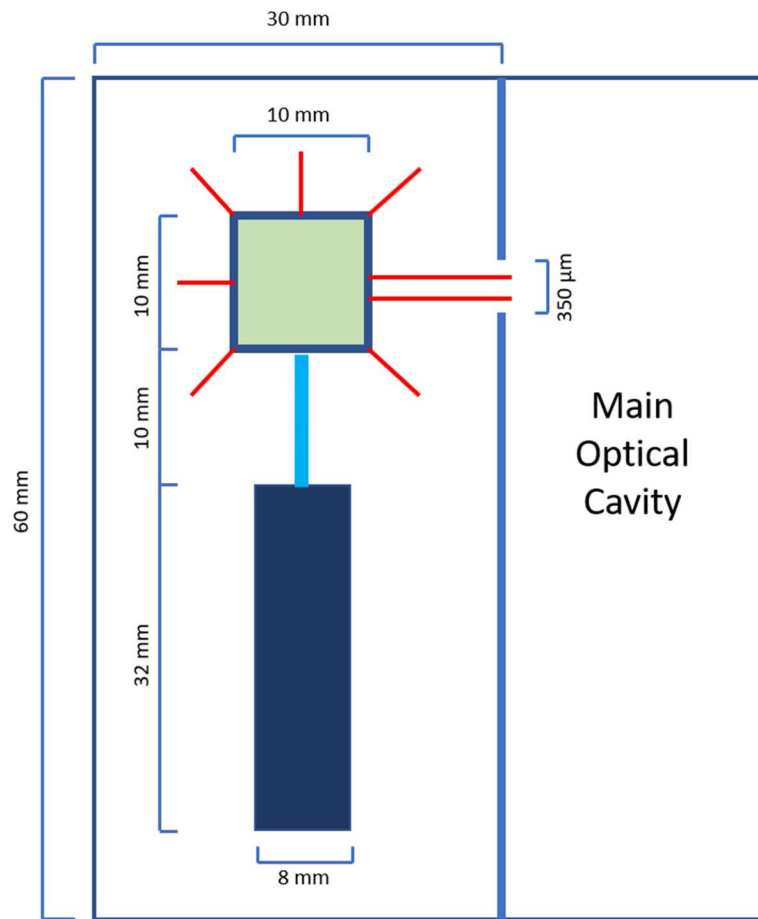


Figure 43. Dimensions of Laser Cavity
Made by Robert Bernson.

5.1.5 Housing Design

The completed housing design is shown in Figure 44. There are several options available for building the housing unit for the chlorophyll fluorescence spectrometer, such as metal, plastics, and wood. A light metal like aluminum or variants tempered with other metals is ideal in most cases, but since the CFS will have wireless capabilities, building the casing out of metal is not advisable. Wood has a significant chance of damaging the sensitive optics as it will rot over time. For this reason, a plastic such as Delrin or Teflon fits as the material for the outside casing and housing for the whole device.

Special care must be taken to not have light leak through from the outside of the enclosure and interfere with the optical instruments within the spectroscopy cavity. The casing must be totally sealed on all sides. To account for this, extra security features have been implemented. Three separate cases will be built: one to house the entire device, one to house and isolate the source and sample, and one to house the spectroscopy cavity. These can be seen in the black outlines in Figure 44.

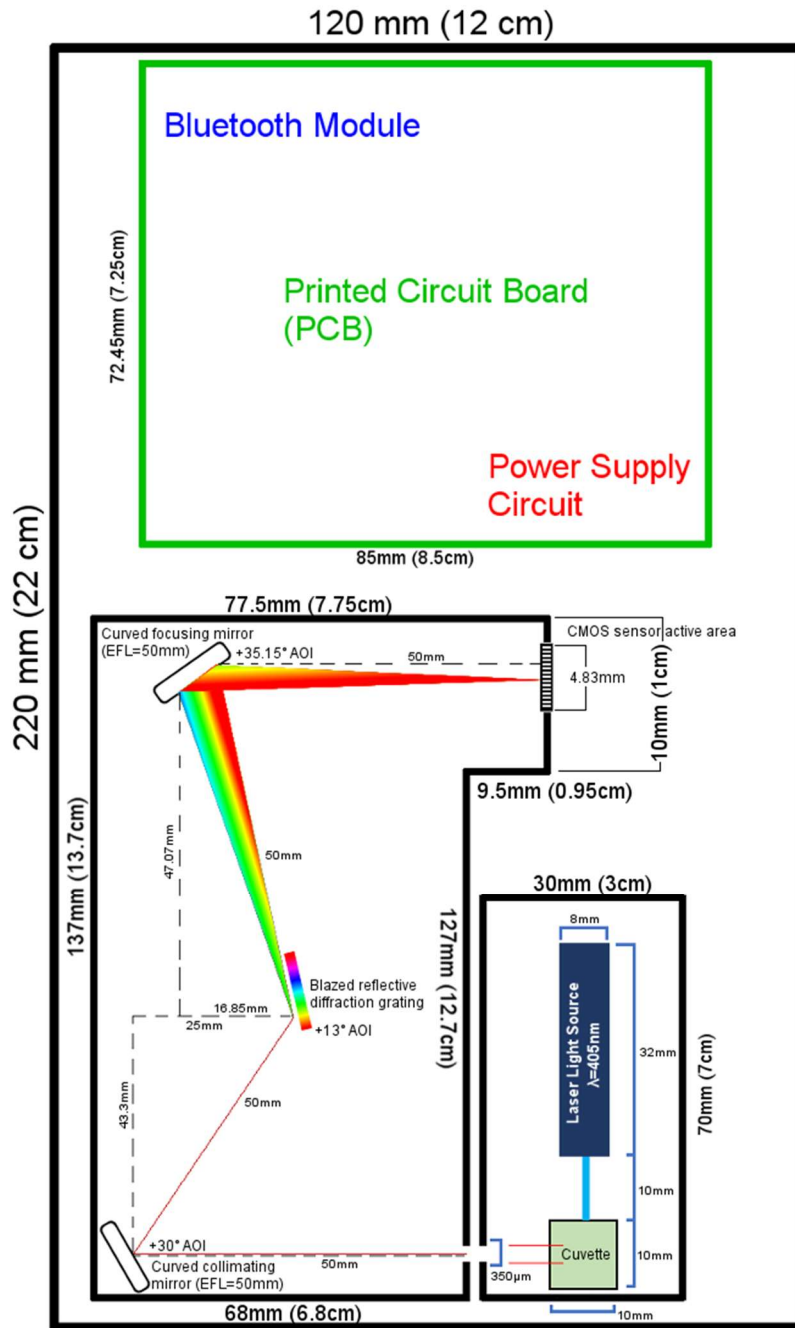


Figure 44. Complete housing design with dimensions, angles, and labels

Made by Samuel Knight

It is critically important, as discussed in 5.1.2 Optical Cavity Loss Calculations, that the sensor reads as much light as possible strictly from the fluorescence of the sample and excludes all other background noise. Thus, firstly, the sample and light source will be enclosed in their own case to ensure no extra light is scattered into the entrance slit. The chlorophyll samples should be excited only by the laser pump and the maximum amount of light should leave the sample and reach the slit. Eliminating all background noise at the source will prevent it from propagating through the spectroscopic system and ruining signal at the sensor. The material anticipated for use in this case design is Delrin or Teflon with the inside coated with antireflective black paint.

Secondly, the spectroscopic cavity will be enclosed in its own case with the dimensions shown in Figure 44. This is the most sensitive part of the CFS and so this case will be both airtight and watertight. This will also keep the case “light-tight”, preventing stray light that got into the housing from entering the spectroscopy cavity and interfering with the signal. The material anticipated for use for this cavity is Delrin or Teflon with the inside spray-coated with antireflective black paint. This case will be hard, but not impossible, to open so that no one can accidentally pop the case open and damage the optics inside. The optical components will be held in place using parts custom-machined from Delrin or Teflon so that the glass surfaces are not scratched. These parts and the case itself have not yet been designed on a detailed level; this is anticipated to occur within the upcoming semester.

Thirdly, the CFS itself will be housed in a case that allows the device to be easily transported, stored, and used in stable areas. The case will have the dimensions shown in Figure 44 and will be made from Delrin or Teflon. The reason plastic was chosen over metal is due to metal’s thermal conductivity. While plastics in general have a lower elastic modulus, impact strength, and tensile strength than metals, they have a much lower thermal conductivity. It is very important that the optics and electronics stay cool during operation so that thermal error is not introduced. While it is not anticipated that the CFS will undergo performance in conditions where the device will be subjected to testing its maximum thermal thresholds, it is an important metric to optimize when possible. The inside of the CFS’s case will be coated with antireflective black paint.

A discussion can be made about how the housing design meets the engineering requirement specifications, specifically the dimension requirement of being volumetrically less than 0.15m^3 . With the length and width given in Figure 44, the area of the device is 0.0264m^2 . In order to reach the volumetric requirement, the device will have to be shorter than 5.682m , a goal which is easily achievable. With that said, it can be said that the housing design above has preliminarily satisfied the dimensions requirement.

Cooling is often an important constraint in building the enclosure of an electronic device. Thermal damage to the electronics or the optics is a serious effect that must be considered. The thermal conductivity of plastic is much lower than metal, so plastic is again a good choice for the optical cavities and the CFS’s case. It is expected that passive cooling will be sufficient with the low power devices we are using which have low heat production.

5.2 Software Design

In the following subsections we will present the details of our software design process and final overall software design. The software design for this product was extremely important, due to the fact that we plan for our software is one of the features that makes our CFS stand out among other similar products. The software in our product will empower the user to effortlessly receive the results of the measurements on their mobile device and allow them to view the results of the analysis in multiple different easy to understand views.

To increase the efficiency of our software design, we divided our design process into two separate design processes: Embedded software design and Mobile software design. This separation was caused by the large differences between the two pieces of software, which we are treating as two separate programs; these differences include different programming languages, runtime environments, and constraints. We will go into more detail about each of these software design processes in the following sections.

In Figure 45 below you can see overall use-case diagram for our CFS. This diagram shows at a high-level how users will interact with the CFS software, and how the embedded and mobile programs will interact with each other. Use case diagrams are a form of UML diagram which overview the usage requirements for the system at a high level. In the diagram you will see the different actors and systems that will be at play throughout the use of our app, as well as the sequences of actions that are possible while using the CFS software.

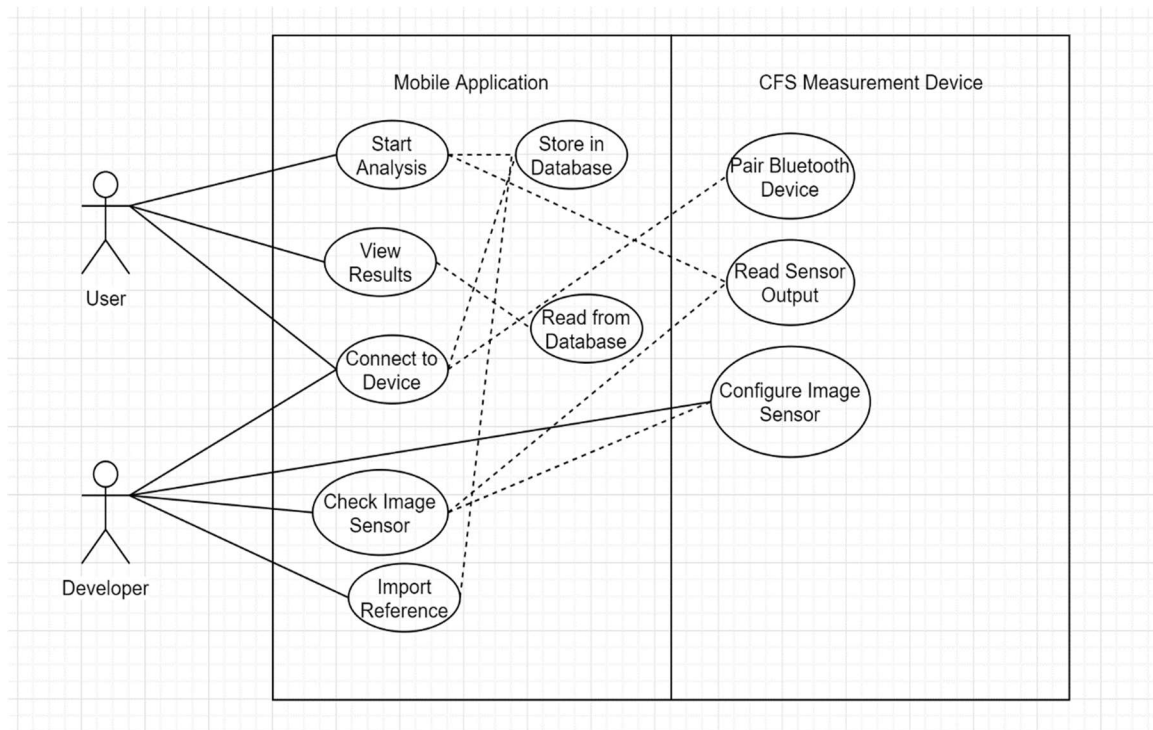


Figure 45. Use Case Diagram

5.2.1 Embedded Software Design

The embedded software design for this project consists of the software design for the firmware that will be running on the CFS measurement device. The firmware we will be developing will be executed on the Cortex-M4 32-bit microcontroller, which uses the ARM architecture. Because the software will be running on an ARM CPU, we have decided to use the C programming language for the development of this software. The C programming language was chosen because it is lightweight and will allow us to manage our memory use, which will be required due to the low amount of memory available to us on the microcontroller. It has also been chosen because there are many compilers that will compile C code into ARM machine code. The development will be done using the Microsoft Visual Studio integrated development environment (IDE).

The firmware will control the coordinating communication between the sensors on the physical device and ensuring that the sensor data during analysis is sent to the mobile application for further processing and visualization. The main sensors that our software will be interacting with on the device will be the image sensor, which will capture the light from the fluorescence of the chlorophyll, and the Bluetooth module, which will be used to send the sensor data to the mobile application. The firmware will also be tasked with properly configuring the sensor modules before analysis. More information about the processes that will be used to control the sensors

5.2.1.1 Block Diagram

In Figure 46, you will find a high-level diagram which illustrates the overall design of the embedded portion of our software design. This control flow diagram shows the main control-flow and logic for our program and is what we will use as a guide when we begin writing the software.

5.2.1.2 Image Sensor Interaction

The image sensor is the most important module in the CFS measurement device. This sensor will measure the amount of light hitting each individual pixel on the sensor, and report that data to the Microcontroller. We will be using this sensor in capture mode instead of video mode, to make the software development easier. Interaction with the image sensor will be achieved via 2 separate digital connections.

To configure the image sensor, we will be using an I2C connection which will allow us to choose an arbitrary register on the module to write to, and then write our data into that register. By writing specific data into the correct registers, we will be able to configure every aspect of the image sensor to ensure that we are properly capturing the information we need. To achieve this, we will be using a pre-written I2C library to facilitate the core I2C functionality, and then write code using that library to send the correct values to the necessary registers to configure the device. The generation of the register contents will be done using bitwise operations in the C programming language.

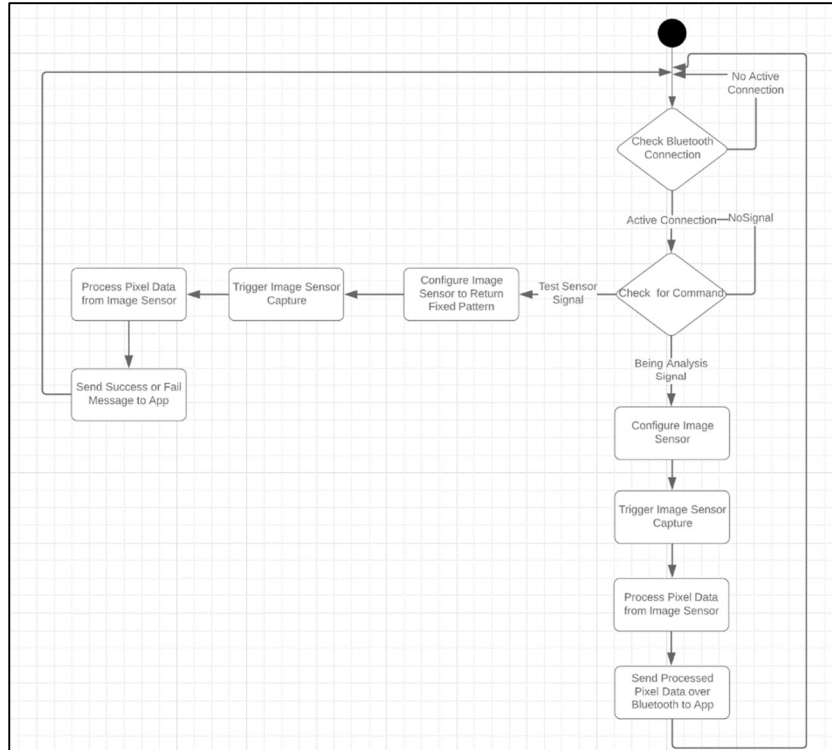


Figure 46. Embedded Software Block Diagram

Unlike the sensor configuration, the pixel data is not transmitted over an I2C connection. The sensor sends the raw pixel data over a parallel data connection line, which we will connect to the microcontroller. Because the image sensor only sends one pixel at a time over the parallel line, and because the data is sent as raw pixel data, we will need to write our own algorithm to read and process the data. This algorithm will be a large loop that will repeatedly read the incoming pixel data and store it for later processing, continuing until it has read the pixel data for all pixels in the image sensor.

Because we will have a limited amount of RAM memory, we will not be able to store all pixels in memory at the same time; to get around this, we have decided that we will only need to store the accumulation of all pixels in each column instead of the individual value of each pixel. This means that in our algorithm, once a pixel comes in the value of that pixel will be added to the current value of the addition of all of the pixels with that same X-axis, which will be stored in an array.

With this method, we will only need to store one array with an integer for each column, which is much less than storing an integer for each pixel. Once all pixels have been iterated over, we will then send this data over Bluetooth to the mobile application for further processing. One challenge that we are anticipating when reading the pixel data is the timing. The Image sensor utilized multiple clocks, and we will need to synchronize those clocks from the microcontroller to be able to have our code read the pixel values without missing any of them. Specifically, our main clock and pixel clock will need to be completely out of phase with each other, so that we may capture the value of the pixels

from the parallel line during the rising edge of the pixel clock, which will be synchronized with the falling edge of the main clock. A more detailed timing diagram of the IO timing can be found in Figure 47.

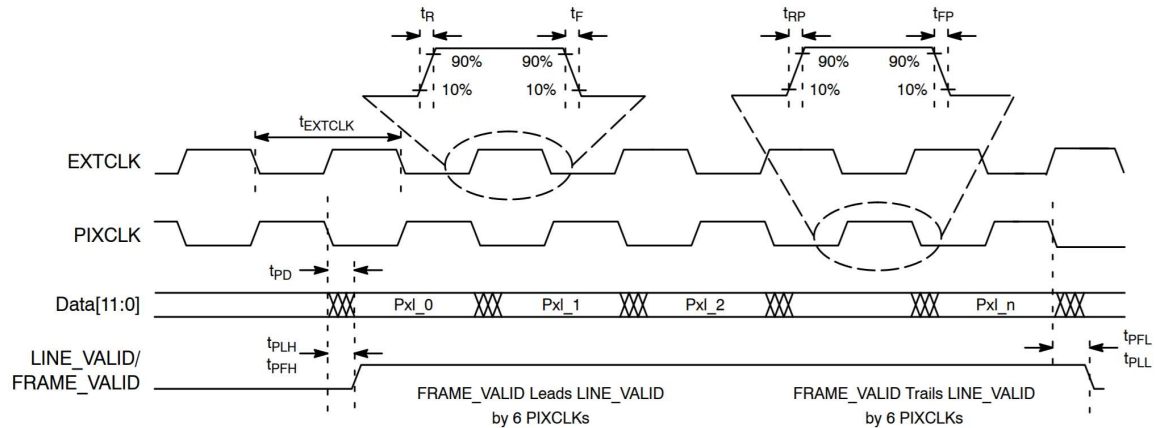


Figure 47. Timing Diagram for Reading Pixel Data

Used with permission from SCILLC dba ON Semiconductor. [ONS.ARO130].

5.2.1.3 Bluetooth Sensor Interaction

The Bluetooth module we will be using on the CFS measurement device is the RN4020 RF module. This module is controlled via ASCII commands over a UART connection. To interface with the module, we will use a pre-written UART library and build our own RN4020 library. The RN4020 library will abstract away the communication of the device using the UART library and allow use to use high-level functions such as “writeData” and “readData”, which will maximize code reuse and reliability. The functions that we will have to write will not be too complex, as we will only be using the basic features of the Bluetooth module. Our software will have to accept connections, keep track of the connection state, receive signals, and send data.

The signals that we will be receiving will be put into a C programming language switch statement to decide what function corresponds with that incoming signal, and what action to take. Once this has been decided, the action will be taken, and the result will be sent to the requesting device over Bluetooth; this data transmission will also have to be designed and coded by us. Throughout our software design, we will also be working to maximize the amount of time that the device spends in sleep mode, to capitalize on the low power capabilities of the Bluetooth module we will be using. To configure sleeps and wakes, we will be using the built-in timer module on the microcontroller with interrupts.

5.2.2 Mobile Application Software Design

The CFS’ Mobile Application will serve as the main user interface for the device. This software will consist of a mobile application which will configure the CFS to prepare it for sample analysis, as well as initiate any analyses and receive the sensor data resulting from

that analysis. The mobile application will be tasked with storing all analysis results and providing the end-user with the results in a multitude of graphics and result summaries which will ensure that the results of the analysis are both simple enough for a layman to get value out of the results, but also detailed enough for expert analysis.

Throughout the initial design process for the mobile application, the team decided to limit the target operating system for the mobile application to Android. This choice was made due to Android being easier to develop for and test on, due to Apple having more restrictions on application development and publishing for iOS. A summary of technical design choices for the mobile application can be found in Table 25 below, and more detailed explanations of the software design can be found in the subsections that follow.

Table 25. Mobile Application Design Choice Summary

| Design Choice | Final Selection |
|--------------------------------|-----------------|
| Supported Operating System(s) | Android |
| Earliest Supported Android API | API level 18 |
| Local Database Technology | SQLite3 |
| User Interface Framework | Kotlin |

5.2.2.1 Block Diagram

In Figure 48 below, you will find a high-level diagram which illustrates the overall design of the Mobile Application portion of our software design. This control flow diagram shows the main control-flow and logic for our program and is what we will use as a guide when we begin writing the software.

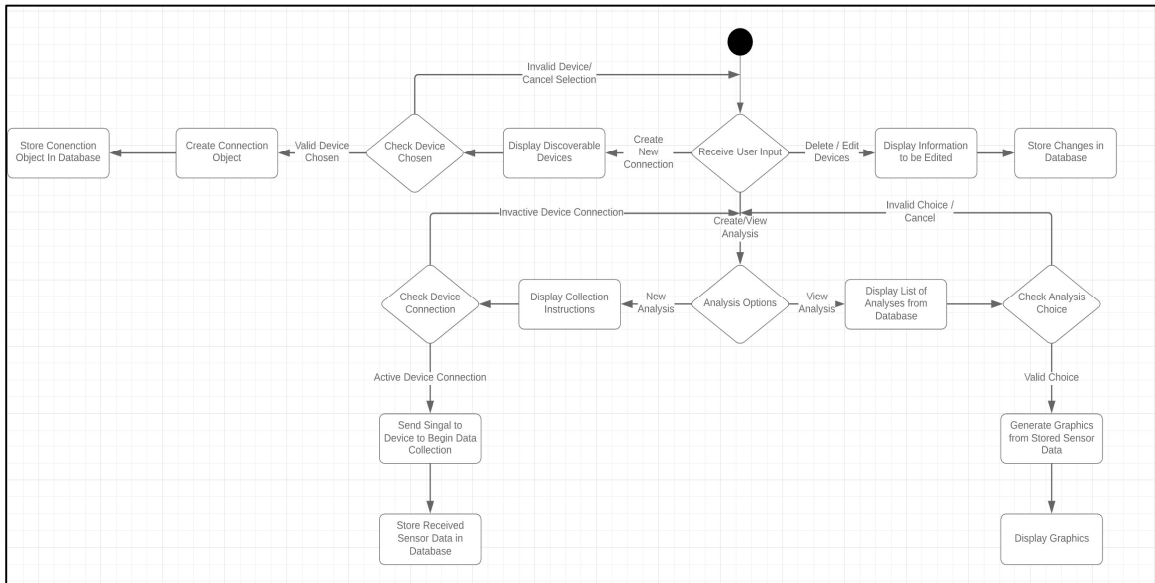


Figure 48. Mobile Application Block Diagram

5.2.2.2 Bluetooth Communication Design

Bluetooth Low Energy support was added to Android in Android version 4.3 (API level 18). This version of android included built-in platform support for BLE, providing APIs that developers can use to facilitate Bluetooth Low Energy communication as long as the phone has a Bluetooth module that supports BLE. The APIs provided by Google allow developers to easily discover devices, discover services, and transmit and receive information with other BLE devices in range of the mobile phone. In this section we will describe how our design leverages this API to allow for the transfer of sensor data between the embedded software and the mobile application.

Our mobile application will require the use of the “BLUETOOTH” and “BLUETOOTH_ADMIN” android permissions to ensure that it can both manage the Bluetooth connections on the device, including discovering and creating connections with new devices, and transmit and receive data. BLE devices can be defined as either central or peripheral devices; in this case the Mobile Application will be defined as a central device, because it will be scanning, while the measurement device will be advertising. The Mobile Application will also be a BLE “Client” device, because it will be receiving data from the measurement device, which will be the “Server”.

Bluetooth Communication in the app will be initiated by the user, who through the GUI will select an option telling the application that they want to pair their device with a nearby CFS device. During this stage the Mobile Application will search for devices that are advertising themselves with a certain device type defined in their metadata and will display these devices to the user so that they can choose which device they would like to pair with. Once a user chooses the CFS device they would like to pair with, the user will be prompted to input information about that CFS device, and all of the information about that device and connection will be stored in the local database.

After a successful Bluetooth connection is made, the mobile application will allow the user to initiate a sample analysis, which will then send a message over the Bluetooth channel to the CFS device to begin measuring. Measurement data will be sent from the CFS to the mobile application via Bluetooth Low Energy in the form of “Generic Attribute Profile (GATT)” metadata. The sensor data that is received via GATT metadata messages will be stored in the local database and associated with a collection time and location.

5.2.2.3 Local Database Design

The mobile application will use a database stored locally on the phone to store data related to the application. This database will contain a structured set of data that will allow the application to efficiently store and retrieve relevant information. The structured and relational properties of the database will allow the application to not only store the data, but also store the relationships between different pieces of data and retrieve that data based on the relationships in an efficient way.

For our application, we have chosen SQLite3 as our database management system. We chose SQLite3 because it is lightweight and does not require an extra program to be running on the mobile device. SQLite databases are stored in a single file, so they are portable, meaning they will work on any mobile device as long as we are able to store files, and require a low amount of resource, which reduces overhead.

The SQLite database will mainly be used to store 2 types of data: CFS device data and analysis data. The CFS device information that will be stored will be information about the different CFS devices that the mobile application has connected to in the past, along with metadata about each device. The metadata that will be stored will include a nickname for the CFS device, the embedded software version that the CFS device is running, the hardware ID for that device, and the last time that the Bluetooth connection with that device was alive. The analysis data will include the results that are read from the image sensor on the CFS device for a given analysis. The analysis data that will be stored will include both reference analyses and user-generated analyses. Reference data will be used to compare the health of the users' plants to known healthy or unhealthy plants.

Because the data we will be storing will have three main types, we have decided to use 3 tables in our Database. There will be one table for user analyses results, one for reference analyses, and one table for CFS device connections. Because we will be using a relational database, the three tables will be related to each other using foreign keys where necessary. Our database design is detailed in the Entity Relationship Diagram in Figure 49.

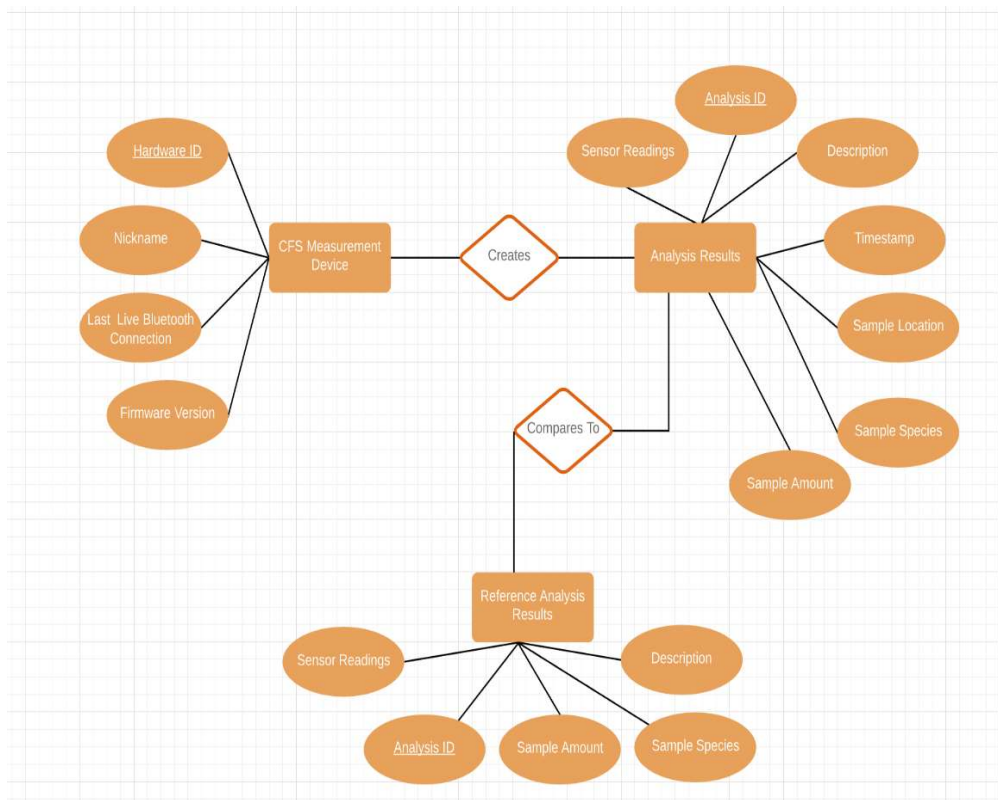


Figure 49. Entity Relationship Diagram for Application Database

5.2.2.4 Graphical User Interface Design

The majority of the software developed for the mobile application will be for the Graphical User Interface of the application. Because the mobile application will be the primary way for users to interface with the CFS device, we have put a lot of time into ensuring that the GUI for the application is well-designed and easy to use. We have chosen to use Android Studio for the overall development of the application, including the graphical user interface development.

When developing an android application, there are many user interface frameworks that are available. For the CFS mobile application, we have chosen to use the Kotlin programming language and framework; this choice will make the development for the GUI portion of the application easier, because Kotlin has been designed to simplify Android application development, especially the GUI portion of the software development.

When designing what the GUI for the application will look like, we will be following the Android Material Design specification. This specification is a comprehensive guide from Google for designing visual, motion, and interaction aspects of an Android application. By closely following the Material Design best practices, we will ensure that our application looks and feels like other android applications; this will increase the ease of use for the mobile application, as well as make it look more appealing to our users.

A common issue that we have seen many other developers run into when designing a graphical user interface is that many people do the software development and visual development simultaneously, which can lead to conflicting design choices and may require a lot of re-development. For this reason, our GUI design process consisted of us sketching out all of the views and actions that will be necessary for our application before we began working on any of the software. In Figure 50. GUI Design Sketch, you will find our initial sketches for the graphical user interface of the CFS mobile application.

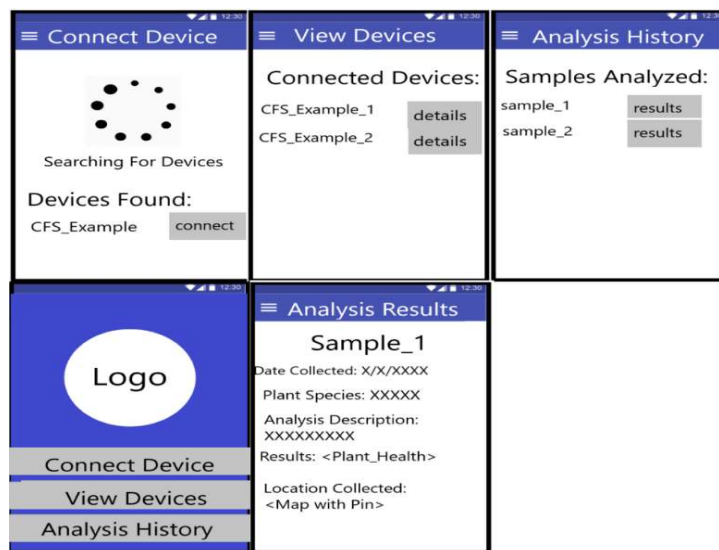


Figure 50. GUI Design Sketch

5.3 Bill of Materials

Table 26 shows the bill of materials for the current hardware design. The bill of materials' Total Price column includes the price of shipping.

Table 26. Bill of materials

| Device | Manufacturer | Description of Purpose | Quantity | Price per unit | Total Price |
|--------------------------------|---------------------------------------|--------------------------------|----------|----------------|-----------------|
| MZH8340550D-AL01A | Zhuhai MZLASER Technology Company LTD | Pump light source | 2 | \$9.00 | \$40.38 |
| CM254-025-P01 | ThorLabs | Collimating/Focusing mirrors | 2 | \$60.34 | \$120.68 |
| 33066FL01-270R | Newport Corporation | Reflective diffraction grating | 1 | \$89.00 | \$89.00 |
| ARDR CMOS Monochromatic Sensor | ON Semiconductor | Imaging sensor | 1 | \$8.38 | \$17.92 |
| OPT3002DNPT | Texas Instruments | Testing power sensor | 20 | - | \$23.23 |
| PCB | TBD | Component Integration | 3 | - | \$25.00 |
| STM32F407VET | STMicroelectronics | CPU | 2 | \$4.41 | \$8.82 |
| STM32F407VET6 | STMicroelectronics | Development Board | 1 | \$8.79 | \$8.79 |
| RN4020 | Microchip | Bluetooth module | 1 | \$15.40 | \$29.85 |
| AP5056 | Wuxi Chipown Microelectronics | Battery Charging | 2 | \$0.11 | \$0.22 |
| INR18650-25R | Samsung SDI Co. | Energy Storage | 2 | \$3.65 | \$7.30 |
| TPS62231DRY | Texas Instruments Inc. | Voltage Regulation | 1 | \$1.23 | \$1.23 |
| TLV71328PDBV | Texas Instruments Inc. | Power Supply | 1 | \$0.20 | \$0.20 |
| TPS62233DRY | Texas Instruments Inc. | Power Supply | 1 | \$1.32 | \$1.32 |
| TPS799195 | Texas Instruments Inc. | Voltage Regulation | 1 | \$0.58 | \$0.58 |
| Total | | | | | \$374.52 |

5.4 Design Summary

The design of the chlorophyll fluorescence spectrometer required the interdisciplinary cooperation of computer, photonics, and electrical engineering. The constraints were largely defined by design decisions relating to the optics of the system. Decisions branched from the choice of sensor and light source, to the choice for processor and Bluetooth module based on the computing, data analysis and connectivity required. The methods for meeting our requirement specifications included some compromises, including the size and weight with battery life, processing power and power consumption. At every stage of the design process, cost was a factor. Communication was required between the designers in order to guarantee that each component of the CFS would function as required.

6. Part Acquisition and Testing

This section describes the timeline of acquisition and testing phase of all component parts researched in section 4. Project Research to complete section 5. Project Design. Included herein is the introduction to the testing phase, individual component testing, and the first attempts at device cohesion through interdisciplinary collaboration on part integration.

6.1 Introduction

One of our team's goals for this semester is to acquire and test all major parts before the end of Senior Design 1; this section will document our progress towards those two goals. Throughout this section we will document our current part acquisition progress for our major parts as well as our testing procedures, progress, and results. Testing for our CFS will be split into two main phases for this semester: the individual module testing phase, and the initial prototyping phase.

The individual module testing phase will be conducted to achieve the following goals for each module tested:

- Ensure the module is in functioning order
- Ensure that we know how to properly use the module
- Ensure that the module produces the expected data in a format that we know how to work with
- Ensure the module is compatible with our MCU
- Confirm power draw of module
- Find any issues with the module that were not found during the research phase of this project

After the individual modules have been fully tested, we will begin the initial prototyping phase. This phase will be conducted to achieve the following goals:

- Ensure that all our components are compatible with each other
- Fully integrate all major components with our development board so that we can have a base circuit to build our schematic and PCB design from
- Test power delivery and power consumption
- Test accuracy of the optics design

6.2 Status Summary

As of 11/15/2019, we have received all major components needed for individual module testing and the initial prototyping stages. Our team has transitioned into the initial testing phase of the project on 11/18/2019. As of 11/25/2019, all major testing of components has been completed.

6.3 Part Acquisition

The following table contains a timeline for the acquisition and testing of the major components of our project.

Table 27. Part Acquisition Timeline

| Part Name | Description | Date Ordered | Date Received | Testing Date |
|--------------------------------|--------------------------------|--------------|---------------|--------------|
| MZH8340550D-AL01A | Light Source | 11/05/2019 | 11/15/2019 | 11/25/2019 |
| 33066FL01-270R | Reflective Diffraction Grating | 11/07/2019 | 11/15/2019 | 11/24/2019 |
| STM32F407VET6 | Development Board | 11/05/2019 | 11/10/2019 | 11/21/2019 |
| ARDR CMOS Monochromatic Sensor | Imaging Sensor | 11/05/2019 | 11/11/2019 | 11/25/2019 |
| OPT3002DNPT | Ambient Light Sensor | 11/05/2019 | 11/08/2019 | -- |
| RN4020 | Bluetooth Module | 11/07/2019 | 11/11/2019 | 11/21/2019 |

6.4 Hardware Testing

This section contains the testing procedures and results for the major components of the CFS. This section will not detail the efforts on any multidisciplinary collaborative efforts. This section is only for testing each individual component to ensure its operability as a standalone device. Once the device has been tested and has been proven to work, the device will be marked as greenlit for the chlorophyll fluorescence spectrometer prototype.

6.4.1 RN4020 – Bluetooth Module Testing

On 11/11/2019 our team received the RN4020 Bluetooth module and has begun planning out our testing procedures for this module. This section contains the testing procedures and the testing results for this module. A photo of the received module can be found in Figure 51.



Figure 51. RN4020 Bluetooth Module

The testing for this module will consist of two tests. The first test will make sure that the module is functioning properly in general. The second test will ensure that the module will connect to our MCU. Before conducting any tests, we had to solder leads onto Bluetooth module so that it could be connected to other devices on a breadboard. For our first test, we wanted to ensure that the module was able to turn on, accept commands, and broadcast a signal properly.

To achieve this, we connected the device directly to a computer via a USB to UART adapter and configured the device using the device's UART command API. Using the UART command API we configured the device to be broadcasting using the name "RN4020_Test", and then used a mobile application on a phone to search for Bluetooth Low Energy devices that were broadcasting to see if we could see a device broadcasting with the proper name. This test was successful, as seen in Figure 52, which shows that the device is working properly and has the ability to broadcast a signal. An image of the device being tested on a breadboard can be found in Figure 52.

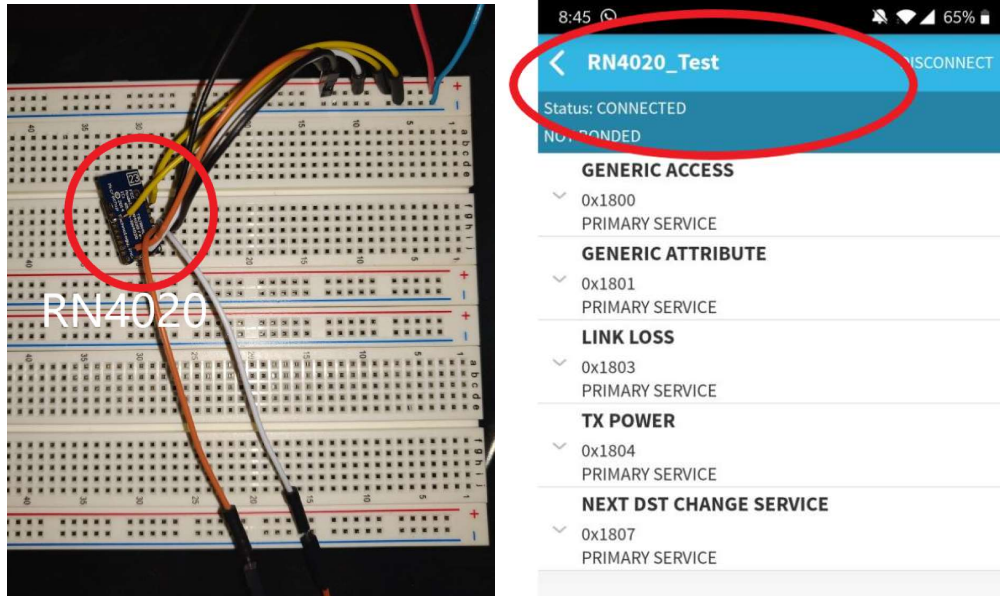


Figure 52. RN4020 Individual Module Testing

For our second test, we needed to make sure that the Bluetooth module could send and receive data from the MCU, as well as be configured automatically via the MCU. To achieve this, we used the STM32CubeMx and Keil IDE software to generate C code that would have the MCU automatically configure the Bluetooth module to broadcast a signal using the name "MCU_Conn_Test". When we initially tried to test this, we ran into an issue where the module would not start broadcasting a signal after the microcontroller was turned on.

After debugging we discovered that this was due to the MCU sending the configuration commands too early before the Bluetooth module was ready to accept commands. To fix this, we implemented a check in our code that waited to receive a signal from the Bluetooth module before sending the configuration commands. This also worked to test to see if the

MCU was properly receiving data from the Bluetooth module. After adding this check to the code, we used a mobile phone application to look for a Bluetooth Low Energy symbol with the proper name. This test was also successful, as seen in Figure 53, which shows that the device was able to send and receive commands to and from the MCU. An image of the device being tested on a breadboard can be found in Figure 53.

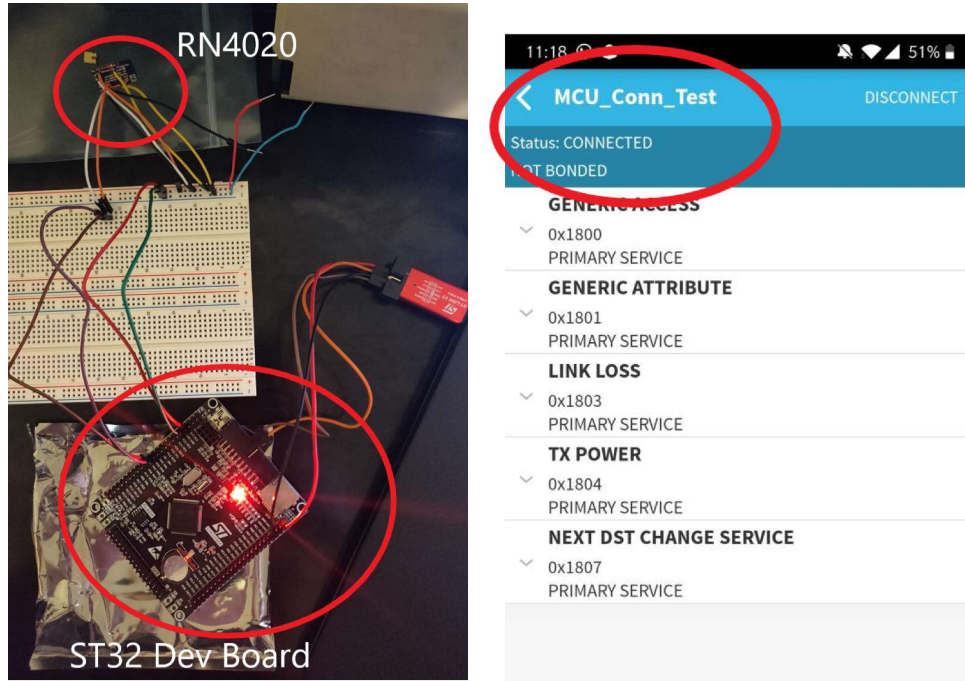


Figure 53. RN4020 Integration Testing

After completing these tests in full, we were able to confirm that the device is indeed working properly, that it can connect to our MCU, and that we can send and receive data between the MCU and the module. A summary of the results of these tests can be found in Table 28.

Table 28. RN4020 Testing Results

| Test | Result |
|------------------------------|------------|
| MCU Connectivity | Successful |
| Module Properly Functioning | Successful |
| Confirm Expected Data Output | Successful |

6.4.2 AR0130CS – CMOS Monochromatic Sensor Testing

The AR0130CS CMOS monochromatic sensor (for short, the ARDR) was received on 11/11/2019 and planning for the testing procedures of this device has begun. This section contains the testing procedures and will eventually contain the testing results for this module. A photo of the received module can be found in Figure 54.

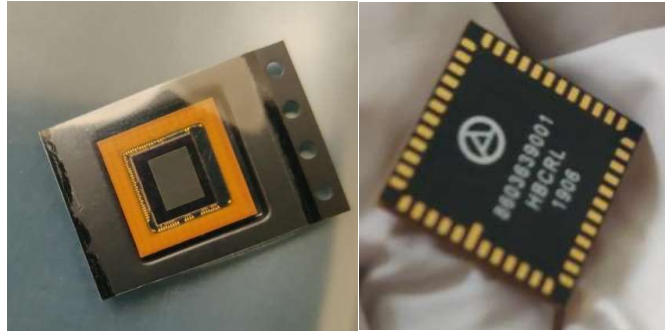


Figure 54. AR0130CS Monochromatic Sensor

The testing for this module will consist of one tests that will make sure that the module is functioning properly, that it will connect to our MCU, that we can properly write to the configuration registers to the module from our development board, and that we can properly parse the raw pixel data that the module is sending back to us. To test all of this, we will solder leads onto sensor module and connect it to our Development board using a breadboard. When doing breadboard testing of this module, we will be using a multichannel DC power supply to provide the different power inputs that the sensor needs. We will also ensure to use .1uF and 10uF decoupling capacitors on each power source for the safety of the module. An image of the sensor connected to our MCU can be seen in Figure 55.

For the first half of the test, we will just make sure that the sensor can communicate with the MCU over I2C. The I2C channel is only used by the sensor for configuration purposes, and we will use this to confirm that the sensor is properly functioning, that the sensor can connect to our MCU, that we are properly powering the sensor, and that our software can write to the configuration registers. This test was completed on 11/25/2019 and was successful.

After connecting the sensor to our MCU we were able to read an example configuration register and print the value to a debug console connected to the device via UART. After confirming that the configuration value read matched the default configuration for the device, we changed the configuration via the I2C connection and then read the register value again. After printing the configuration value to the debug console the second time, we confirmed that this value matched the new configuration value that we had written. The fact that these tests were successful shows that the sensor is working properly and can interact with our MCU and software.

During the previously described I2C configuration testing process, one of the solder joints on the sensor broke. This was an expected issue due to how small the pads on the sensor are, making soldering leads onto the sensor very hard. Due to the timing of this issue, it delayed our second stage of testing for this device, which was supposed to test not only the configuration of the device, but reading the pixel data from the device. After we re-solder the lead onto the sensor, we will continue testing the device to see if we can properly get pixel data out of the sensor. To do this, we will connect the MCU to the parallel data output bus of the image sensor and see if we can parse the pixel output from the sensor.

To ensure that we are properly reading and receiving the raw pixel data, we will configure the image sensor using the I2C connection to display a “test pattern”. When configured in this manner, the sensor pixels will always return the configured pattern, which we can compare against the pixel data that we are receiving to ensure that we are reading the expected pattern. The results of all of our testing can be found in Table 29.



Figure 55. Monochromatic Sensor Configuration Testing
Table 29. Monochromatic Sensor Testing Results

| Test | Result |
|------------------------------|------------|
| MCU Connectivity | Successful |
| Software Interaction | Successful |
| Module Properly Functioning | Successful |
| Confirm Expected Data Output | Successful |

6.4.3 STM32F407VET6 – Development Board Testing

The STM32F407VET6 development board arrived on 11/10/2019 and planning for the testing procedures of this device has been completed. This section contains the testing procedures the testing results for this device. An image of the received development board can be found in Figure 56.

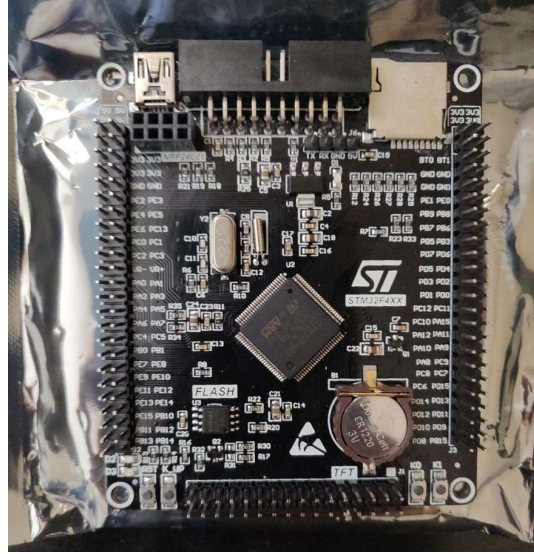


Figure 56. STM32 Development Board

The testing for this module will consist of one test that will make sure that the board is functioning properly, that we can properly write software to the MCU using our integrated development environment, and that we can properly view the results of our software. To test all of this, we will generate, compile, and deploy C code using the STM32CubeMX and Keil IDE software. Once deployed to the development board, this code will cause the board to send a string of data over a UART channel. Once the code has been deployed, we will connect a computer to the UART channel and ensure that we can receive the string that the board is sending, which will confirm that the MCU is working properly, and that we can successfully write code to the MCU.

The testing for this module was completed on 11/21/2019. We had a few unexpected complications come up during our testing of this module, but after getting all complications ironed out, we were able to get a successful result from the test described in this section. The complications that were encountered mainly stemmed from the team's lack of experience with an STM development board; our team only had experience working with MSP430 development boards and we expected this board to function similarly to the MSP430 boards, which was not the case.

The first complication came when trying to flash our compiled code to the device. With other development board we had used in the past, it was possible to flash the board using a USB connection to the board, and due to the fact that the STM32 board we were using had a USB connection we expected it to be possible to use this USB connection to flash the device. When we began testing, we realized that the USB connection could not be used for flashing the device, and we would need a separate "STM-LINK" device to be able to write code to the device, this process can be seen in Figure 57. This complication delayed our testing schedule due to having to wait for the STM-LINK device to arrive to be able to test all modules.

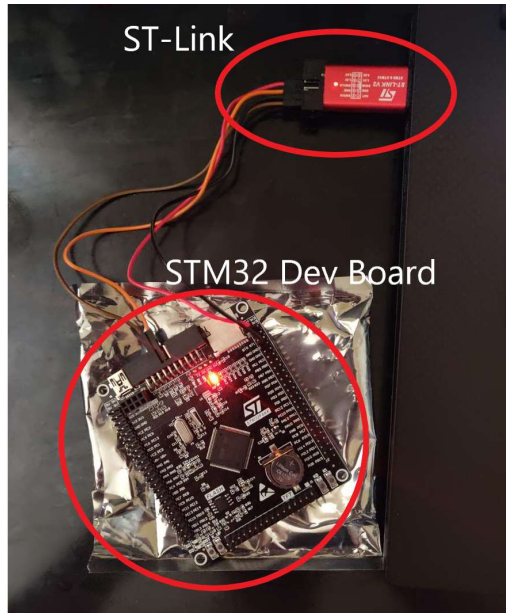


Figure 57. Flashing Development Board

The other complication we encountered was similar to the first; much like in the first complication, we expected to be able to use the USB connection on the board for our UART communication due to being able to do that with other boards we had used in the past. This was not the case, and we also needed to buy a separate USB to UART adapter to be able to receive UART signals from the board, further delaying the testing process. As soon as our UART and STM-LINK devices arrived we were able to conduct the test as described earlier. After we deployed the code to the device and connected the device to a computer via a USB to UART connection, we were able to receive the expected string and confirm that the device was working as expected. Figure 58 shows the development board connected to a laptop via a USB to UART adapter for the purposes of this test.

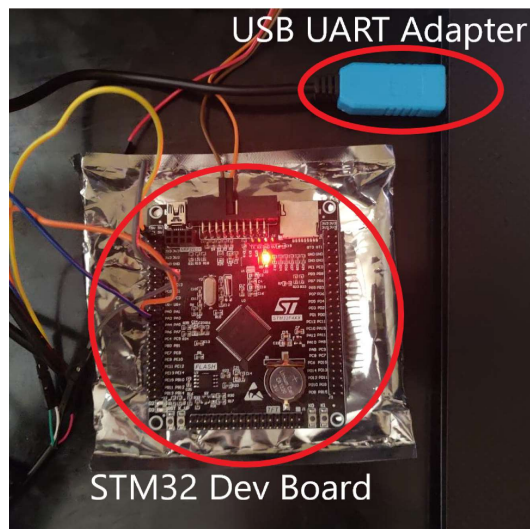


Figure 58. Testing Development Board

Table 30. Development Board Testing Results

| Test | Result |
|----------------------------|------------|
| IDE Connectivity | Successful |
| Software Deployment | Successful |
| Board Properly Functioning | Successful |

6.4.4 Newport 33066FL01-270R Diffraction Grating Testing

The Newport Corporation’s diffraction grating 33066FL01-270R was received on 11/14/2019, shown unopened in Figure 59 due to the extreme sensitivity of the optic. Table 31 shows the sources which the diffraction grating was tested against and whether the grating produced a spectrum in line with traditional research findings of similar sources. The grating produced ideal rainbow spectra for the two different white light sources and effectively diffracted the laser source, satisfying the testing procedure.

Table 31. Diffraction grating spec test

| Source | Waveband | Status |
|---|--------------|------------|
| Uncollimated white LED (phone flashlight) | 400 – 700 nm | Successful |
| MZH8340550D-AL01A laser light source | 405 nm | Successful |
| 60W non-dimmable soft white LED bulb | 400 – 700 nm | Successful |



Figure 59. Richardson Diffraction Grating (unopened)

6.4.5 Laser Testing

The laser module being used for this CFS was ordered from Zhuhai MZLASER Technology Co., Ltd in Guangdong, China. Two laser modules were ordered in case there was any electrical malfunctions during testing which could render one of the modules unusable. The lasers were received on November 15, 2019 and Table 32 displays the laser specifications which were tested for accuracy on November 25, 2019.

Table 32. Tested Specifications for Laser Module

| Specification | Company Listed | Manually Tested |
|--------------------|----------------|-------------------|
| Peak Wavelength | 405 nm | 405 nm @ 23°C |
| Optical Power | 40-45 mW | 44.4 mW @ 33.5 cm |
| Beam Spot Diameter | 6 mm @ 10 m | 4.4 mm @ 33.5 cm |

For testing, the laser module was connected to a Keithley 2231A-30-3 triple channel DC power supply with a DC operating voltage of 2.8 V. The beam spot diameter was measured using a micrometer on a white screen. The peak wavelength and the optical power were determined using a gentec- ϵ Maestro 234907 power meter. All the devices were set up on a Thorlabs optical bench and the setup to measure the beam spot diameter at 33.5 cm can be seen in Figure.

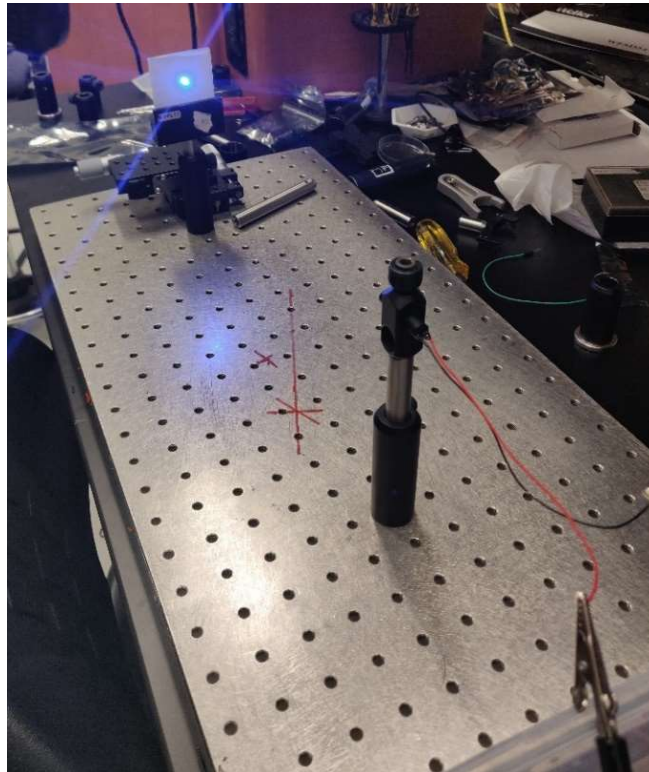


Figure 60. Setup for Measuring Laser Beam Spot Size

6.5 Software Testing

This section describes the testing procedures that will be used throughout the entire software development process to ensure that the software is functioning properly on our hardware and is free of any major bugs. This section includes procedures for testing both the embedded software and the mobile application.

6.5.1 Development Board Emulation

When developing embedded software, it is often difficult to fully test the code that is being written due to a lack of debugging capabilities on the embedded device, which reduces the visibility that you have on the code as it is running. To circumvent this restriction, we will be using an emulator to run and debug our embedded software before deploying it to our microcontroller.

One large limitation of this testing method is that it will not allow us to test any of the code that requires interaction with our sensors, as that cannot be emulated. This testing will mainly be useful for ensuring that the code compiles and runs correctly, and that there are no major bugs. When conducting this testing, we will use the Qemu emulator to run and debug our code. When debugging our code, we will specify breakpoints where we will pause the execution of the code and ensure that the variables in memory at that time are what they should be. We can also use debugging features to set breakpoints before crucial parts of the code that need to be tested and step through those sections of code one instruction at a time. This will give us insight into how exactly the code will be running on our microcontroller; this increased understanding of how our code will execute will make debugging issues on the physical microcontroller much easier.

6.5.2 Physical Measurements

Even though we will be using an emulated environment to test our embedded software, this environment will not allow us to test the effects that our software will have on the physical MCU and how this will affect our external sensor modules. Testing that the physical effects reflect what is expected by the developer is important to avoid damaging the microcontroller or even our external modules. The main limitation of this testing method is that it will require expensive equipment, such as an oscilloscope, which will always not be available to our team. Because of this limitation, we will not be conducting physical measurement tests as often as the emulation tests for our embedded software.

The physical testing for our software will require separate equipment; the main pieces of equipment that we will be using will be Oscilloscopes and Multimeters. The oscilloscopes will be used to measure waveforms generated by specific pins on the development board to ensure that our software is generating the waveforms at the correct frequency. Specifically, we will be using this to test the external clock signal that our MCU will have to provide our image sensor with. To test this, we will run our software that will generate the proper clock signal and use an oscilloscope to measure the frequency of the clock signal and ensure that it is in the proper range needed by the image sensor. We will also use an

oscilloscope to observe I2C and UART communication between the MCU and our external modules, to ensure the communication reflects what is expected based on what the software should be doing. We will also use multimeters to check the GPIO pins that are used by our software after running the software to ensure that the software is setting every GPIO pin to the expected value.

6.5.3 Mobile Application Automated Testing

When developing the mobile application, we will need to constantly test the software to ensure that the changes being made do not break previously added functionality or introduce bugs. Because this testing will need to be conducted often, we will be using an automated testing suite named Junit5 to achieve this testing. Junit 5 will allow us to write automated tests that will run every time before the code is compiled. The main drawback for this testing method is the amount of time needed when initially setting up the tests to learn the testing framework and create the automated tests.

While the unit tests that we mentioned in the previous section will allow us to test the core logic of the business application, we will still need to test the user interface to ensure the buttons and functionality on the user interface work as expected. To automate user interface testing, we will be using another framework named Espresso. Espresso is similar to Junit in the sense that we will have to spend time initially to learn the framework and create our test cases, but once they are created, they will automatically run and update us whenever the mobile application has lost functionality.

7. Administrative

The section herein describes the administrative content not pertinent to the overall design, construction, or research for the CFS. Covered in this section are milestones and timelines for the group, budget for the project, avenues of financing, and division of labor.

7.1 Milestones

To ensure the Chlorophyll Fluorescence Spectrometer is designed properly meeting various design and timing constraints, several deadlines were enacted. The necessary objectives to be completed for each deadline during the first semester appear in Table 33. Possible objectives to be completed over the next semester are listed in Table 34.

Table 33. Milestones for Senior Design 1

| Objective | Start Date | End Date | Status | Lead |
|--------------------------------|-------------------|-----------------|---------------|-------------|
| Administrative | | | | |
| Project Concept | 8/26/2019 | 8/30/2019 | Complete | Group 1 |
| Role Assignment | 8/30/2019 | 9/5/2019 | Complete | Group 1 |
| Initial Research | 9/5/2019 | 9/19/2019 | Complete | Group 1 |
| D&C Document | 9/9/2019 | 9/20/2019 | Complete | Group 1 |
| Component Research | 9/21/2019 | 10/31/2019 | Complete | Group 1 |
| Initial Document | 9/25/2019 | 11/1/2019 | Complete | Group 1 |
| Component Ordering | 11/2/2019 | 11/14/2019 | Complete | Group 1 |
| Draft Document | 11/5/2019 | 11/15/2019 | Complete | Group 1 |
| Initial Optics Design | 11/5/2019 | 12/1/2019 | Complete | PSE |
| Initial PCB Design | 11/5/2019 | 12/1/2019 | Complete | EE |
| Initial Software Design | 11/5/2019 | 12/1/2019 | Complete | CE |
| Final Document | 11/16/2019 | 12/4/2019 | Complete | Group 1 |
| Research and Design | | | | |
| Optical Cavity | 11/1/2019 | 11/20/2019 | Complete | PSE |
| Sensor | 10/1/2019 | 10/23/2019 | Complete | PSE |
| Housing | 11/1/2019 | 12/1/2019 | Complete | PSE |
| PCB Design | 11/5/2019 | 11/29/2019 | Complete | EE |
| Mobile App UI | 11/5/2019 | 12/1/2019 | Complete | CE |
| Sample Preparation | 11/19/2019 | 11/19/2019 | Complete | PSE |
| Wireless Components | 11/5/2019 | 12/1/2019 | Complete | CE |
| Parts Ordered | 11/5/2019 | 11/15/2019 | Complete | Group 1 |
| Parts Tested | 11/18/2019 | 11/30/2019 | Complete | Group 1 |
| Parts Confirmed | 12/1/2019 | 12/1/2019 | Complete | Group 1 |

Table 34. Milestones for Senior Design 2

| Objective | Start Date | End Date | Status | Lead |
|-----------------------|------------|-----------|-------------|---------|
| Final Optics Design | 1/6/2020 | 1/30/2020 | Researching | PSE |
| Final PCB Design | 1/6/2020 | 1/30/2020 | Researching | EE |
| Final Software Design | 1/6/2020 | 1/30/2020 | Researching | CE |
| CDR Presentation | -- | -- | Not Started | Group 1 |
| Peer-Review | -- | -- | Not Started | Group 1 |
| Conference Paper | -- | -- | Not Started | Group 1 |
| Initial Demonstration | -- | -- | Not Started | Group 1 |
| Final Presentation | 4/17/2020 | 4/17/2020 | Not Started | Group 1 |
| Exit Interview | 4/22/2020 | 4/22/2020 | Not Started | Group 1 |

7.2 Budget and Avenues of Financing

The University does not provide us with any funding for our materials. We have asked several companies if they were willing to sponsor us for our project with any amount of funding, but none have responded to our queries. Therefore, it should be noted that this project is being funded entirely by the four students who are building this device.

Table 35 shows details of the budget for this project. Since this project has no external funding, we are trying to minimize the cost for the CFS while meeting every one of our design constraints and standards. We have borrowed several components for testing that may need to be purchased during the next phase of our design.

Table 35. Budget details for CFS

| Component | Area of Device | Provided By | Quantity | Price per unit | Total Price |
|---------------------|----------------|--------------|----------|----------------|-----------------|
| Housing | Housing | Students/UCF | 1 | \$80.00 | \$80.00 |
| Laser Source | Laser Cavity | Students | 1 | \$9.00 | \$9.00 |
| Quartz Cuvette | Laser Cavity | UCF | 1 | Borrowed | Borrowed |
| Mirrors | Optical Cavity | Students | 2 | \$60.34 | \$120.68 |
| Diffraction Grating | Optical Cavity | Students | 1 | \$89.00 | \$89.00 |
| Imaging Sensor | Optical Cavity | Students | 1 | \$8.38 | \$8.38 |
| CPU | PCB | Students | 2 | \$4.41 | \$8.82 |
| Development Board | PCB | Students | 1 | \$8.79 | \$8.79 |
| Bluetooth Module | PCB | Students | 1 | \$15.40 | \$15.40 |
| Power Supply | PCB | Students | 1 | \$10.85 | \$10.85 |
| Total | | | | | \$350.92 |

It should be noted that the budget shown above does not match the bill of materials shown in Table 26. This is because minor parts and the TI OPT3002 testing sensor were omitted from this list.

7.3 Division of Labor

Shown below is Table 36 is the division of labor for the task of building, designing, and executing the chlorophyll fluorescence spectrometer. Table 36 shows all tasks attempted, the lead executor, the helping executor(s), and the college major associated with each task.

Table 36. Division of labor for the CFS

| Task | Lead | Helpers | Major |
|----------------------------|-------------|----------------|--------------|
| Light source cavity design | Robert | -- | PSE |
| Sample holder design | Robert | -- | PSE |
| Spectroscopy cavity design | Samuel | Robert | PSE |
| CFS Housing design | Samuel | Robert, Luke | PSE |
| PCB design | Luke | David | EE, CE |
| Power circuit | Luke | -- | EE |
| Embedded software design | David | -- | CE |
| Mobile application design | David | -- | CE |

8. Project Summary/Conclusion

The design of the chlorophyll fluorescence spectrometer is a result of overcoming design challenges, meeting engineering requirements, collaborating with different fields of engineering, and agreeing on standards, constraints, and compromises. The engineering requirement specifications that started out as a design table on a screen has evolved into a device capable of observing fluorescence from samples and categorizing them based on intensity.

The CFS consists of three major components: the source cavity, the spectroscopic cavity, and the PCB. The source cavity excites a chlorophyll sample to fluorescence using low-visible light at 405nm. The spectroscopic cavity splits the fluorescence into its component wavelengths using a diffraction grating and two concave mirrors and directs it to an imaging sensor. The PCB powers every component of the CFS, reads data from the sensor, and transmits said spectroscopy data to a user via a mobile app for ease of review and consideration.

The group consensus is that the work included herein is a result of individuals collaborating to produce an idea of original design and implementation. It is expected that the project shown in this document will be successfully produced within the next semester and will work exactly according to specification. With the ease of access to the CREOL machine shop and with knowledge and experience of hardware design already in place among the majority of group members, it is expected that there will be no major problems building the physical body of the CFS.

Problems that may occur during the build semester include modeling issues, 3-D printing, and component burn-out. If the report needs to be updated to include three-dimensional models of the CFS, this will be an issue since only the minority of team members have experience using modeling software. The same issue goes for 3-D printing, especially if components need to be custom-made since they are not readily available commercially or from the CREOL machine shop. Also, there is a chance that components become damaged or unusable during the build and testing process in the coming semester. If this happens and replacement parts need to be ordered, especially the optics, then the cost requirement of the device will increase dramatically. Time is also a large consideration in this regard. If we have a problem with our PCB design and it needs to be remade, that can take weeks to get the next revision. While coming up to our deadlines in senior design two, we may not have the time to order another printed circuit board. This is why it is crucial to design, build, and test the printed circuit board as soon as possible.

A brief discussion can be made about the engineering requirement specifications and whether, so far, the CFS has met the specifications listed in 2.3 Requirement Specifications and 2.4 Engineering Trade-Off Matrix. The dimensions need to be less than or equal to 0.15m^3 , the power consumption needs to be less than or equal to 115 Watts, the device should last at least 6 hours on its battery, should cost under 500 USD to build, should use Bluetooth 4.0 Bluetooth Low Energy technology, and should analyze a sample in less than 2 seconds.

As described in 5.1.5 Housing Design, the dimensions requirement is satisfied as long as the device is not taller than 5.8 meters. A design consideration for the housing is that it not produce excessive attenuation impeding the signal of the Bluetooth antenna. Solutions for this problem include using different materials such as polycarbonate or fiberglass as well as changing the design so that the Bluetooth module is not entirely enclosed in the metal housing.

The original design specification for power consumption was made at a time when we were considering a 100 Watt broadband source as our light source. This accounted for the vast majority of our power budget because the electronics we needed were only a couple hundred milliwatts. We decided later on in the research stage that we would like to use a laser diode which consumes a peak 285 milliwatts. While our requirement specification states a maximum of 115 Watts for total system power consumption, the sum of peak power consumption for each of our major components is only 829.3 milliwatts. Actual power consumption will be obtained from testing.

There will be other losses in the power supply, voltage regulation and PCB traces, but we are still two orders of magnitude lower than we need to be on the power supply constraint. Another important consideration is the fact that this power consumption figure is calculated with the assumption that each component will always be drawing its peak power consumption, which is extremely conservative. Depending on software development, our processor will be entering various levels of low power mode which can cut power consumption dramatically. Additionally, our laser diode will not be under continuous operation, a sample will be taken with the source powered for about one second and the data will then be sent over Bluetooth.

According to 5.3 Bill of Materials, the CFS will cost less than 500 USD to create and thus the budget still has enough room to include housing design and material implementation to stay under that mark. The CFS is designed to use Bluetooth 4.0 Bluetooth Low Energy technology for its wireless communications. The only metric that cannot be discussed yet is the sample analysis time since the device is not complete. Once the device has been built and is ready to test samples, then the analysis time engineering requirement specification can be discussed.

It is also important to remember that the project design must meet or exceed commercially available products. The Spectral Evolution spectrometer discussed in 4.1 Similar Products can and should be used as a benchmark for comparison during the testing and building phases of the upcoming semester. Due to budget limitations, this device will not be purchased by the group, but it is reasonably well documented online and has been used by several third-party groups to conduct research and study. Information on Spectral Evolution's broadband UV-Vis-NIR spectrometer can be used to judge whether the CFS meets or exceeds a commercial product in price, dimensions, functionality, power consumption, and power delivery. While this is not a make-or-break metric, it will prove impressive if the CFS can beat a commercially produced product.

Another option is to use the industrial-grade laboratory spectrometers available in the various labs in CREOL. These devices cost five to six figures in USD and are used for broadband, precise spectral measurement. While it is unlikely that the CFS will meet the metrics established by these spectrometers, it is important to note that they can and should be used as references due to their reliability, versatility, and functionality. These spectrometers are not for handheld use like the CFS is designed to be, so these industrial-grade laboratory spectrometers can serve as perfect benchmarks instead.

With the extent of the work done on the CFS, the team feels confident and competent going into the upcoming semester. Problems with the design were addressed before design completion, possible issues were brought up and documented, and all relevant standards have been met and implemented. Looking forward to the upcoming semester, the CFS is poised to be a successful senior design project that operates according to specifications and performs as outlined in this report.

The team responsible for the optical design of the CFS would like to thank Dr. David Hagan, Mr. Richard Zotti, Dr. Kyle Renshaw, and Dr. Kyu Young Han from CREOL, the College of Optics and Photonics at the University of Central Florida for assisting with and mentoring the design process.

Appendix A – References

[MC.aprs] Measurement Computing. *TechTip: Accuracy, Precision, Resolution, and Sensitivity*. <https://www.mccdaq.com/TechTips/TechTip-1.aspx>

[TL.dfg] Thor Labs. *Optics Catalog: Introduction to Diffraction Gratings*. <https://www.thorlabs.com/catalogpages/802.pdf>

[TgO.Dnk] Dereniak, Eustace L.; Dereniak, Teresa D. *Geometrical and Trigonometric Optics*. 2008.

[MD.WUUES] Micro Digital. *Ways to Use USB in Embedded Systems*. http://www.smxrtos.com/articles/usb_art/waysusb.htm

[ARM.CPU] Arm Ltd. *Classic Processors*.
<https://www.arm.com/products/processors/classic/arm7/index.php>

[EET.I2C] EETech Media, LLC. *Introduction to the I2C Bus*. <https://www.allaboutcircuits.com/technical-articles/introduction-to-the-i2c-bus/>

[EET.UART] EETech Media, LLC. *Back to Basics: The Universal Asynchronous Receiver/Transmitter (UART)*. <https://www.allaboutcircuits.com/technical-articles/back-to-basics-the-universal-asynchronous-receiver-transmitter-uart/>

[EET.SPI] EETech Media, LLC. *Back to Basics: SPI (Serial Peripheral Interface)*. <https://www.allaboutcircuits.com/technical-articles/spi-serial-peripheral-interface/>

[LFI] LightForm, Inc. *Prism and Diffraction Grating Spectral Properties Compared*. <https://lightforminc.com/prism-grating/>

[Hct] Hecht, Eugene. *Optics*. 4ED.

[HL.A] Healthline; reviewed by Xixi Luo, MD. *Acetone Poisoning*. <https://www.healthline.com/health/acetone-poisoning#symptoms>

[OFC] Keiser, Gerd. Optical Fiber Communication, Fourth Edition. McGraw-Hill, New York, NY. 2011.

[LE] Kuhn, Kelin J. Laser Engineering. Prentice-Hall, Inc. Upper Saddle River, NJ. 1998.

[HGIC] Blake, James H.; Kluepfel, Marjan; Williamson, Joey (ed.). Clemson Cooperative Extension Home & Garden Information Center.
<https://hgic.clemson.edu/factsheet/houseplant-diseases-disorders/>

[ONS.AR0130] SCILLC dba ON Semiconductor. *AR0130CS Datasheet*.
<https://www.onsemi.cn/PowerSolutions/document/AR0130CS-D.PDF>

[Qck.Htn] Quick, W.P.; Horton, P. *Studies on the induction of chlorophyll fluorescence in barley protoplasts. I. Factors affecting the observation of oscillations in the yield of chlorophyll fluorescence and the rate of oxygen evolution.*

<https://www.jstor.org/stable/35689>

Appendix B – Permissions

Permission for [TgO.Dnk]

Re: Requesting Permission to Use Material



Eustace Dereniak <eustace@optics.arizona.edu>
To: Samuel Knight

Reply Reply All Forward ...
Wed 10/23/2019 6:57 PM

Sure,
Yes

Sent from my Verizon, Samsung Galaxy smartphone

----- Original message -----

From: Samuel Knight <sknight@Knights.ucf.edu>
Date: 10/23/19 3:50 PM (GMT-07:00)
To: Eustace Dereniak <eustace@optics.arizona.edu>
Cc: Robert Bernson <bermson91@Knights.ucf.edu>, David Maria <DavidMaria@Knights.ucf.edu>
Subject: Requesting Permission to Use Material

Dr. Dereniak,

Hello; I'm an undergraduate student at CREOL at the University of Central Florida. I'm enrolled in my senior design capstone course and I'm working on a project about chlorophyll fluorescence spectrometry. I'm emailing you today to request your permission to use Figure 4.8 from Geometric and Trigonometric Optics, first edition, in my capstone course's research paper with the appropriate citation included in the references. The paper will not be published for monetary gain.

Regards,
Samuel Knight

Permission for [MD.WUUES]

RE: Request for Permission



David Moore <davidm@smxrtos.com>
To: David Maria
Cc: Samuel Knight; Robert Bernson; Luke Preston

Sat 10/26/2019 7:38 PM

Hi David,

Sure that's fine. You might get a better quality image if you open the PDF version (link in upper right of web page), zoom in, and then use the Windows Snipping Tool to lift it.

David Moore
Vice President

Micro Digital Inc www.smxrtos.com
Voice 714-437-7333 ext 304

From: David Maria [<mailto:DavidMaria@Knights.ucf.edu>]
Sent: Saturday, October 26, 2019 2:20 PM
To: davidm@smxrtos.com; yingbohu@smxrtos.com
Cc: Samuel Knight; Robert Bernson; Luke Preston
Subject: Request for Permission

Hello,

I'm an undergraduate student in the College of Engineering and Computer Science at the University of Central Florida. I'm working on a research paper for my senior design capstone course and I was wondering if I could use one of your figures in my paper, which will not be published for monetary gain. The image is Figure 1 on this page: http://www.smxrtos.com/articles/usb_art/waysusb.htm. I will cite the source appropriately, as well, and state that the image was republished with permission.

Regards,
David Maria

Permission for [EET.UART], [EET.I2C], [EET.SPI]

Re: Request for Permission



Adam LaBarbera <adam@eetech.com>
To: David Maria
Cc: admin@eetechmedia.com

We removed extra line breaks from this message.

Thanks for asking.

You are permitted to use AAC content.
Best of luck.

Best,
Adam

> On Oct 27, 2019, at 12:25 PM, David Maria <davidjmaria@knights.ucf.edu> wrote:
>
> University of Central Florida
> 7542343157
> Hello,
>
> I'm an undergraduate student in the College of Engineering and
> Computer Science at the University of Central Florida. I'm working on
> a research paper for my senior design capstone course and I was
> wondering if I could use some of your figures in my paper, which will
> not be published for monetary gain. The figures will come from the following pages:
> <https://nam02.safelinks.protection.outlook.com?url=https%3A%2F%2Fwww.allaboutcircuits.com%2Ftechnical-articles%2Fspi-serial-peripheral-interfacing%2F&data=02%7C01%7Cdavidjmaria%40knights.ucf.edu%7Cc456f998ad%55454e2b6708d75b17829f%7C5b16e18278b3412c919668342689eeb7%7C0%7C1%7C63%7078028854830384&data=BI1dEI5Nm18%2FgiwGrXvc%2BuHgl%2BtTwa7Hfh856%2DtOdM%3D&reserved=0>
> d2tOdM%3D&reserved=0,

Permission for [LFI]

Re: Request for Permission



jlerner lightforminc.com <jlerner@lightforminc.com>
To: Samuel Knight; jlerner lightforminc.com
Cc: Robert Bernson; David Maria

Reply Reply All Forward
Thu 10/24/2019 5:09 PM

Bandpass-QE_Composite.xlsx 36 KB Effic_Curves_Composite.xlsx 28 KB Spectral_Imaging_Hardware.pdf 4 MB

Action Items

+ Get more add-ins

Hi Sam,

Fine with me.

I think the bandpass spreadsheet contains the figure you are looking for. I used the data in the spreadsheets in the attached paper and subsequently my website. Use, tweak it / them however you wish.

The second spreadsheet compares the efficiency of various devices used in imaging spectroscopy.

Should you publish please be so kind as to send me a copy, or a link to the final publication.

If you need more or different just ask.

Good luck!!

Jeremy

Cell: (908)963-4262

On 10/24/2019 4:18 PM, Samuel Knight wrote:

Hello,

I'm an undergraduate student at CREOL at the University of Central Florida. I'm working on a research paper for my senior design capstone course and I was wondering if I could use one of your images in my paper, which will not be published for monetary gain. The image is Figure 3 on this page: <https://lightforminc.com/prism-grating/>. I will be using it to highlight the differences between gratings and prisms in spectrometers. I will cite the source appropriately, as well, and state that the image was republished with permission. I was also hoping, if permission was granted, that there is a higher resolution copy available for use in my paper, and if I could have access to it.

Regards,
Samuel Knight

Proof of permission request for Young's double slit and [Hct] Request for Permission



Samuel Knight

To: hecht@adelphi.edu

Cc: Bobby Bernson; davidjmaria@knights.ucf.edu; lukepreston@knights.ucf.edu

Reply

Reply All

Forward



Mon 10/28/2019 2:00 PM

Dr. Hecht,

I'm an undergraduate student at CREOL at the University of Central Florida. I'm working on a research paper for my senior design capstone course and I was wondering if I could use some images from your book *Optics* 4th Edition. My paper will not be published for monetary gain. I will be using the images in chapter 10 to highlight the differences between gratings and prisms in spectrometers. I will cite the source appropriately, as well, and state that the images were republished with permission. If I need to use other pictures in my paper, I will be sure to email you before adding them.

Regards,
Samuel Knight

Proof of permission from Scott Prahl



Scott Prahl <Scott.Prahl@oit.edu>

Wed 10/30/2019 12:11 AM

Robert Bernson

You have permission

On Oct 29, 2019, at 9:03 PM, Robert Bernson <rberkson91@knights.ucf.edu> wrote:

Hello Scott,

My name is Robert Bernson and I would like to use the figures you made for the absorption and emission spectra of Chlorophyll A you made and posted on the following page: <https://omlc.org/spectra/PhotochemCAD/html/1122.html>

I will be using them for my capstone course's research paper on chlorophyll fluorescence spectroscopy and will use proper citation.

Sincerely,
Robert

Proof of permission from Greg Sun

RE: Requesting permission to use figures



Greg Sun <Greg.Sun@umb.edu>

Wed 10/30/2019 8:32 AM

Robert Bernson

Dear Robert,

Please go ahead with the figure. Thanks for checking.

Greg

From: Robert Bernson [mailto:rberkson91@Knights.ucf.edu]

Sent: Wednesday, October 30, 2019 4:25 AM

To: Greg Sun <Greg.Sun@umb.edu>

Subject: Requesting permission to use figures

[EXTERNAL SENDER]

Greg,


My name is Robert Bernson and I would like to use Figure 1 in your paper "Intersubband approach to silicon based lasers—circumventing the indirect bandgap limitation."

I will be using it for my capstone course's research paper on chlorophyll fluorescence spectroscopy and will use proper citation.

Sincerely,
Robert

Proof of permission from Edmund Optics

Edmund Optics Technical Support - Photo Permission

 Austin O'Neill <AO'Neill@edmundoptics.com>
Thu 10/31/2019 2:15 PM
Robert Benson; Gretchen Morris <GMorris@edmundoptics.com>

Hi Robert,

Thank you for contacting Edmund Optics Technical Support.


I have CC'd our Director of Creative Services, Gretchen Morris, she will be happy to work with you to get the correct permissions for use in your research paper.

Good Luck in your academic endeavors!

Best Regards,

Austin O'Neill | Product Support Technician

Edmund Optics® Headquarters
p: +1 856.547.3488 ext. 6143



The Future Depends on Optics

From: eo-service@edmundoptics.com <eo-service@edmundoptics.com>
Sent: Thursday, October 31, 2019 1:55 PM
To: Technical Support USA <techsup@edmundoptics.com>
Subject: Edmund Optics: Technical Support : EN - 15798

Edmund Optics: Technical Support : EN - 15798

| | |
|----------------------------|--|
| Reason for Contact: | Technical Support |
| Country: | United States |
| First Name: | Robert |
| Last Name: | Benson |
| Company: | UCF |
| Job Title: | Student |
| Phone Number: | 4109716713 |
| Ext: | |
| Email Address: | rbenson91@knights.ucf.edu |
| Military/Defense Related?: | False |
| Comments: | My name is Robert Benson and I am a student at the University of Central Florida working on a research paper. I would like to use the image comparing shortpass, longpass, and bandpass filters on this page: https://www.edmundoptics.com/campaign/high-performance-optical-filters/ . This image will be properly cited and the paper will not be used for monetary gain. Sincerely, Robert Benson https://www.edmundoptics.com/contact-support/ |
| Referring Page URL: | |
| User Agent: | Mozilla/5.0 (Windows NT 10.0; Win64; x64) AppleWebKit/537.36 (KHTML, like Gecko) Chrome/77.0.3865.120 Safari/537.36 |
| UserIp: | 72.238.31.131, 108.162.212.119 |

This email has been automatically generated. Please do not reply to this message.

(10/31/2019 05:54 PM EST)

Permission for [ONS.AR0130]

Re: Request for Permission SR#241395



Steve West <Steve.West@onsemi.com>
To: David Maria
Cc: Steve West

Tue 11/26/2019 6:15 PM

Hello David,

Please consider this email as official permission from ON Semiconductor (Semiconductor Components Industries, LLC) to use Figure 29 from the AR0130CS/D data sheet in your capstone research paper as indicated in the information outlined below. Please make sure to provide the following attribution statement: *Used with permission from SCILLC dba ON Semiconductor.*

In the future, any and all copyright requests may be sent directly to me.

Best Regards,
Steve



Steve West | ON Semiconductor
Global Technical Publications Manager
Marketing Communications
602.616.5816 (W)
480.619.0930 (M) | 866.435.1399 (F)
steve.west@onsemi.com

Follow us: [Twitter](#) | [Facebook](#) | [LinkedIn](#) | [YouTube](#) | [Blog](#)

Proof for Richardson grating efficiency curve

Request to use grating curve in a paper



Samuel Knight
To gratings@newport.com
Cc Bobby Bernson; davidjmaria@knights.ucf.edu; Luke Preston

Reply Reply All Forward ...

Sat 11/30/2019 5:36 PM

Hello,

I am an undergraduate student at CREOL, the College of Optics and Photonics, at the University of Central Florida. I'm doing a chlorophyll fluorescence spectrometer for my senior design capstone project and I'd like to use your efficiency curve from your 53-*270R data sheet as part of my report since I used this same grating in my design. This report will not be published for monetary gain but will be hosted online for peer review. I will cite the source appropriately and give reference to the owner.

Regards,
Samuel Knight

Proof for ON Semiconductor sensor efficiency

| | |
|---------------------------------------|---|
| First Name | Samuel |
| Last Name | Knight |
| Company name | N/A |
| Phone | * |
| Email Address | knightsc@knights.ucf.edu |
| Country | UNITED STATES |
| Product Type | Sensors |
| Part Number | AR0130CS |
| Estimated Annual Usage | 3 |
| Subject | Request for permission |
| Description (max. 2000 characters) | Hello, I am an undergraduate student at <u>CREOL</u> , the College of Optics and <u>Photonics</u> , at the University of Central Florida. I'm doing a chlorophyll fluorescence spectrometer for my senior design capstone project and I'd like to use your monochromatic efficiency curve from your <u>AR0130CS</u> data sheet as part of my report since I used the monochrome sensor in my design. This report will not be published for |
| First Name | Samuel |
| Last Name | Knight |
| Company name | N/A |
| Phone | * |
| Email Address | knightsc@knights.ucf.edu |
| Country | UNITED STATES |
| Product Type | Sensors |
| Part Number | AR0130CS |
| Estimated Annual Usage | 3 |
| Subject | Request for permission |
| Description (max. 2000 characters) | I'm doing a chlorophyll fluorescence spectrometer for my senior design capstone project and I'd like to use your monochromatic efficiency curve from your <u>AR0130CS</u> data sheet as part of my report since I used the monochrome sensor in my design. This report will not be published for monetary gain but will be hosted online for peer review. I will cite the source appropriately and give reference to the owner. |

Appendix C – Extra Tables and Figures

Table 37. (Appendix) Efficiency and loss at relevant interfaces

| | 600nm | 683nm | 700nm |
|---------------------------------|--------------|--------------|--------------|
| Sensor quantum efficiency (%) | 78 | 69 | 68 |
| Sensor loss (dB) | 1.0790 | 1.6115 | 1.6749 |
| Concave mirror reflectance (%) | 97 | 98 | 98 |
| Concave mirror loss (dB) | 0.1323 | 0.0877 | 0.0877 |
| Grating spectral efficiency (%) | 73 | 63 | 62 |
| Grating spectral loss (dB) | 1.3668 | 2.0066 | 2.0761 |

Loss calculated using $10 \log_{10} \left(\frac{1}{\Gamma} \right)$, where Γ is the quantum efficiency/reflectance/spectral efficiency in decimal form. Modified from $10 \log_{10} \left(\frac{P_0}{P_f} \right)$ where P_0 is the incident power and P_f is the power after the surface interaction. Table 37 assumes the only loss at that surface comes from the efficiency or reflectance and thus does not include losses from scratches, digs, or settled surface particles.